MICROTEXTURED SURFACES

EDWIN T. DEN BRABER

MICROTEXTURED SURFACES

CIP-GEGEVENS KONINKLIJKE BIBLIOTHEEK, DEN HAAG

den Braber, Edwin Teunis

Microtextured Surfaces / Edwin Teunis den Braber. - [S.L. : s.n.]
Thesis Katholieke Universiteit Nijmegen. - With ref.
ISBN 90-9010431-3
Subject headings:biomaterials / microtexture / grooves / biologic response / cell-material interactions / surface modification

The picture of the Borg™ on the cover of this thesis is a still taken from the movie "*Star Trek®: First Contact™*", and was reproduced with the kind permission of Paramount Pictures/UIP/Viacom.

Microtextured Surfaces

Een wetenschappelijke proeve op het gebied van de Medische Wetenschappen

P R O E F S C H R I F T

ter verkrijging van de graad van doctor
aan de Katholieke Universiteit Nijmegen,
volgens het besluit van het College van Decanen
in het openbaar te verdedigen op
dinsdag 20 mei 1997
des namiddags om 1.30 uur precies

door

Edwin Teunis den Braber

geboren op 22 april 1965 te Rotterdam

Promotores : Prof. dr. J.A. Jansen
Prof. dr. L.A. Ginsel

Manuscript committee : Prof. dr. C.G. Figdor
Dr. J.C. Maltha
Prof. dr. E.J.J. van Zoelen

This project was a part of program VI of the Faculty of Medical Sciences and the Dutch Institute for Dental Sciences, and was performed at the unit Oral Function/Dept. for Biomaterials of the University of Nijmegen, The Netherlands. The research, which is described in this thesis, was supported by the Technology Foundation STW, applied science division of NWO and the technology program of the Ministry of Economic Affairs.

The publication of this thesis was supported financially by contributions of:

--- Stichting Technische Wetenschappen (STW)
--- Nederlandse Vereniging voor Biomaterialen (NVB)
--- Nederlandse Vereniging voor Microscopie (NVvM)
--- Stichting Electonenmicroscopie Nederland (SEN)
--- Peehaka$_I$ Excellence Foundation
--- BELIN Project Development B.V.
--- Cordis Europa N.V.
--- Ortomed B.V.
--- J.J. Bos B.V.
--- Drukker Internationaal B.V.
--- H. Drijfhout & Zoon's Edelmetaalbedrijven (Engelhard-CLAL)
--- Sigma-Aldrich Chemie Nederland B.V.
--- Medtronic Bakken Research Center
--- Ethicon (Johnson & Johnson Medical)
--- Foster Findlay Associates

Doctor You see, her eyes are open.
Gentlewoman Ay, but their sense is shut.

Macbeth (Act V, Sc. 1) by William Shakespeare

"Have you also forgotten patience, Spock?
It is one of the most important lessons your father taught me."
"For myself, and my career, I have no need to rush. 'For life is long and there is much to be learned in unhurried contemplation,'" Spock quoted. "However, my concern for speed is on behalf of others."
[...] Sytok closed his eyes and sighed.
"Humans are always so agitated and in too much of a hurry."
"Indeed, the life of a human is short compared to ours," Spock observed.

Prime Directive by Judith and Garfield Reeves-Stevens

This thesis is based on the following publications:

-1- E.T. den Braber, J.E. de Ruijter, H.T.J. Smits, L.A. Ginsel, A.F. von Recum, and J.A. Jansen, "Effect of parallel surface micro grooves and surface energy on cell growth," *J. Biomed. Mater. Res.,* **29,** 511-518 (1995)

-2- E.T. den Braber, J.E. de Ruijter, H.T.J. Smits, L.A. Ginsel, A.F. von Recum, and J.A. Jansen, "Quantitative analysis of cell proliferation and orientation on substrata with uniform parallel surface micro-grooves," *Biomaterials,* **17,** 1093-1099 (1996)

-3- E.T. den Braber, J.E. de Ruijter, L.A. Ginsel, A.F. von Recum, and J.A. Jansen, "Quantitative analysis of fibroblast morphology on microgrooved surfaces with various groove and ridge dimensions," *Biomaterials,* **17,** 2037-2044 (1996)

-4- J.A. Jansen, E.T. den Braber, and Y.C.G.J. Paquay, "Percutaneous implants," *In: Materials in Clinical Applications; Advances in Science and Technology,* **12,** 779-790 (1995)

-5- E.T. den Braber, J.E. de Ruijter, and J.A. Jansen, "The effect of a subcutaneous silicone rubber implant with shallow surface micro grooves on the surrounding tissues in rabbits," *J. Biomed. Mater. Res.,* accepted, (1996)

-6- E.T. den Braber, J.E. de Ruijter, H.J.E. Croes, L.A. Ginsel, and J.A. Jansen, "Transmission electron microscopical study of fibroblast attachment to microtextured silicone rubber surfaces," *Cells and Materials,* accepted, (1997)

-7- E.T. den Braber, J.E. de Ruijter, L.A. Ginsel, A.F. von Recum, and J.A. Jansen, "Confocal laser scanning microscopical study of fibroblast cytoskeletal architecture, attachment complexes, and ECM protein deposition on silicone microgrooved surfaces," *J. Biomed. Mater. Res.,* accepted conditionally, (1997)

-8- E.T. den Braber, H.V. Jansen, M.J. de Boer, H.J.E. Croes, M. Elwenspoek, L.A. Ginsel, and J.A. Jansen, "SEM, TEM, and CLSM observation of fibroblasts cultured on microgrooved surfaces of bulk titanium substrata," *J. Biomed. Mater. Res.,* submitted, (1996)

TABLE of CONTENTS

CHAPTER 1

General introduction

CHAPTER 1

General introduction

Implants, biomaterials, and tissue engineering

During the last two decades the availability and application of medical implants has increased dramatically. For example, the Dutch National Medical Registration Office LMR/SIG approximates that over 100,000 implants were used in 1995 in the Netherlands alone. This concerns a broad variety of medical implants ranging from knee protheses to heart valves, and from breast protheses to pace makers. More estimate figures were presented by Ratner[1] in his Presidential Address for the Society for Biomaterials in 1993 (Table I). Although both sources emphasize that these figures are estimates, it is clear that the use of implants is considerable. Long term projections even suggest that implant applications are going to rise in the future. Factors that contribute to this increase can be ascribed roughly to three major causes. First, the life expectancy of humans increases. This will inevitably lead to a raise in the demand of implants like hip replacements or artificial lenses for the treatment of geriatric diseases and defects. Second, more and more medical treatments are going to include the use of implants in the future. One example of such a development is the use of percutaneous implants in dialysis[2]. In stead of treating patients with chronic renal failure though intermittent haemodialysis, percutaneous implants enable continuous ambulatory peritoneal dialysis (CAPD). Third, technologies are evolving that open new ways in treating specific disorders or defects. This is demonstrated by techniques that are being developed in the field of tissue engineering[3]. Basically, tissue engineering combines the principles and methods of the life sciences with those of engineering to elucidate fundamental understanding of structure-function relationships in normal and diseased tissues, to develop materials and methods to repair damaged or diseased tissues, and to create entire tissue replacements[4]. Tissue engineering thus spans from controlling cellular responses to implant materials, manipulating the healing environment to control the structure of the regenerated tissue, producing

TABLE I

Selected biomedical implant applications; magnitude of use[a]

Application	Numbers Used per Year
Ophthalmologic	
Intraoccular lenses	1,400,000
Contact lenses	250,000,000[b]
Retinal surgery implants	50,000
Prothesis after enucleation	5,000
Cardiovascular	
Vascular grafts	350,000
Arteriovenous shunts	150,000
Heart valves	75,000
Pace makers	130,000
Blood bags	30,000,000
Reconstructive	
Breast protheses	100,000
Nose, chin	10,000
Penile	40,000
Dental	200,000
Orthopaedic	
Hips	90,000
Knees	65,000
Shoulders, finger joints	50,000
Other devices	
Ventricular shunts	21,500
Catheters	200,000,000
Oxygenerators	500,000
Renal dialysers	16,000,000
Wound drains	3,000,000
Sutures	20,000,000

[a]Approximate annual usage in United States of America

[b]Worldwide

cells and tissues for transplantation into the body, and developing a quantitative understanding of many biological equilibrium and rate processes[5].

Biomaterials play an important role in many of these activities. Originally, inertness was thought to be one of the major contributions of the performance of an implant or biomaterial but later Williams adapted the definition of biocompatibility to include the idea that a biomaterial performed with an appropriate host response in a specific application[6]. However, most currently used implant materials do not possess these desirable qualities. At his Presidential Address, Ratner[1] voiced this problem very vividly by saying: "For the majority of our widely used biomaterials, no one sat down in advance and said `how can I engineer the surface of this material to produce the desired biological response?'" He stressed that most currently used biomaterials, although demonstrating generally satisfactory clinical performance, were "ad-hoc" biomaterials, developed upon a trail-and-error optimization, rather than being engineered to produce a desired interfacial interaction. One of these interactions of major importance is cell adhesion to the surface of a biomaterial.

Cell-substratum interactions

Recent advances in the understanding of cell biology have led to a realization that cells are highly sensitive to their immediate environment[7]. Most normally growing cells, both in artificial culture conditions and *in vivo*, attach to surfaces of some kind. These surfaces are usually neighbouring cells of a similar or different type, accumulations of natural extracellular materials such as collagen, or non-cellular substrata. These non-cellular substrata can be either natural or artificial. In addition to the fundamental importance of these cell-substratum interactions during embryogenesis and organogenesis, they also play a critical role in the interactions between surgically implanted materials and the surrounding body tissues. Cell-substratum interactions are concerned not only with the more or less static processes of adhesion and cytotoxicity, but also with the dynamic process of cell locomotion. Mainly through the use of *in vitro* experiments, major progress has been made in the understanding of the interactions between different cell types with the implanted material surface. In the following paragraphs, some cell structures and mechanisms related with fibroblast-substratum interactions will be discussed with a focus on their morphological and molecular structure.

The fibroblast cytoskeleton

The cytoskeleton is a distinct part of the fibroblast. It consists of a cohesive framework of filaments formed by the self-assembly of protein molecules[8]. It is known that the cytoskeleton is involved intimately in producing, coordinating and directing movement of the entire cell, as well as various components within the fibroblast[8-12].

Morphologically, the cytoskeleton consists of three different components, i.e. the microfilaments, intermediate filaments, and microtubules[7, 9, 13]. The presence of fibres within the cytoplasm of cultured cells has been recognized since the description by Lewis and Lewis[14] in 1924 of so called `tension striae' in cultures of mouse endothelium and mesothelium. Later, these striae were also observed in other cell types and were called stress fibres because they are found frequently in regions where the cytoplasm appears to be under stress or tension. Their presence in living cells can be detected by using bright field, phase contrast, Normanski interference contrast, or polarized light microscopy. Specific labelling of these fibres for visualization with fluorescence, confocal laser scanning, or transmission electron microscopy was until recently only possible in fixed cells. However,

recent developments[15] show that fluorescent labelling of stress fibres is now also possible in living cells, enabling for instance confocal laser scanning microscopical time lapse studies.

Stress fibres, commonly more often referred to as microfilaments, consist of parallel bundles of closely packed filaments, 5-7 nm in diameter[8, 10]. Microfilaments are often associated with contacts of the cell and the substratum. In such areas the bundles seem to be attached to the plasma membrane and to run obliquely back into the cytoplasm, rising gradually from the lower to the upper surface of the cell, ending usually in the region of fibrous material around the nucleus (Figure 1). Microfilaments are however not confined to cell/substratum contact areas. The leading lamellipodium contains a cross-weave of microfilaments[16]. Furthermore, microfilaments are present in a cortical layer of cytoplasm immediately beneath the plasma membrane on both the upper and lower surfaces of the cell. This cortical layer has a variable thickness (0.1-0.5 μm) and, in contrast to the orderly arrangement the microfilament bundles, consists of an irregular meshwork of microfilaments[11, 16]. On the lower surface of the fibroblast, the cortical cytoplasm layer is interrupted by obliquely running stress fibres (Figure 1).

Biochemically, microfilaments consist of proteins. These proteins, i.e. actin, myosin and the associated proteins tropomyosin, troponin, α-actinin and filamin, are involved supposedly in the cellular contraction mechanism[8-12]. Up to 15% of the total protein in actively motile cells consists of actin (Mw ±42 kDa). Actin can be present as globular actin (G-actin), although in non-muscle cells much of the actin is also found in the filamentous form (F-actin). These filaments have a double helical structure with a diameter of

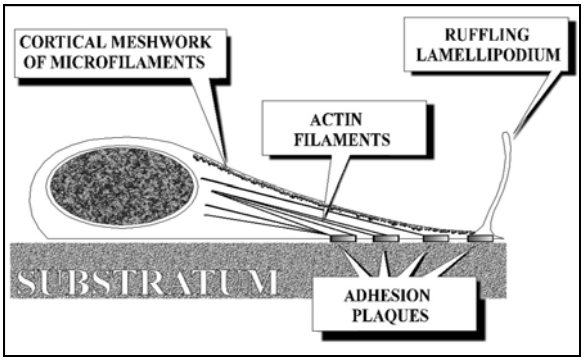

Figure 1 Schematic drawing of a vertical section through a fibroblast[17].

40-70 nm. Electron microscopically they have a characteristic beaded appearance with an axial repeat of about 37 nm. Next to the filaments, a portion of the cellular actin (± 50%) can be present in an unpolymerised form. This may represent a pool of stored actin which can be converted into filaments when required.

Cytoplasmic myosin accounts for about 0.5-1.5% of the total protein in non-muscle cells. The structure and function of this protein is beyond the scope of this study and will therefore not be discussed here. This also applies for the associated proteins tropomyosin, troponin, α-actinin and filamin.

In addition to the microfilaments, another important filamentous system is found in the cytoplasm of many cells from higher eukaryotes. This system consists of filaments with a diameter of 10 nm[8]. Because they are wider than the 6 nm actin filaments, but narrower than the myosin filaments, they are collectively known as the intermediate filaments. Based on their occurrence in specific cell types and their subunit composition, intermediate filaments have been separated into five distinct classes:

-1- Keratin (or prekeratin) filaments restricted to epithelial cells.
-2- Neurofilaments, found characteristically in neurons.
-3- Glial filaments, in glial cells.
-4- Desmin filaments, found mainly in

smooth, skeletal and cardiac muscle.

-5- Vimentin filaments in cells of mesenchymal origin like fibroblasts.

Of all these different categories, only vimentin filaments will be discussed in detail, since these filaments are present in fibroblasts, the cells used in this thesis.

As apparent from the name, the major subunit of vimentin filaments is vimentin. This protein has a molecular weight of 52 kDa[8]. Immunofluorescence of cultured fibroblasts demonstrated that characteristically wavy vimentin fibres extend through the cytoplasm of a cell in a more-or-less radial fashion. Immunofluorescence has also revealed an abundant presence of vimentin filaments around the nucleus. The function of these filaments is however not completely clear. There is some evidence that they are capable of interacting with desmosomes, cellular membranes, and nucleus. One common supposition is that these proteins give mechanical support to the nucleus to maintain its position within the cell. An additional hypothesis is that vimentin filaments are capable of interacting with microtubules.

The presence of elongated tubular structures in cilia and flagella was recognized during the early days of electron microscopy and led to the introduction of the term microtubule by Slauterback[18] in 1963. The widespread occurrence of microtubules in the cytoplasm is a feature of virtually all types of eukaryotic cells, including fibroblasts. Within the cytoplasm, microtubules may occur individual, in bundles, or in more extensive organized arrays. Irrespective of these different patterns, they display a common basic structure in electron micrographs[8]. In a transverse section they usually appear as rings with a diameter of 25 nm. The electron translucent central region is approximately 10 nm across, and the electron dense wall is about 5 nm thick. In longitudinal sections they appear as two electron dense parallel lines. Their total length is difficult to estimate, but immunofluorescence showed that individual microtubules may extend without interruption for at least 50 μm in the cytoplasm of cultured fibroblasts. Furthermore, microtubules are not straight, rigid structures. They usually form extensive networks within the cytoplasm, for the most part conforming to the shape of the cell. The exact function of the microtubules is still unclear.

Tubulin, the predominant protein in microtubules, exists in aqueous solution as a dimer with a sedimentation coefficient of 6S[8]. When denatured, the dimer yields two monomers, each with a diameter of 4 nm, called α- and β-tubulin. These two monomers, which have the same molecular weight of 50 kDa, polymerize and form a microtubule with a hollow cylindrical form, an outer diameter of 25 nm, and a central canal or lumen of about 10 nm diameter.

The fibroblast adhesion mechanism

In vitro, fibroblast adhesion in serum free and serum containing culture medium are two different processes. Adhesion without serum occurs presumably through non-specific physico-chemical forces, while with serum more specific interactions occur between cell and serum components. Since the behaviour of fibroblasts in the absence of serum is beyond the scope of our experiments, only the reactions of these cells in the presence of serum will be reviewed.

Fibroblasts *in vitro* form cell-substratum and cell-cell contacts. These contacts can be differentiated by morphological criteria, i.e. the gap distances between the plasma membrane and the substratum surface and the presence of submembranous densities. Three types of these contact sites have been described[13, 19-22], i.e. focal adhesions, close contacts, and extracellular matrix (ECM) contacts.

Focal adhesions, also called focal con-

tacts, focal adhesion points, or adhesion plaques, are often found on the perimeter of the fibroblasts. They are oval patches, roughly 1 micron long, and characterized by the presence of narrow gaps (10-20 nm) between the ventral surface of the fibroblast and the substratum. Although they occupy only a small fraction of the interface, they are the site of the strongest cell-substratum adhesion. Fibroblasts detached from a substratum with a micro-electrode or a jet of fluid for example leave their adhesion plaques behind on the surface[12]. This suggests that focal contacts are not only points of close contact, but also sites of mechanical anchorage.

Close contacts, often found surrounding focal adhesion points, are characterized by larger gaps of 30-50 nm between the plasma membrane and the substratum. At these contact sites, a meshwork of microfilaments is often seen in the cytoplasm.

ECM contacts are observed at sites where the cell membrane is separated from the substratum surface by a large distance (>100 nm). They are characterized by the presence of strands of extracellular proteinaceous material, which connect the ventral cell membrane to the substratum.

In the formation of focal contacts, two proteins present in serum are involved, i.e. fibronectin and vitronectin[23-28]. *In vitro*, these multi-domain proteins adhere to the glass or plastic surface of a culture dish and expose specific sequences that are recognized by cell surface receptors. The amino acid sequence Arg-Gly-Asp (RGD), found in the cell binding domain of both fibronectin and vitronectin, is especially important in this process. Both, endogenous and plasma fibronectin, possess this amino acid sequence, but that does not mean that the two forms of this protein are identical. Endogenous fibronectin is the major surface glycoprotein of many fibroblastic cell lines. The plasma fibronectin differs from the endogenous form in both molecular weight and biological activity. At present, plasma fibronectin has been demonstrated to mediate several cellular functions, like cell attachment to substrata, maintenance of cellular morphology, wound repair, and non-immune opsonization[23-31].

Focal contacts and integrin

Many models have been developed to describe the cell adhesion process. One of these models[8, 22, 32-41], which now is regarded as most likely, will be presented here in order to describe the construction of a focal contact.

During cell adhesion, the stress fibres of the cytoskeleton are linked to the glycoproteins on the substratum surface through a cascade of proteins. One of these proteins in the cascade is the transmembrane protein integrin (Figure 2).

An integrin molecule is a non-covalently bound complex of two distinct, high molecular weight polypeptides, called α- and β-integrin. Integrin acts as a transmembrane linker in a variety of cells. Beside fibroblasts, integrins are for example also found on blood platelets, where they are involved in blood clotting. Furthermore, they are also present on lymphocytes and macrophages, where they play a role in the crucially important matrix interactions. Integrin spans the plasma membrane in the region of a focal contact (Figure 2). Its cytoplasmic domain binds to the 215 kDa protein talin, which in turn binds to the 130 kDa protein vinculin. Vinculin interacts with α-actinin, which connects with the actin filaments, but may also associate directly with the cytoplasmic domain of integrin. However, the binding affinity of vinculin for α-actinin is quite weak, and in its embryonic form it does not bind to α-actinin at all. Addition of other proteins to the cascade, like the 400 kDa protein tenuin, will strengthen this association between vinculin and α-actinin. With the binding of α-actinin to the stress fibres, a chain of proteins is formed which extends from the

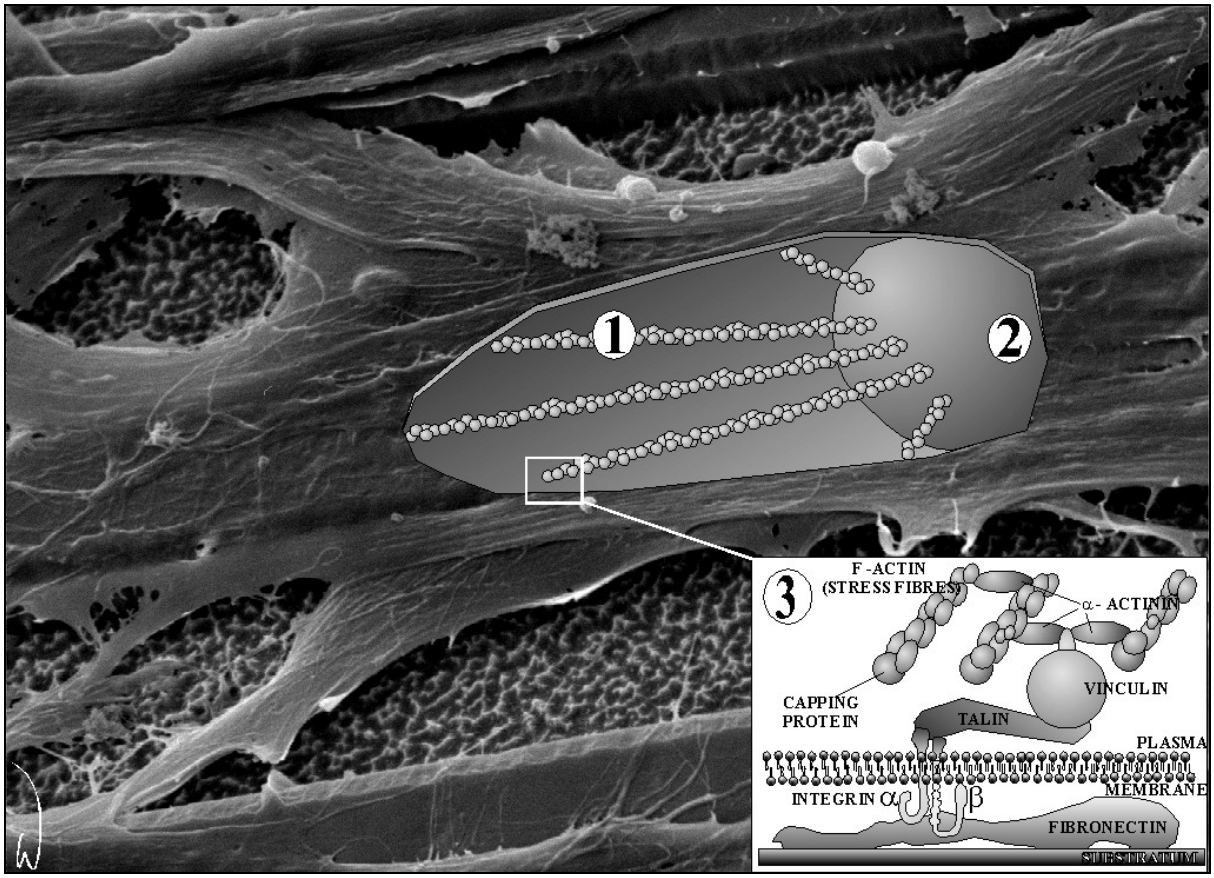

Figure 2 The stress fibres (1) of the cytoskeleton run obliquely from the region near the nucleus (2) to the ventral membrane of the cell. Here the F-actin binds to a cascade of proteins (see inset 3), linking it up with the transmembrane protein integrin that protrudes through the cell membrane and connects to ECM components like fibronectin[8, 22, 32-41].

ECM across the plasma membrane to the cortical cytoskeleton (Figure 2).

Fibroblast locomotion

Most animal cell types possess the capacity to crawl across a substratum. This process of cell locomotion plays a key role in both normal physiology and pathological situations[10-12, 22]. Certain cell types, like neutrophils and free living amoebae, are specialized for locomotion, but in most cells the capacity for locomotion is repressed. As with fibroblasts, cell locomotion is normally only activated by wounding or oncogenic transformation.

Fibroblast locomotion on a rigid substratum is continuous process, which is undoubtedly complex and consists of a delicate interplay between various cellular components. The most important components in this process are the fibroblast cytoskeleton and adhesion mechanism. When the process during fibroblast movement is simplified and broken down into a sequence of separate events (Figure 3), it can be presented as follows[10-12, 22]:

-1- protrusion of the leading edge by assembly of a actin mesh-network;
-2- formation of new distal adhesions of the newly formed protrusion;
-3- contraction of the meshwork by the interaction of microfilaments linked proximally;
-4- forward movement of the cell centre as the microfilament array contracts;
-5- decay of the adhesion as it becomes proximally located; the decay of ad-

hesion, associated with the disassembly of the contractile system, provides recycled subunits for another cycle.

The formation of the lamella is vital for locomotion in general, and the protrusion of the leading edge in particular. The broad, 0.5 μm thick lamella at the front of the fibroblast is devoid of organelles. From the leading edge of this lamella, which is anchored by focal adhesion points, the lamellipodium is projected forward and parallel to the substratum (Figure 3). This extension of the lamellipodium and additional microspikes is driven by the polymerization of actin filaments. Therefore, free actin molecules, also called G-actin, move to the region of the advancing margin of the cell through diffusion. However, how the actin filament actually formed, is not known[11]. One model suggest that new actin can only be generated by polymerization onto the existing barbed ends, thus resulting in elongation of the actin filaments. A second model however, proposes that nucleation of new filaments precedes the elongation of the existing filaments. This would result in "tailor-made" actin extensions that are fitted on the existing filaments. Up to now, results of experiments have not provided sufficient data to rule out one of these two possible models. After the elongation of the actin filaments, the membrane has to be driven forward. As with the elongation of the actin filaments, the exact mechanism of this membrane protrusions is not known. Again, two models are for the generation of the protrusive force have been proposed[11]. The first model suggests that the forward movement of the membrane is driven by an ATPase driven motor (e.g. myosin I), that moves the filament barbed ends backwards and the membrane forward. As a result, the polymerization of actin can fill the created gap. The second model proposes that the membrane is moved forward by thermal fluctuations.

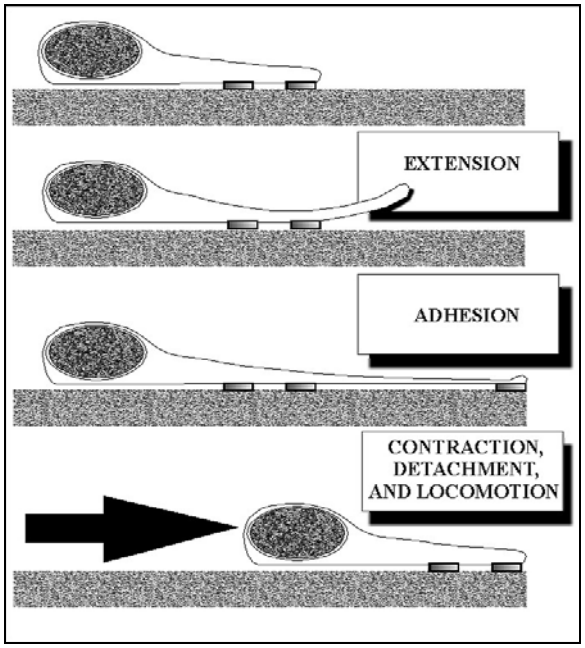

Figure 3 Highly schematic illustration of the principal events during fibroblast locomotion[10-12, 22].

Polymerization again fills the resulting gap, thus preventing backward movement of the membrane.

If the lamellipodium, an extremely thin cytoplasmic sheet of 110-160 nm, contacts the substratum, this results in the formation of focal contacts. An accumulation of transmembrane proteins (integrins) will occur, followed by a polymerization of actin. If the lamellipodium however fails to adhere to the substratum, it extends upwards, moves backwards across the dorsal surface of the lamella in a wave-like manner, and disappears. As one such lamellipodium migrates posteriorly, another takes it place, trying to establish a stable contact with the substratum. The posteriorly directed traffic of lamellipodia on the dorsal surface of the fibroblast is generally called ruffling, and is considered an universal aspect of cell locomotion on planar surfaces *in vitro*. *In vivo* however, it appears that ruffling is uncommon, since these cells advance usually by means of filopodia or blunt protrusions.

After adhesion of the lamellipodium, the cortical network contracts. The contraction

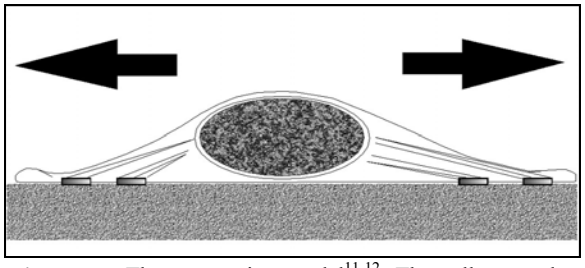

Figure 4 The contraction model[11-12]. The cell centre becomes the focus of a competitive tug-of-war ...

is most prominent in the tail region of the cell and has two important consequences. First, it squeezes the cytoplasm, producing hydrostatic pressure which drives cytoplasmic constituents to the front of the cell. Second, the contraction generates a polarized flow of cortical actin.

After anchorage of the fibroblast to the substratum surface, traction will be applied on the newly focal contacts. According to the two most accepted models[11-12] out of many, this traction will be generated by myosin II. With the contraction model, the myosin II filaments will pull on actin filaments of opposite polarity, thus creating cortical tension that pulls the cell equally in all directions. The cell centre becomes the focus of a competitive tug-of-war (Figure 4) and the area with the greatest number of adhesion sites or exerting the greatest pull will determine the direction of movement. The directed transport model however suggests a more gentile approach. This model postulates that the pull of myosin II is not random, but along an orientated track of actin filaments. As a result of the directive pull, the cell would then move into the direction of the actin filaments.

With both the contraction and the directed transport model, it is essential that the adhesions to which the motor system is anchored, are temporary. If these adhesion plaques do not decay or detach, the cell will not be able to move because of the fact that it is held down by its own adhesion points. Furthermore, the rate at which adhesion anchorages are relinquished also has important consequences for the behaviour of the fibroblast. If isometric tension in the contractile system is maintained, the supply of subunits needed for actin polymerization will become restricted, and forward protrusion at the leading edge will slow down. Hence, cells with tightly adhering adhesion plaques are less likely to be motile. This clearly demonstrates that there is an inverse correlation between the duration of adhesive interactions and the rate of movement. The control of adhesion decay must therefore be of considerable interest. Currently, little is known about the mechanisms involved in the adhesion decay process. Results of experiments indicate that proteolytic degradation of the adhesions almost certainly plays no part in this mechanism[42]. Another possibility is based on the fact that the stability of focal adhesions seems to depend on the lateral, rather than the converse stabilization of the microfilament bundle. Probably, this stabilization is provided by vinculin. However, it is also known that vinculin is one of the cytoplasmic targets of the protein kinase that phosphorylates a tyrosine residue, and kinase is abundantly present in all non-transformed cells. Earlier studies have shown that phosphorylation of vinculin results in the loss of focal adhesions[43-44], and this theory is supported by the observation that intracytoplasmic injection of anti-vinculin antibodies leads to the dissolution of focal contacts[45]. However, one problem with this hypothesis is that only a small proportion of the vinculin becomes phosphorylated. Furthermore, it is not clear whether the phosphorylation of vinculin is a primary cause or a secondary consequence of the altered microfilament distribution. Finally, in more recent models that have been proposed, integrin plays a very important role in the decay of the cell adhesion[22]. With the growing insight in the different functions of integrin and its position in many signalling pathways, it will be not be surprising to learn that integrin is involved in the process of

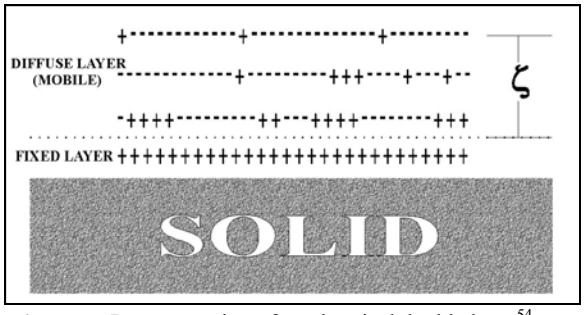

Figure 5 Representation of an electrical double layer[54]

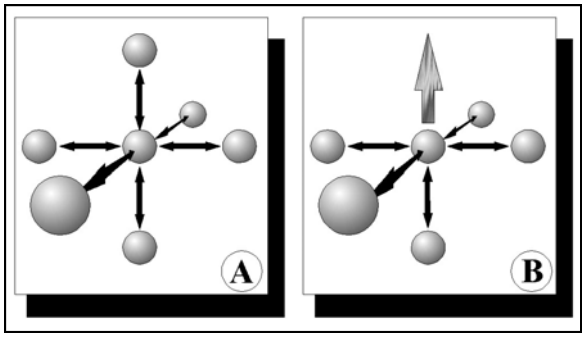

Figure 6 Diagram illustrating the creation of surface energies by unsaturated chemical bonds[62]

adhesion decay. However, regarding the fact that integrin too is directed by other mechanisms[39] will make it a complex, but interesting puzzle to unravel.

The role of the substratum in cellular adhesion

Although cells are able to adhere to different kinds of non-cellular substrata[46], it is known that certain physicochemical properties of the substratum can influence the interactions between cells and the substratum surface. These physicochemical properties include surface chemistry, surface composition, surface charge density[47], surface (free) energy[48-49], surface oxidation[50], solidity[51], curvature[52], and surface morphology[53], which have been shown to affect cellular behaviour. In the following paragraphs the surface charge density, surface free energy, and surface topography will be discussed.

It was suggested by H. von Helmholz[54] in 1879, that an electrical double layer of positive and negative charges exists at the surface of separation between two phases. According to modern views, this double layer at a solid-liquid interface is made up of a layer of ions that are firmly held to the solid, and a more diffuse mobile layer that extends into the solution (Figure 5). The charge of the firmly held or fixed layer is a result of the surface charge density. The surface charge density on its turn a result of the chemical composition of the solid interface. The resultant (net) charge of the diffuse layer is equal in magnitude but of opposite sign to that of the firmly held layer. As a result of the electrical charges, there is a potential between the separation of the bulk of the solution and the fixed and diffuse layer (Figure 5). This is called the electrokinetic potential, represented by the Greek letter zeta, ζ[54].

The role of surface charge density in cell adhesion has been discussed by Curtis[55], Maroudas[47], Grinnell[56], and Weiss[57]. They proposed that negatively charged groups on the substratum surfaces should be present for cell adhesion to occur. It was suggested that these charged groups might be composed of either carboxyl or sulphonate. However, more recent research[56-61] has indicated that the presence of a high surface density of hydroxyl groups is probably more important for the adhesion of cells.

The energy at the surface of a substratum is greater than in its interior. For example, consider a crystal consisting of a cubic lattice. Inside this crystal the atoms are held in place by an equilibrium of attracting and repulsive forces, which are a result of the physicochemical properties of these atoms (Figure 6A). However, at the surface of the crystal this equilibrium is disturbed because of a discontinuity in the three dimensional lattice of forces between the atoms of this crystal (Figure 6B). As a result, the energy at the surface of the crystal is larger because the outermost atoms are not equally attracted or repelled in

all directions. This amount of energy present at the surface of a material is called the surface (free) energy or the surface tension. The latter is represented by the symbol γ. The conventional unit to describe the magnitude of the surface free energy and the surface tension are dynes per centimeter and ergs per square centimeter. These units are numerically similar since 1 erg equals 1 dyne cm. Taking into account that 1 erg equals 10^{-7}J and 1 dyne equals 10^{-5}N, it is easy to deduce that the SI-unit for the surface free energy and surface tension is N/m[62-63].

It was recognized many years ago[64] that surface free energy is a determinant in cell attachment and spreading. Since then, many studies have demonstrated that cellular adhesion, defined in terms of attachment, spreading and growth, tends to correlate with the surface free energy of the substratum surface[65-71]. Surfaces with critical surface tension of 20-30 dynes/cm are reportedly less "adhesive" than surfaces with a critical surface tension between 30 and 50 dynes/cm[72-73]. Therefore, low energy surfaces appear to be non-ideal supports for cellular adhesion.

For the improvement of cellular behaviour it is possible to modify low energy surfaces so that they are energetically similar to high energy surfaces in order to enhance cell attachment and spreading. Polystyrene tissue culture dishes are the best known example of such a modification to enhance cell adhesion. Although the nature of this pretreatment process is a trade secret, it is supposed to consist of a glow discharge treatment[74]. Glow discharge is phenomenon that has been know for some time. It consists of the passage of electrons between two electrodes through a gas at low pressure, creating an ionized atmosphere. The latter is supposed to impart negatively charged groups on the polystyrene surfaces which, as mentioned earlier, seems to facilitates cell attachment.

Despite the above mentioned relationship between cellular behaviour and the substratum surface energy, it should be noted that several investigators have demonstrated that this relation is also influenced by the cell type and the presence of serum in the culture medium[49, 75-78].

Surface topography, microtextured surfaces, and cellular behaviour

In 1912, Harrison[79] cultured cells on a spiderweb and noticed that the direction of movement of the cells was influenced by the structure of the fragile substrata these cells were incubated on. Later, this phenomena was confirmed by Loeb and Fleisher[80] and Weiss[81], who termed the by Harrison observed cell behaviourial change "contact guidance". A few decades later, the ability of the substratum surface to manipulate cellular behaviour was rediscovered Rovensky and Maroudas. Rovensky[82-83] studied the behaviour of fibroblast-like cells on different kinds of substratum surfaces with orderly distributed 40 μm deep grooves with a triangle profile. He reported that the cells became orientated after adhesion and grew parallel to the grooves. Maroudas[52, 84] studied the growth of fibroblasts on small glass beads (diameter 20-60 μm), fibres, and platelets. He observed that cells grown on beads with a large diameter tended toward forming multilayers, while smaller beads progressively failed to support growth.

Since these early studies by Rovensky and Maroudas, several investigators have studied the behaviour of various types of cells to a variety of grooved substrata materials. These studies have been reviewed recently by von Recum and van Kooten[85], and Singhvi et al.[53]. Therefore, only a small recapitulation of some studies with microgrooved surfaces will be given here.

Since the ability emerged to produce standardized microgroove patterns into substratum surfaces, many investigators have tried to answer the question of which surface feature

is responsible for cell orientation and directive movement. In 1982, Dunn[86] studied the response of chick heart fibroblasts (CHF) to grooved substrata. A mask pattern was contact printed onto photoresist-coated quartz by ultraviolet irradiation (200-260 nm). Subsequently, grooves were produced in the quartz substratum by ionmilling. The resulting grooves ranged in width from 1.65 to 8.96 μm, and had a repeat spacing from 3.0 to 32.0 μm. The grooves were of constant depth, i.e. 0.69 μm. After 24 hours of incubation, it appeared that the cells aligned parallel to the long axis of the grooves. In addition, he also observed that the F-actin, associated with focal contacts on the bottom of the grooves, ran almost always parallel to the groove axis. Based on the results of his study, Dunn concluded that groove width has only a small effect in the cellular alignment process. Quantitative analysis of the alignment of populations of fibroblasts demonstrated that the ridge width is the main parameter affecting cell alignment. Finally, he also concluded that the shape and orientation adopted by the cells in response to the grooves, are not governed by independent cellular mechanisms, but a result of actions from the cell as a whole. Later, Dunn, together with Brown[87], would repeat these experiments on quartz surfaces with an identical micropattern as in 1982. However, this time they used a mathematical approach to describe the cell shape, and reached three important conclusions. First of all, they stated that the change of the cell shape on the differently grooved surfaces were entirely due to cell elongation. Secondly, they found that the spreading of the cells on the grooved substrata was generally less than that of cells on smooth substrata. Third and finally, they concluded from their mathematical calculations that the width of the ridges accounted for 90% of the orientational cellular response. The resulting 10% was contributed by the groove width, thus neglecting a possible influence of the groove depth.

This hypothesis contradicted the conclusions of Clark et al.[88-89], who cultured fibroblasts, epithelial-like, and neuronal cells on polymethylacrylate surfaces with a groove/ridge width configuration of 4-24 μm and a groove depth of 0.2-1.9 μm. On results of these studies, Clark et al. concluded that not ridge width, but groove depth is the major factor for cellular orientation. They based this conclusion on the fact that a reduction of the groove depth to 260 nm or 100-400 nm still resulted in cellular orientation, but led to a decrease of the axial polarization of the cells along the surface grooves. In addition to these findings concerning the groove depth, Clark et al.[89] made another interesting observation during this study. They reported that the neuronal cells did not align on 1.0 μm deep grooves, while they did on 2.0 μm deep grooves. This could be a very important indication for a discrepancy in "topography sensitivity" between different cell types, since the neuronal cell only aligned on 2.0 μm deep grooves, while the fibroblasts and epithelial-like cells already orientated on grooves of 100 nm deep.

Next to the different responses of various cell types to identical surfaces, discrepancy in cellular behaviour can also be caused by using different substratum materials. Unfortunately, no reports are known that compare the cellular behaviour of a single cell type to identical groove patterns in different substratum materials. Such a study could clarify the mechanism of cell adhesion, orientation, and movement on microtextured surfaces. The fact that such a study has not been preformed yet, could be caused by the fact that the choice of a suitable substratum material is a difficult one. Although many potential biomaterials are available, it is often difficult to produce micropatterns into the surfaces of these materials.

Titanium is a clear example of such a biomaterial, since it is widely used and ex-

cepted as implant material. Therefore, it seems a logical choice to compare the cellular behaviour of various cell types on smooth and microtextured titanium surfaces. But, due to its structural properties, it is difficult to produce micropatterns into titanium. Furthermore, as reviewed by Singhvi et al.[53], the surface homogeneity, with respect to the surface chemistry and surface energy, can be changed by the production methods used to produce microtextured titanium. Despite this, many investigators have attempted to investigate the behaviour of cells on microtextured titanium.

Lowenberg et al.[90] for example investigated the *in vitro* response of human gingival fibroblasts to two different dental implant materials, titanium alloy and zircalloy. These materials were provided with either a ground surface or a porous structured surface. Based on their observations, Lowenberg et al. reached the very general conclusion that surface geometry could affect attachment and orientation of cells *in vitro* and *in vivo*.

Like Lowenberg, Inoue et al.[91] studied the *in vitro* migration and orientation of human gingival fibroblasts in relation to the rim of smooth-surfaced and porous-coated titanium discs. In these cultures, they found that the fibroblasts migrated from the multilayer onto the smooth-surfaced discs, forming cellular bridges between them. The fibroblasts orientated themselves along parallel circumferential grooves in the rim of the discs. They concluded that in this way the geometrical configuration of implants could influence the development of a capsule or induce an orientated fibrous attachment to implants *in vivo*.

Könönen et al.[92] studied the adhesion, orientation and proliferation of human gingival fibroblasts on electropolished, etched, and sandblasted titanium surfaces. After 3 and 7 days of incubation they found that the fibroblasts attached, spread, and proliferated on all titanium surfaces. However, cells on electropolished titanium exhibited an extremely flat morphology and seemed to form cellular bridges with adjacent cells, whereas the etched and sandblasted titanium surfaces harboured both round and flat cells with many long protrusions. The fibroblasts on the electropolished titanium appeared to grow in thick multilayers with no specific orientation, whereas the cells on the etched surfaces were migrating along the parallel, irregular minor grooves caused by mechanical polishing. On the sandblasted substrata the cells seemed to grow in clusters. Könönen et al. also reported that stress fibre type actin bundles and vinculin containing focal adhesions were present in fibroblasts spreading on the electropolished and etched titanium surfaces, but not on the sandblasted titanium substrata. They concluded that finely grooved titanium surfaces could be optimal with implants adjacent to soft tissues, because they could support the attachment and growth of human gingival fibroblasts.

In all three studies[90-92], the investigators were interested in the cellular response to surface topography. However, being unable to produce standardized surface patterns into titanium, they used methods to create an aspecific surface roughness[90-92] and observed cells on surface features that were created as a by-product of the production process, eg the scratches caused by mechanical polishing[92].

Brunette et al.[93-94] however, approached this problem differently. They cultured human gingival fibroblasts and porcine epithelial cells on uncoated and titanium coated grooved substrata. V-shaped grooves (0.5 μm, 2.0 μm, 3.0-60 μm deep) were produced in silicon wafers by micromachining and subsequently replicated in Epon. They found fibroblast and epithelial cell alignment parallel to the long axis of the grooves. Furthermore, they reported that transmission electron microscopy showed that the cellular filamentous cytoskeletal elements reflected the orientation of the cell as a whole. Fibroblasts

on grooved substrata proved to have more filopodia and to round up more frequently than cells on flat surfaces.

In an additional study, Brunette et al.[95] performed *in vitro* and *in vivo* experiments with the same surfaces. They reported that *in vitro*, grooves as small as approximately 0.5 μm in depth aligned and directed the migration of both fibroblasts and epithelial cells. Tightly spaced grooves (pitch < 30 μm) were found to be more effective in orienting cells than widely spaced grooves. Furthermore, the experiments indicated that the guidance of cell locomotion resulted from interactions of the grooves with the leading lamellae, rather than from the mechanical stiffness of the long cytoskeletal elements. When the grooved, titanium-coated epoxy surfaces were implanted percutaneously in rats, the length of epithelial attachment increased and the rate of epithelial migration towards of the base of the implant was slowed. On basis of these findings, Brunette et al. concluded that surface topography can influence cell migratory and attachment behaviour at implant surfaces significantly.

Objectives of the study

As described above, it has been reported that, except from the physicochemical properties, surface morphological features of a substratum can influence cellular behaviour. Still, little detailed knowledge is available about the interaction between microtextured substratum surfaces and biological tissues. Consequently, the main objective of the studies described in this thesis will be to obtain a better understanding of the mechanisms underlying the relationship between substratum surface microtopography and connective tissue behaviour through *in vitro* and *in vivo* experiments.

In view of this, it will be attempted to answer the following questions:

-1- How does the cellular response of fibroblasts *in vitro* relate to standardized, well defined surfaces? Do microgrooves for instance alter the proliferation rate of cells incubated on these surfaces?

-2- If the proliferation rate of cells is changed by microtextured surfaces, is this a result from the presence of the micro-events or a change due to other physicochemical properties of the substratum material?

-3- What will be the cellular response to surface events with different dimensions? Is there a minimum or maximum micro-event dimension to provoke a certain cellular response?

-4- Many investigators have reported on the overall orientation of cells on microgrooved surfaces. But does the orientation of the intracellular cytoskeletal components differ between textured and non-textured surfaces?

-5- Will it be possible to visualize the intracellular components together with the microtextured surfaces, so that they can be analyzed adequately?

-6- Do microtextured surfaces influence the adhesion of the cell to the surface? Is it possible to manipulate the site of attachment of the cells?

-7- Do microtextured surfaces also influence extracellular matrix formation or protein deposition on these surfaces?

-8- What will the *in vivo* response be to microgrooved surfaces with specific dimensions?

-9- Will it be possible to produce microtextured surfaces in a generally accepted biomaterial like titanium? And if so, will the cellular response to this microtextured titanium surface be comparable to the response of cells on another microtextured material?

-10- How do the obtained results relate to earlier published results and hypotheses?

REFERENCES

1. B.D. Ratner, "New ideas in biomaterial science - a path to engineered biomaterials," *J. Biomed. Mater. Res.*, **27,** 837-850 (1993)

2. A.F. von Recum and J.B. Park, "Permanent percutaneous devices," *CRC Crit. Rev. Bioeng.*, **5,** 37-77 (1981)

3. J.A. Hubbell, "Biomaterials in tissue engineering," *Biotechnology,* **13,** 565-576 (1995)

4. R. Langer and J.P. Vacanti, "Tissue engineering," *Science,* **260,** 920-926 (1993)

5. N.A. Peppas and R. Langer, "Challenges in Biomaterials," *Science,* **263,** 1715-1720 (1994)

6. D.F. Williams, *Definitions in Biomedicals. Progress in Biomedical Engineering*, Vol. 4, Elsevier, New York, U.S.A., 1987

7. I.A.P. Gwynn, "Cell biology at interfaces," *J. Mater. Sci.*, **5,** 357-360 (1994)

8. B. Alberts, D. Bray, J. Lewis, M. Raff, K. Roberts, and J.D. Watson, *Molecular biology of the cell*, Third edition, Garland Publishing Inc., New York, U.S.A., 1994

9. C.A. Middleton and J.A. Sharp, *Cell locomotion in vitro; techniques and observations*, ed. P.J. Baron, Croom Helm Ltd., Kent, U.K., 1984

10. T.P. Stossel, "On the crawling of animal cells," *Science,* **260,** 1086-1094 (1993)

11. T.J. Mitchinson and L.P. Cramer, "Actin-based cell motility and cell locomotion," *Cell,* **84,** 371-379 (1996)

12. D.A. Lauffenburger and A.F. Horowitz, "Cell migration: a physically integrated molecular process," *Cell,* **84,** 359-369 (1996)

13. D. Bray, *Cell Movements*, Garland Publishing Inc., New York, U.S.A., 1992

14. W.H. Lewis and M.R. Lewis, "Behaviour of cells in tissue cultures" *In: General Cytology*, ed. E.V. Cowdry, University of Chicago Press, U.S.A., 1929, pp. 385-447

15. T. Doyle and D. Botstein, "Movement of yeast cortical actin cytoskeleton visualized *in vivo*," *Proc. Natl. Acad. Sci. USA,* **93,** 3886-3891, 1996

16. D. Cox, J.A. Ridsdale, J. Condeelis, and J. Hartwig, "Genetic deletion of ABP-120 alters the three-dimensional organization of actin filaments in Dictyostelium pseudopods," *J. Cell. Biol.,* **128,** 819-835 (1995)

17. T.M. Preston, C.A. King, and J.S. Hyames, *The cytoskeleton and cell motility*, Blackie and Son Ltd., Glasgow, U.K., 1990

18. D.B. Slauterback, "Cytoplasmic microtubules: I. Hydra," *J. Cell Biol.,* **18,** 367 (1963)

19. W-T. Chen and S.J. Singer, "Immunoelectron microscopic studies of the sites of cell-substratum and cell-cell contacts in cultured fibroblasts," *J. Cell. Biol.,* **95,** 205-222 (1982)

20. J.M. Schakenraad et al., "Kinetics of cell spreading on protein precoated substrata: a study of interfacial aspects," *Biomaterials,* **10,** 43-50 (1989)

21. G.A. Truskey, J.S. Burmeister, E. Grapa, and W.M. Reichert, "Total internal reflection fluorescence microscopy (TIRFM); II. Topographical mapping of relative cell/substratum separation distances," *J. Cell Sci.,* **103,** 491-499 (1992)

22. B.M. Gumbiner, "Cell adhesion: the molecular basis of tissue architecture and morphogenesis," *Cell,* **84,** 345-357 (1996)

23. R.J. Klebe, K.L Bentley, and R.C. Schoen, "Adhesive substrates for fibronectin," *J. Cell. Physiol.,* **109,** 481-488 (1981)

24. A. Horwitz, E. Duggan, C. Buck, M.C. Beckerle, and K. Burridge, "Interaction of the plasma membrane fibronectin receptor with talin-a transmembrane receptor," *Nature*, **320,** 531-533 (1986)

25. I.I. Singer, S. Scott, D.W. Kawka, D.M. Kazazis, J. Gailit, and E. Ruoslahti, "Cell surface distribution of fibronectin and vitronectin receptors depends on substrate composition and extra cellular matrix accumulation," *J. Cell Biol.*, **106,** 2171-2182 (1988)

26. S.K. Akiyama, S.S. Yamada, W.-T. Chen, and K.M. Yamada, "Analysis of fibronectin receptor function with monoclonal antibodies: roles in cell adhesion, migration, matrix assembly, and cytoskeletal organization," *J. Cell Biol.*, **109,** 863-875 (1989)

27. J.G. Steele, G. Johnson, and P.A. Underwood, "Role of serum vitronectin and fibronectin in adhesion of fibroblasts following seeding onto tissue culture polystyrene," *J. Biomed. Mater. Res.*, **26,** 861-884 (1992)

28. V.J. Uitto, H. Larjava, J. Peltonen, and D.M. Brunette, "Expression of fibronectin and integrins in cultured periodontal ligament epithelial cells," *J. Dent. Res.,* **71,** 1203-1211 (1992)

29. P.A. Underwood, J.G. Steele, and B.A. Dal-

ton, "Effects of polystyrene surface chemistry on the biological activity of solid phase fibronectin and vitronectin, analyzed with monoclonal antibodies," *J Cell Sci,* **104,** 793-803 (1993)

30. F. Grinnell, C-H. Ho, and A. Wysocki, "Degradation of fibronectin and vitronectin in chronic wound fluid: analysis by cell blotting, immunoblotting, and cell adhesion assays," *J. Invest. Dermatol.,* **98,** 410-416 (1992)

31. L.S. Chou, J.D. Firth, V.J. Uitto, and D.M. Brunette, "Substratum surface topography alters cell shape and regulates fibronectin mRNA level, MRNA stability, secretion and assembly in human fibroblasts," *J. Cell Sci.,* **108,** 1563-1573 (1995)

32. D.J.G Rees et al., "Sequence and domain structure of talin," *Nature,* **347,** 685-689 (1990)

33. C.A. Otey, F.M. Pavalko, and K. Burridge, "An interaction between α-actinin and the ß1 integrin subunit in vitro," *J. Cell Biol.*, **111,** 721-729 (1990)

34. A.P. Gilmore, P. Jackson, G.T. Waites, and D.R. Critchley, "Further characterization of the talin-binding site in the cytoskeletal protein vinculin," *J. Cell Sci.,* **103,** 719-731 (1992)

35. E.J. Luna and A.L Hitt, "Cytoskeleton-plasma membrane interactions," *Science,* **258,** 955-964 (1992)

36. G. Isenberg and W.H. Goldmann, "Actin-membrane coupling: a role for talin," *J. Muscle Res. Cell Mot.,* **13,** 587-589 (1992)

37. R.L. Juliano and S. Haskill, "Signal transduction from the extra cellular matrix," *J. Cell Biol.*, **120,** 577-585 (1993)

38. M.D. Schaller and T.J. Parsons, "Focal adhesion kinase and associated proteins," *Curr. Opin. Cell Biol.*, **6,** 705-710 (1994)

39. N.A. Hotchin and A. Hall, "The assembly of integrin adhesion complexes requires both extracellular matrix and intracellular rho/rac GTPases," *J. Cell Biol.*, **131,** 1857-1865 (1995)

40. A.P. Gilmore, and K. Burridge, "Cell adhesion-cryptic sites in vinculin," *Nature*, **373,** 197 (1995)

41. R.P. Johnson and S.W. Craig, "F-actin binding site masked by the intramolecular association of vinculin head and tail domains," *Nature*, **373,** 261-264 (1995)

42. J.V. Forrester, J.M. Lackie and A.F. Brown, "Neutrophil behaviour in the presence of protease inhibitors," *J. Cell Sci.,* **59,** 213-230 (1983)

43. B.M. Sefton et al., "Cytoskeletal targets for vital transforming proteins with tyrosine protein kinase activity," *Cold Spring Harbor Symp.,* **46,** 939-952 (1982)

44. L. Rohrschneider, M. Rosok, and K. Shriver, "Mechanism of transformation by Rous sarcoma virus: events within adhesion plaques," *Cold Spring Harbor Symp.,* **46,** 953-966 (1982)

45. W. Birchmeier, T.A. Libermann, B.A. Imhof, and T.E. Kreis, "Intracellular and extracellular components involved in the formation of ventral surfaces of fibroblasts," *Cold Spring Harbor Symp.,* **46,** 755-768 (1982)

46. A.S.G. Curtis, *The cell surface: Its molecular role in morphogenesis*, Logos Press, London, U.K. (1967)

47. N.G. Maroudas, "Adhesion and spreading of cells on changed surfaces," *J. Theor. Biol.,* **47,** 417-424 (1975)

48. N.G. Maroudas, "Sulphonated polystyrene as an optimal substratum for the adhesion and spreading of mesenchymal cells in monovalent and divalent saline solutions," *J. Cell. Physiol.,* **90,** 511-520 (1977)

49. J.M. Schakenraad, H.J. Busscher, C.R.H. Wildevuur, and J. Arends, "The influence of substratum free surface energy on growth and spreading of human fibroblasts in the presence and absence of serum proteins," *J. Biomed. Mater. Res.,* **20,** 773-784 (1986)

50. W.S. Ramsey, W. Hertl, E.D. Nowlan et al., "Surface treatment and cell attachment," *In Vitro,* **20,** 802-808 (1984)

51. N.G. Maroudas, "On the low adhesiveness of fluid phospholipid substrata," *J. Theor. Biol.,* **79,** 101-116 (1979)

52. N.G. Maroudas, "Anchorage dependence: correlation between amount of growth and diameter of bead, for single cells grown on individual glass beads," *Exp. Cell Res.,* **74,** 337-342 (1972)

53. R. Singhvi, G. Stephanopoulos, D.I.C. Wang, "Review: effects of substratum morphology on cell physiology," *Biotechnology and Bioengineering,* **43,** 764-771 (1994)

54. S. Glasstone and D. Lewis, *Elements of physical chemistry,* Macmillan & Co Ltd., London, U.K. (1961)

55. A.S.G. Curtis, "Cell adhesion," *In: Prog.*

Biophys. Mol. Biol., A.J.V. Butler and D. Noble (eds.), Pergamon Press, Oxford; 317-386 (1973)

56. F. Grinnell, "Cellular adhesiveness and extracellular substrata," *Rev. Cytol.*, **57,** 65-144 (1978)

57. L. Weiss, "Cell adhesion," *Int. Dent. J.*, **28,** 7-17 (1978)

58. F. Grinnell and K. Feld, "Fibronectin absorption on hydrophillic and hydrophobic surfaces detected by antibody binding and analyzed during cell adhesion in serum-containing medium," *J. Biol. Chem.*, **257,** 4888-4893 (1982)

59. A.S.G. Curtis, J.V. Forrester, C. McInnes, and F. Lawrie, "Adhesion of cells to polystyrene surfaces," *J. Cell. Biol.*, **97,** 1500-1506 (1983)

60. D. Yu and R.E. Marchant, "Formation of hydroxyl groups in plasma polymerized N-vinyl-2-pyrrolidone by reduction with sodium borohydride," *Macromolecules,* **22,** 2957-2961 (1989)

61. T.G. van Kooten, J.M. Schakenraad, H.C. van der Mei, and H.J. Busscher, "Influence of substratum wettability on the strength of adhesion of human fibroblasts," *Biomaterials,* **13,** 897-904 (1992)

62. R.W. Phillips, *Skinner's Science of dental materials*, 9th edition, W.B. Saunders Co., Philadelphia, U.S.A., 1991

63. J.B. Park and R.S. Lakes, *Biomaterials; an introduction,* 2nd edition, Plenum Press, New York, U.S.A., 1992

64. L. Weiss, "The adhesion of cells," *Int. Rev. Cytol.*, **9,** 187-225 (1960)

65. R.E. Baier, "Surface properties influencing biological adhesion," *In: Adhesion in Biological Systems*, R.S. Manly (ed.), Academic Press, New York, U.S.A., 1970, pp 15-48

66. H. Kawahara, "Cellular responses to implant materials: biological, physical and chemical factors," *Int. Dent. J.*, **33,** 350-375 (1983)

67. P. van der Valk et al., "Interactions of fibroblasts and polymer surfaces: relationship between free surface energy and spreading," *J. Biomed. Mater. Res.,* 17; 807-817 (1983)

68. M.J. Lydon, T.W. Minett, and B.J. Tighe, "Cellular interactions with synthetic polymer surfaces in culture," *Biomaterials,* **6,** 396-401 (1985)

69. D.R. Absolom, L.A. Hawthorn, and G. Chang, "Endothelialization of polymer surfaces," *J. Biomed. Mater. Res.,* **22,** 271-285 (1988)

70. S.D. Johnson, J.M. Anderson, and R.E. Marchant, "Biocompatibility studies on plasma polymerized interface materials encompassing both hydrophobic and hydrophillic surfaces," *J. Biomed. Mater. Res.,* **26,** 915-935 (1992)

71. K. Lewandowska, "Cell-type specific adhesion mechanisms mediated by fibronectin adsorbed to chemically substrata," *J. Biomed. Mater. Res.*, **26,** 1343-1363 (1992)

72. R.E. Baier and A.E. Meyer, "Future directions in surface preparation of dental implants," *J. Dent. Education,* **52,** 788-791 (1988)

73. R.E. Baier and A.E. Meyer, "Implant surface preparation," *Int. J. Maxillofac. Impl.,* **3,** 9-20 (1988)

74. C.F. Amstein, "Adaptation of plastic surfaces for tissue culture by glow discharge," *J. Clin. Microscopy,* **2,** 46-54 (1975)

75. R.E. Stallard, A.K. ElGeneidy, and H.J. Skerman, "Vitreous carbon implants: an aid to alveolar bone maintenance," *Oral Impl.,* **6,** 286-308 (1975)

76. J. Ricci, H. Alexander, J.R. Parsons, and A.G. Gona, "Dynamics of cell growth on synthetic fiber materials in vitro," *Proceedings 2nd World Congress on Biomaterials*, 298 (1984)

77. J.A. Jansen, J.P.C.M. van der Waerden, and K. de Groot,"Fibroblast and epithelial cell interactions with surface-treated implant materials," *Biomaterials,* **12,** 25-31 (1991)

78. H.J. Grevstad and K.N. Leknes, "Epithelial adherence to polytetrafluoroethylene (PTFE) material," *Scand. J. Dent. Res.,* **100,** 236-239 (1992)

79. Harrison RG. The cultivation of tissues in extraneous media as a method of morphogenetic study. *Anat Rec* 1912; **6:** 181-193

80. Loeb L, Fleisher MS. On the factors which determine the movements of tissues in culture media. *J Med Res* 1917; **37:** 75-99

81. Weiss P. Experiments on cell and axon orientation in vitro: the role of colloidal exudates in tissue organization. *J Exp Zool* 1945; **100:** 353-386

82. Y.A. Rovensky, I.L. Slavnaya, and J.M. Vasiliev, "Behaviour of fibroblast-like cells on grooved surfaces," *Exp. Cell Res.,* **65,** 193-

201 (1971)

83. Y.A. Rovensky and I.L. Slavnaya, "Spreading of fibroblast-like cells on grooved surfaces," *Exp. Cell Res.,* **84,** 199-206 (1974)

84. N.G. Maroudas, "Growth of fibroblasts on linear and planar anchorages of limiting dimensions," *Exp. Cell Res.,* **81,** 104-110 (1973)

85. A.F. von Recum and T.G. van Kooten, "The influence of micro-topography on cellular response and the implications for silicone implants," *J. Biomater. Sci. Polymer Edn.,* **7,** 181-198 (1995)

86. G.A. Dunn, "Contact guidance of cultured tissue cells: a survey of potentially relevant properties of the substratum," *In: Cell Behaviour,* R. Bellairs, A.S.G. Curtis, G.A. Dunn (eds.), Cambridge University Press, Cambridge, U.K., 1982, pp 247-280

87. G.A. Dunn, and A.F. Brown, "Alignment of fibroblasts on grooved surfaces described by a simple geometric transformation," *J.Cell Sci.,* **83,** 313-340 (1986)

88. P. Clark, P. Connolly, A.S.G. Curtis, J.A.T. Dow, and C.D.W. Wilkinson, "Topographical control of cell behaviour: II. multiple grooved substrata," *Development*, **108,** 635-644 (1990)

89. P. Clark, P. Connolly, A.S.G. Curtis, J.A.T. Dow, C.D.W. Wilkinson, "Cell guidance by ultrafine topography in vitro," *J. Cell Sci.* **99,** 73-77 (1991)

90. B.F. Lowenberg, R.M. Pilliar, J.E. Aubin, G.R. Fernie, and A.H. Melcher, "Migration, attachment, and orientation of human gingival fibroblasts to root slices, naked and porous-surfaced titanium alloy discs, and zircalloy 2 discs in vitro," *J Dent Res,* **66,** 1000-1005 (1987)

91. T. Inoue, J.E. Cox, R.M. Pilliar, and A.H. Melcher, "Effect of the surface topography of smooth and porous-coated titanium alloy on the of in vitro," *J. Biomed. Mater. Res.,* **21,** 107-126 (1987)

92. M. Könönen, "Effect of surface processing on the attachment, orientation and proliferation of human gingival fibroblasts on titanium," *J. Biomed. Mater. Res.,* 26; 1325-1341 (1992)

93. D.M. Brunette, "Fibroblasts on micromachined substrata orient hierarchically to grooves of different dimensions," *Exp Cell Res,* **164,** 11-26 (1986)

94. D.M. Brunette, "Spreading and orientation of epithelial cells on grooved substrata,"*Exp Cell Res,* **167,** 203-217 (1986)

95. D.M. Brunette, "The effect of surface topography on cell migration and adhesion," *Surface Characterization of Biomaterials,* 203-217 (1988)

CHAPTER 2

Effect of parallel surface micro grooves and surface energy on cell growth

E.T. den Braber[1], J.E. de Ruijter[1],
H.T.J. Smits[2], L.A. Ginsel[2], A.F. von Recum[3] and J.A. Jansen[1]

[1]University of Nijmegen, Dental School, Department of Oral Function, Laboratory of Biomaterials,
POB 9101, NL-6500 HB Nijmegen, The Netherlands.
[2]University of Nijmegen, Faculty of Medical Sciences, Department of Cell Biology and Histology,
POB 9101, NL-6500 HB Nijmegen, The Netherlands.
[3]Clemson University, Department of Bioengineering, College of Engineering, 301 Rhodes Research Center,
Clemson SC 9634-0905, U.S.A.

CHAPTER 2

Effect of parallel surface micro grooves and surface energy on cell growth

INTRODUCTION

All cell types that adhere to substrata, reside in an environment with some form of topography. This topography may consist of other cells, extracellular matrix, other organisms, or artificial materials. The first observation of such a topographical reaction of cells dates from the beginning of this century[1]. Until the early 70's, almost no further attention was paid to this phenomenon. Then, Rovensky et al.[2-3] and Maroudas[4-5] rediscovered that cells are able to react on the topography of substratum surfaces. From this moment on, research of this process has flourished, resulting in a host of publications[6-17]. The underlying mechanism of this altered cellular behavior remains unknown. Several applicable theories are available. Some of them assume that the geometrical surface properties impose mechanical restrictions on the cytoskeletal components, which are involved in cell spreading and locomotion[6-17].

Besides geometrical properties, it is also recognized that physicochemical properties are able to influence cellular behavior. For example, it has been described that cellular adhesion tends to correlate with the surface free energy of the substratum material[18-24]. Surfaces with a low surface free energy are reported to be less adhesive than surfaces with a high surface free energy.

Similar to the influence of surface topography, several mechanisms have been proposed to explain the influence of the wettability or surface free energy on cellular behavior. The most widely accepted theory is that these properties have a selective effect on the configuration or conformation of the proteins, which are deposited on the substratum surface[19,25]. These proteins play an important role in the cellular adhesion process. In this context, it has also been noted that the wettability of a substratum surface is primarily determined by the nature and packing of the outermost or exposed surface atoms in a solid. Therefore, it is independent of the chemical nature or arrangement of the underlying atoms and molecules[26].

Recognizing the potential effect of surface properties on cellular behaviour, there are two other factors that need to be considered. First, it has been found that surface roughness or surface topography can have a disturbing effect on the wettability characteristics of a solid[27]. This may especially occur when a material has a uniform roughness or surface texture, but has been disputed by Schmidt and von Recum[38]. Second, in various experiments investigating the influence of the substratum surface topography on cellular behaviour, several methods of surface treatment were used, like ultraviolet irradiation[28], and radio frequency glow discharge[39]. However, there is sufficient evidence that the applied surface treatment can modify the wettability properties and the biological performance of a material[29].

Taking these factors into consideration, it is possible to suggest that the effect of surface topography on cellular behaviour is not only caused by the surface pattern, but also by the altered wettability characteristics as a result of the applied surface treatments. Therefore, the aim of this study was to evaluate the cellular growth rate

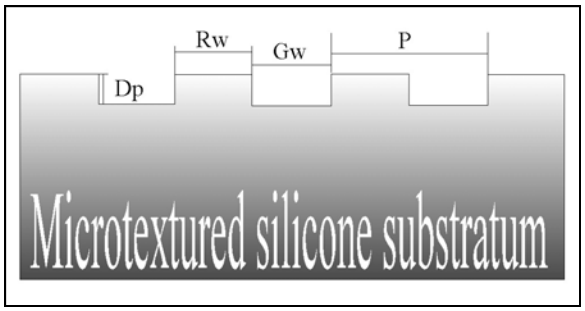

Figure 1 Cross-section through a microtextured substratum (not to scale); Dp=groove depth, Gw=groove width, Rw=ridge width, and P=pitch.

and orientation on well defined surfaces, which received a different surface treatment.

MATERIAL AND METHODS

Production of the substrata

The experimental substrata were produced as described by Schmidt and von Recum[30,31]. Briefly, photolithography was used to manufacture smooth and textured silicon wafers. These produced textured silicon wafers, which had parallel surface grooves with a 2, 5, or 10 μm width. All these grooves had a depth of 0.5 μm and were distributed uniformly with a spacing or ridge similar to the groove width. The configuration and dimensions of these surfaces are summarized in Table I and Figure 1. In order to obtain the final experimental substrata, these wafers or molds were covered with polydimethylsiloxane (silicone elastomer A-2186, FACTOR II). After polymerization, the silicone rubber sheets were removed by peeling them off the wafers.

Surface treatment of the substrata

Prior to use, the microtextured silicone sheets were cut into 15 mm diameter round discs. These experimental substrata were washed manually in 10% Liquinox solution (Alconox Inc.), rinsed, cleaned ultrasonically for 6 hours in a 1% Liquinox solution, and given two 15 minute ultrasonic rinses in distilled, deionized water. Subsequently, they were given a Soxhlet rinse for 24 hours in distilled, deionized water to remove residue. Finally, the substrata were air-dried and divided randomly into 4 groups. These groups of substrata were either left untreated (NT) or were treated by: (1) ultraviolet irradiation (UV; 254 nm, 8 hours); (2) radio frequency glow discharge (RFGD) treatment (PDC-3XG, Harrick; Argon, 0.15 Torr, 5 minutes); (3) 8 hour UV irradiation, followed by RFGD treatment (UVRFGD).

Surface characterization of the substrata

After applying these treatments, the following methods were used to characterize the smooth and microtextured surfaces:

TABLE I

Designer values of the silicon molds and the actual values of the micro events on the silicone rubber substratum surface (Dp=groove depth, Gw=groove width, Rw=ridge width, and P=pitch).

	Designer values				***Actual values***			
Surface	*Dp (μm)*	*Gw (μm)*	*Rw (μm)*	*P (μm)*	*Dp (μm)*	*Gw (μm)*	*Rw (μm)*	*P (μm)*
SilD00	0.00	----	----	----	± 0.02	----	----	----
SilD02	0.50	2.00	2.00	4.00	0.45	1.71	1.68	3.87
SilD05	0.50	5.00	5.00	10.00	0.45	4.65	4.98	9.49
SilD10	0.50	10.00	10.00	20.00	0.46	9.58	9.77	18.98

1. Scanning Electron Microscopy (SEM 500, Philips) and Scanning Probe Microscope (SPM, SP300, Polaron) for qualitative and quantitative inspection of the various surface textures.
2. Wettability measurements by using the Wilhelmy plate technique. The substrata for this particular analysis consisted of two square pieces of silicone rubber (15 mm x 15 mm) attached back to back, thus creating a substratum with two identical smooth or microtextured surfaces. A DCA 322/DACS (Cahn Instruments Inc.) was used to perform the wettability analysis in water and ethylene glycol, according to the two liquid method[27].

The dip and retraction speed during contact angle measurements was 2.5 μm/sec. To exclude an effect of the groove orientation on the advancing and receding contact angles, the measurements were performed with three different substratum orientations (Fig. 2). Nine test pieces of each substratum were used. In addition to the measured contact angles, the surface tension of the various substrata was calculated (DCA Applications Software Version 1.0, Cahn Instruments Inc.), according to the geometric mean method[27,32-34].

Cell culture

Rat dermal fibroblasts (RDFs) were isolated from ventral skin grafts, taken from male Wistar rats, 40 to 43 days of age (100-120 gram). After dissociation, these cells were incubated at 37°C in sterile atmosphere of 5% CO_2-95% air in α-MEM with Earl's Salts and with L-glutamine (Gibco), supplemented with 15% (v/v) heat treated fetal calf serum (Gibco), 2.5 μg/ml amphotericin B (Gibco) and 50 μg/ml gentamicin (Gibco). After approximately 3 days of culturing the RDFs were rinsed with phosphate buffered saline without magnesium and calcium (PBS Dulbeco; pH 7.2), supplemented with 5 μg/ml amphotericin B and 100 μg/ml gentamicin to remove non-attached cells. Subsequently, the growth medium was replaced every two days by fresh growth medium. Upon confluence, the RDFs were detached by trypsinization [0.25% (w/v) crude trypsin and 1 mM EDTA (pH 7.2)] and resuspended at a lower cell concentration in new culture flasks (Nunc) in fresh growth medium. The cells were identified as fibroblasts by phase contrast morphology analysis as described by Freshney[35]. Fifth generation cells were used in all experiments.

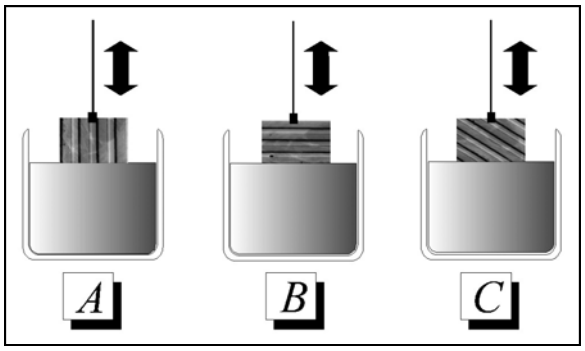

Figure 2 Illustration of the orientation of the micro grooves during wettability analysis.

Cell growth assay

Smooth and microtextured surface treated substrata were placed randomly in the wells of 24 well plates (Greiner). The orientation of the grooves was random, since the micro grooves are not macroscopically visible during this procedure. Subsequently, approximately 1.0 $x10^4$ viable RDFs ml^{-1} suspended in sterile growth medium were added to each substratum. In addition, cell suspension was added to wells without substrata to serve as a control group (CTRL). The cultures were incubated for 1, 3, 5 and 7 days (37°C, 5% CO_2-95% air) under static conditions. The growth medium was changed every two days. At the end of the various incubation periods, the cultures were rinsed with PBS Dulbeco to remove non-attached cells. The remaining RDFs on the substrata were detached by tryp-

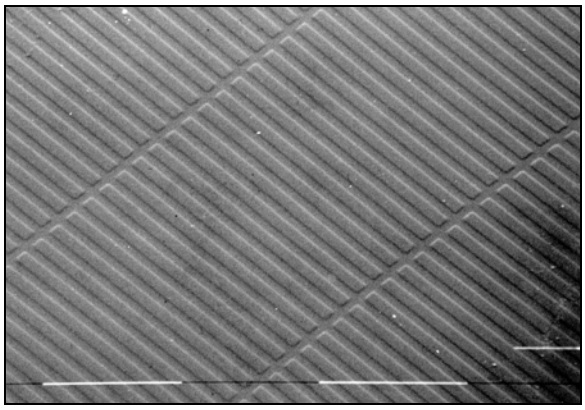

Figure 3 Scanning electron micrograph of the grooved surface of a SilD05 substratum (1 division equals 100 μm).

sinization and counted using a Coulter Counter. After trypsinization, the substrata were observed routinely with a phase contrast microscope to check whether all cells were removed. The results presented are based on the average of four experimental runs, which were counted in triplicate.

To demonstrate the effect of the surface microgeometry on the shape and orientation of the RDFs, additional cultures of smooth and microtextured substrata were evaluated by SEM. After incubation, the attached RDFs were fixed and dehydrated by rinsing with 100% methanol for 5 minutes. Finally, the samples were air dried, mounted on stubs, sputter-coated with gold and investigated by SEM. This experiment was performed in triplicate.

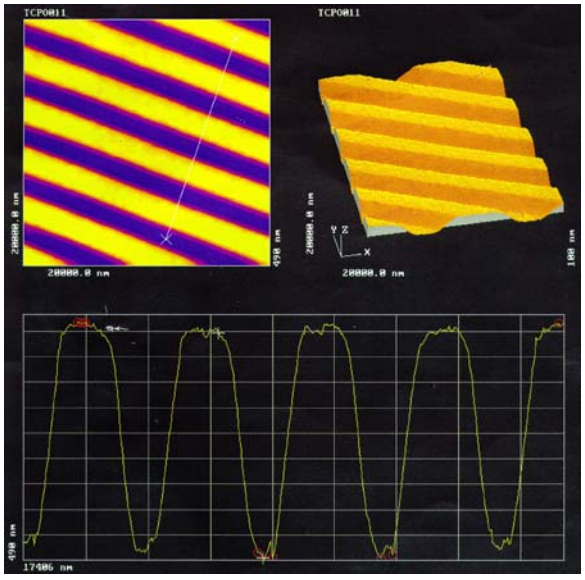

Figure 4 Results of SPM measurements on a SilD02 substratum. The two figures represent a two dimensional and a three dimensional height distribution plot. The graph shows the data points of the SPM measurements. X- and Y-axis have different magnifications.

RESULTS

Surface characterization

SEM and SPM examination showed that none of the duplicated silicone surfaces had defects or irregularities in their surface pattern (Fig. 3 and 4). However, SPM measurements also showed a deviation between the values of the micro events on the silicone casted substrata and the designer values of the silicon molds (Table I and Fig. 4).

The advancing and receding contact angle (θ_{ADV} and θ_{REC}) of the various substrata were measured, followed by calculation of the surface free energy. The results are listed in Table II. The values were averaged over the three orientations as used for wettability analysis, but were statistically tested separately. Statistical testing of these findings, using a Kruskal-Wallis test, showed that the orientation of the surface grooves had no measurable effect on the contact angles and surface free energies of equally treated substrata with an identical surface texture. The various topographical dimensions also did not influence the advancing and receding contact angles and surface energies. Furthermore, statistical testing revealed that UV treatment had no influence ($p>0.05$) on the contact angles and surface energies of substrata with an identical surface topography. However, a significant difference was detected between identical textured substrata of the NT and RFGD ($p=0.0001$), the NT and UVRFGD ($p=0.0001$), the UV and RFGD ($p=0.0001$), and the UV and UVRFGD group ($p=0.0001$).

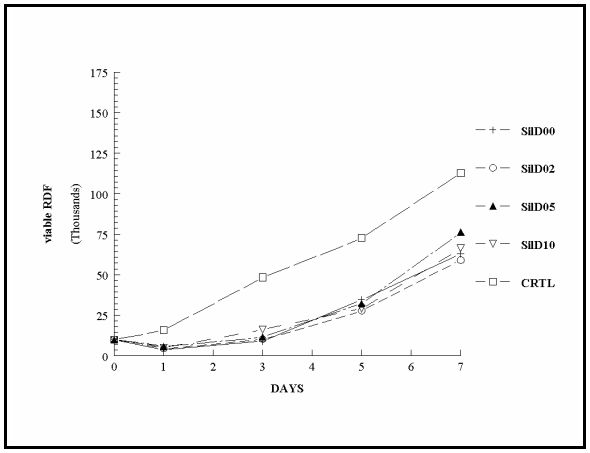

Figure 5 Growth of RDFs on substrata of the UV group ($CV_{average}$=24.4). The growth data of the control group (CTRL) is also plotted ($CV_{average}$=4.3). Differences were found between CTRL and UV treated surfaces ($0.0001 \leq p \leq 0.0005$).

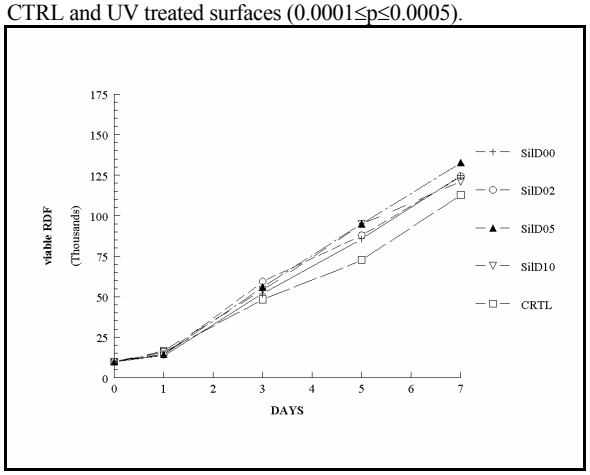

Figure 6 Growth of RDFs on substrata of the RFGD group ($CV_{average}$=11.7). The growth data of the control group (CTRL) is also plotted. No statistic significant differences were found between CTRL and RFGD treated surfaces.

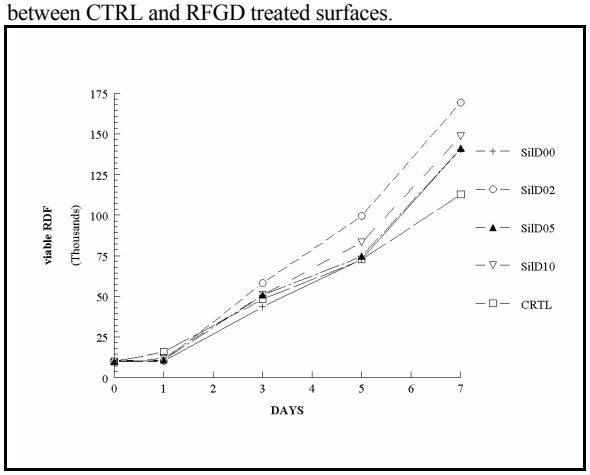

Figure 7 Growth of RDFs on substrata of the UVRFGD group ($CV_{average}$=13.84). The growth data of the control group (CTRL) is also plotted. No statistic significant differences were found between CTRL and UVRFGD treated surfaces.

TABLE II

Average contact angles (θ_{ADV} and θ_{REC}) and surface tension (γ_S) of the smooth and microtextured substrata; σ_{n-1} is given between brackets (n=9).

Sample	θ_{ADV} *(degrees)*	θ_{REC} *(degrees)*	γ_S *(dynes/cm)*
SilD00 NT	111 (10.7)	68 (3.9)	24.9 (2.6)
UV	104 (2.4)	75 (1.6)	24.9 (1.6)
RFGD	17 (1.0)	17 (1.2)	125.8 (12.5)
UVRFGD	15 (1.5)	16 (1.7)	110.5 (14.5)
SilD02 NT	96 (1.5)	66 (3.1)	14.9 (0.9)
UV	98 (0.8)	74 (0.3)	23.6 (2.9)
RFGD	17 (0.6)	15 (0.6)	133.1 (11.7)
UVRFGD	17 (0.7)	15 (0.8)	131.8 (10.3)
SilD05 NT	100 (2.2)	66 (3.2)	17.7 (3.7)
UV	100 (1.5)	70 (2.0)	14.4 (1.4)
RFGD	29 (1.2)	18 (0.6)	111.4 (28.3)
UVRFGD	18 (1.2)	17 (1.2)	123.4 (4.1)
SilD10 NT	90 (2.8)	67 (2.6)	16.6 (2.4)
UV	98 (2.0)	69 (3.1)	14.0 (0.3)
RFGD	23 (0.9)	23 (0.6)	127.5 (18.8)
UVRFGD	18 (0.7)	19 (0.4)	137.3 (12.4)

Cell growth assay

Figures 5, 6, and 7 show the growth curves of the RDFs on the various substrata. As indicated by these graphs, the RDF cell growth on RFGD and UVRFGD treated substrata is higher than on UV treated substrata. Statistical evaluation of the data, using a Kruskal-Wallis test, confirmed this observation (p=0.0001). Statistical testing also revealed that the cell growth of the RDFs of the CTRL group was significantly higher than the growth of these cells on the UV treated substrata ($0.0001 \leq p \leq 0.005$). No significant difference in growth rate was found between

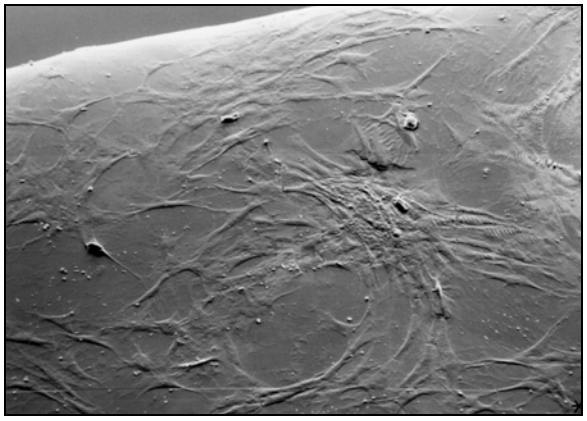

Figure 8 Scanning electron micrograph of RDFs on a SilD00 surface after an incubation period of 3 days (1 division equals 100 μm). Note the random orientation.

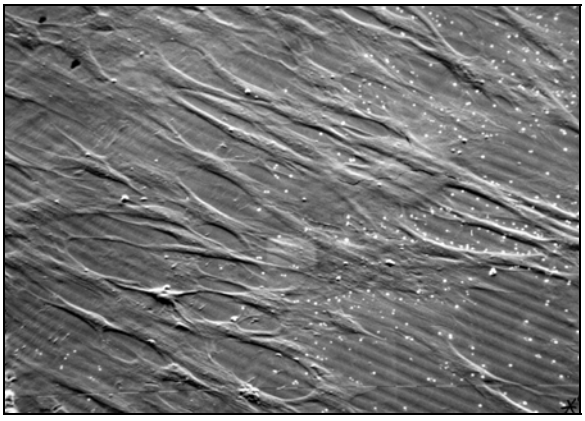

Figure 10 Scanning electron micrograph of RDFs on a SilD05 surface after an incubation period of 3 days (1 division equals 10 μm). The RDFs are aligned parallel to the surface grooves.

RDF cultured on the different treated substrata and CTRL surfaces. Statistical comparison of the growth data for each individual treatment group produced no evidence for a constant significant influence of the surface topography on the RDF growth rate. For example, in the RFGD group cell growth on SilD10 substrata was significantly higher than on SilD02 substrata on DAY 1 ($p=0.0376$), while on DAY 3 the reverse was found ($p=0.0002$). Furthermore, many non-significant differences in cell growth were found. These findings were consistent for all treatment groups.

In contrast with these growth rate findings, SEM evaluation revealed a clear influence of the surface topography of the substrata on the shape and orientation of the cells. This influence was independent of the surface treatment used. Scanning electron micrographs of cells cultured on the various patterned surfaces are shown in Figures 8 to 11. These micrographs show that cells grown on the SilD00 substrata are spread randomly and orientated. Although no quantitative procedures were performed, it is clear that cells on the SilD02 and SilD05 substrata are aligned parallel to the surface grooves. Furthermore, it has to be noted that, despite their orientated

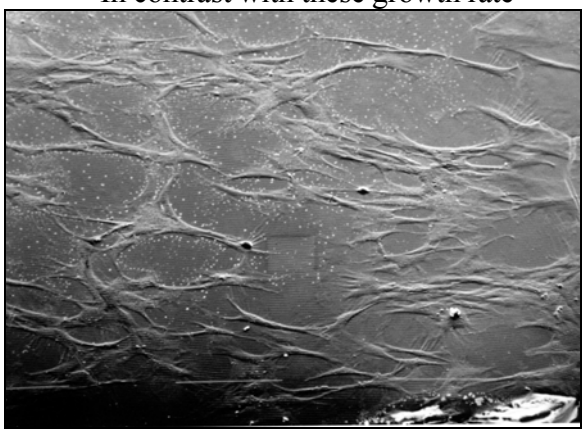

Figure 9 Scanning electron micrograph of RDFs on a SilD02 surface after an incubation period of 3 days (1 division equals 100 μm). The RDFs are aligned parallel to the surface grooves.

Figure 11 Scanning electron micrograph of RDFs on a SilD10 surface after an incubation period of 3 days (1 division equals 10 μm). Orientation of the RDFs becomes more random compared to RDFs cultured on SilD02 and SilD05 substrata.

shape, some of these cells also possess protrusions, which extend over several grooves and ridges. RDFs, growing on SilD10 substrata, differed in two ways from cells cultured on the other surfaces. First, these cells were elongated, but their body was not aligned parallel to the surface pattern. Second, these RDFs were not orientated randomly like the cells observed on the smooth SilD00 substrata. These findings proved to be comparable for all incubation periods.

DISCUSSION AND CONCLUSIONS

SPM measurements showed a deviation between the designer values of the silicon mold and the actual values of the micro events on the silicone substratum surface. These dimensional changes are probably caused by polymerization shrinkage, due to the minimal amount of filler that is added to the polymer[26]. However, it has to be noted that only the dimensions of the casts were determined. Therefore, it can not be completely excluded that the dimensions of the textured wafers deviated from the original designer values.

During the cell culture experiments the NT group was excluded, because the growth rate could be very seriously affected by a possible microbiological contamination. The effect of such a contamination on the growth rate would introduce an additional variable, which would obscure the relation between surface treatment and cell growth. Application of conventional sterilization methods like sterilization by heat, gas, or gamma irradiation can have negative effects, or cause damage to silicone rubber substrata and the growth behaviour of cells cultured on these substrata[19,36]. Therefore, UV irradiation was chosen as an additional surface treatment. This choice was guided by the fact that UV treatment is commonly used for the sterilization of cell culture specimens. Furthermore, as demonstrated by our contact angle measurements, the wettability properties of the NT and UV substrata are similar.

The experimental data in Table II show that substrata of the same treatment group have the same contact angles and surface energy, despite their different surface grooves. The contact angles and surface free energies were only increased after RFGD treatment. These results also demonstrated that RFGD treatment increased the wettability of UV treated substrata to the same level as RFGD alone did. Therefore, a correlation between wettability and surface topography or roughness was not demonstrated. Although this observation is not in agreement with some earlier studies[37], it corroborates the findings of Schmidt and von Recum[38], who reported that square 2, 5, 8, and 10 μm events on silicone surfaces did not increase the critical surface tension and energy of these surfaces compared with smooth silicone substrata.

Our study showed that the growth rate of the RDFs on UV treated substrata was lower than the growth rate of these cells on the substrata of the RFGD, UVRFGD, and CTRL group. A difference between the RFGD, UVRFGD and CTRL groups was not detected. We found no clear evidence that, within a single treatment group, the dimension of the micro features on the substratum surface did facilitate a higher growth rate.

Furthermore, the SEM micrographs demonstrated a marked influence of the various surface structures on the orientation of RDFs. These results confirm the findings of other investigators[3-4,6-17], who also observed contact guidance of cells cultured on microtextured surfaces. However, contrary to the substrata used in our study, their substrata did not possess 0.45 μm deep grooves but grooves of at least 1 μm deep. It was not surprising to find that some RDF cells were able to span several grooves and ridges on all our microtextured surfaces, since this has already been observed by other investigators[39]. In addition, our results showed that SilD02 and SilD05 substrata were able to

induce a stronger contact guidance than SilD10 substrata. The random orientation of the RDFs on SilD00 substrata proved that no contact guidance was evident on these substrata. These last two observations support the studies of Meyle et al.[16] and Schmidt and von Recum[31], who concluded that especially surface features in the range of 1-5 μm promote cellular conformation.

Finally, a comment has to be made about the SEM fixation and dehydration method used. The authors realize that the use of methanol is not accepted widely to fixate and dehydrate cells, which can cause a great loss of delicate cell structures[40]. Nevertheless, this method was chosen since other accepted methods, like critical point drying, freeze drying, and dehydration with tetramethylsilane, which cause severe damage to cells cultured on silicone rubber, make it impossible to gather information about cell orientation. This damage occurs probably because the substrata consist of polydimethylsiloxane. During critical point drying, high pressure compresses the silicone rubber, thus causing cell damage or detachment of the RDFs. Freeze drying results in a rapid drop in temperature which acts as a fixative. However, during this process silicone rubber acts as an insulator, retaining heat and permitting crystals to form which destroy the cell. Dehydration with tetramethylsilane, on the other hand, causes the silicone rubber substrata to swell. Consequently, the cells that are attached to the silicone rubber are exposed to forces which deform, and ultimately detach or damage the cells.

By combining all our findings, the most important conclusion that can be drawn, is that physicochemical parameters, such as wettability and surface free energy, play no measurable role in the shape and orientation of cells on microtextured surfaces. Apparently, the cells are forced into place by the surface texture. For example, as already mentioned earlier by Meyle et al.[15], it can be hypothesized that the strong induction of contact guidance by 2 and 5 μm grooves indicates the need of cells for mechanical stabilization against interfacial movement. However, it cannot be excluded that this orientation phenomenon is caused by the efforts of the cell to reach a biomechanical equilibrium with the net sum of forces minimized[39,41-43].

Finally, it has to be concluded that, in light of earlier reports[28,31], no effect of surface features on the fibroblast growth rate could be proven undeniably in this study. This growth rate is however changed significantly by the applied surface treatment method.

ACKNOWLEDGEMENT

This study is supported by the Technology Foundation (STW).

REFERENCES

1. R. G. Harrison, "The reaction of embryonic cells to solid structures," *J. Exp. Zool.*, **17**, 521-544, (1914)

2. Y.A. Rovensky, I.L. Slavnaya, and J.M. Vasiliev, "Behaviour of fibroblast-like cells on grooved surfaces," *Exp. Cell Res.*, **65**, 193-201 (1971)

3. Y.A. Rovensky, and I.L. Slavnaya, "Spreading of fibroblast-like cells on grooved surfaces," *Exp. Cell Res.*, **84**, 199-206 (1974)

4. N.G. Maroudas, "Anchorage dependence: correlation between amount of growth and diameter of bead, for single cells grown on individual glass beads," *Exp. Cell Res.* **74**, 337-342 (1974)

5. N.G. Maroudas, "Growth of fibroblasts on linear and planar anchorages of limiting dimensions," *Exp. Cell Res.*, **81**, 104-110 (1973)

6. G.A. Dunn, and A.F. Brown, "Alignment of fibroblasts on grooved surfaces described by a simple geometric transformation," *J.Cell Sci.*, **83**, 313-340 (1986)

7. D.M. Brunette, "Fibroblasts on micromachined substrata orient hierarchically to grooves of different dimensions," *Exp. Cell Res.*, **164**, 11-26 (1986)

8. D.M. Brunette, "Spreading and orientation of

epithelial cells on grooved surfaces," *Exp. Cell Res.*, **167**, 203-217 (1986)

9. D.M. Brunette, "The effect of surface topography on cell migration and adhesion," *Surface Characterization of Biomaterials*, 203-217 (1988)

10. T. Inoue, J.E. Cox, R.M. Pilliar, and A.H. Melcher, "Effect of the surface topography of smooth and porous-coated titanium alloy on the orientation of fibroblasts in vitro," *J. Biomed. Mater. Res.*, **21**, 107-126 (1987)

11. P. Clark, P. Connolly, A.S.G. Curtis, J.A.T. Dow, and C.D.W. Wilkinson, "Topographical control of cell behaviour. 1. Simple step cues," *Development*, **99**, 439-448 (1987)

12. P. Clark, P. Connolly, A.S.G. Curtis, J.A.T. Dow, and C.D.W. Wilkinson, "Cell guidance by ultrafine topography in vitro," *J. Cell. Sci.*, **99**, 73-77 (1991)

13. A. Wood, "Contact guidance on microfabricated substrata: the response of teleost fin mesenchyme cells to repeating topographical patterns," *J. Cell. Sci.*, **90**, 667-681 (1988)

14. A.S.G. Curtis, and P. Clark, "The effects of topographic and mechanical properties of materials on cell behaviour," *Critical Reviews in Biocompatibility*, **5**, 343-362 (1990)

15. J. Meyle, A.F. von Recum, B. Gibbesch, W. Hüttemann, U. Schlagenhauf, and W. Schulte, "Fibroblast shape conformation to surface micromorphology," *J. Applied Biomat.*, **2**, 273-276 (1991)

16. J. Meyle, K. Gültig, H. Wolburg, and A.F. von Recum, "Fibroblast anchorage to microtextured surfaces," *J. Biomed. Mater. Res.*, **27**, 1553-1557 (1993)

17. P.T. O'Hara, and R.C. Buck, "Contact guidance in vitro. A light, transmisson, and scanning electron microscopic study," *Expl. Cell Res.*, **121**, 235-249 (1979)

18. R.E. Baier, "Surface properties influencing biological adhesion," *Adhesion in Biological Systems*, Academic Press, New York, 15-48, 1970

19. R.E. Baier, and A.E. Meyer, "Implant surface preparation," *Int. J. Maxillofac. Impl.*, **3**, 9-20 (1988)

20. H. Kawahara, "Cellular responses to implant materials: biological, physical and chemical factors,"*Int. Dent. J.*, **33**, 350-375 (1983)

21. P. van der Valk, A.W.J. van Pelt, H.J. Busscher, H.P. de Jong, Ch. R.H. Wildevuur, and J. Arends,"Interactions of fibroblasts and polymer surfaces: relationship between free surface energy and spreading," *J. Biomed. Mater. Res.*, **17**, 807-817 (1983)

22. M.J. Lydon, T.W. Minett, and B.J. Tighe, "Cellular interactions with synthetic polymer surfaces in culture," *Biomaterials*, **6**, 396-401 (1985)

23. D.R. Absolom, L.A. Hawthorn, and G. Chang, "Endothelialization of polymer surfaces," *J. Biomed. Mater. Res.*, **22**, 271-285 (1988)

24. S.D. Johnson, J.M. Anderson, and R.E. Marchant, "Biocompatibility studies on plasma polymerized interface materials encompassing both hydrophobic and hydrophilic surfaces," *J. Biomed. Mater. Res.*, **26**, 915-935 (1992)

25. V.J. Uitto, H. Larjava, J. Peltonen, and D.M. Brunette, "Expression of fibronectin and integrins in cultured periodontal ligament epithelial cells," *J. Dent. Res.*, **71**, 1203-1211, 1992

26. R.W. Phillips, *Skinner's Science of dental materials*, W.B. Saunders Co., Philadelphia, 1991

27. R.J. Good, "Contact angle, wetting, and adhesion: a critical review," *J. Adhesion Sci.*, **6**, 1269-1302 (1992)

28. A.M. Green, J.A. Jansen, and A.F. von Recum, "The fibroblast response to microtextured silicone surfaces: texture orientation into or out of the surface," *J. Biomed. Mater. Res.*, accepted, 1994

29. J.H. Doundoulakis, "Surface analysis of titanium after sterilization: Role of implant-tissue interface and bioadhesion," *J. Prosth. Dent.*, **58**, 471-478, 1987

30. J.A. Schmidt, and A.F. von Recum, "Texturing of polymer surfaces at the cellular level," *Biomaterials*, **2**, 385-389 (1991)

31. J.A. Schmidt, and A.F. von Recum, "Macrophage response to microtextured silicone," *Biomaterials*, **13**, 1059-1061 (1992)

32. L.A. Girifalco, and R.J. Good, "A theory for the estimation of surface and interfacial energies. I. Derivation and application to interfacial tension," *J. Phys. Chem.*, **61**, 904-909 (1957)

33. F.M. Fowkes, "Determination of interfacial tensions, contact angles, and dispersion forces in surfaces by assuming additivity of intermolecular interactions in surfaces," *J. Phys. Chem.*, **66**, 382 (1962)

34. D.H. Kaelble, "Dispersion-polar surface ten-

sion properties of organic solids," *J. Adhesion*, **2**, 66-81 (1970)

35. R.I. Freshney, *Culture of animal cells; a manual of basic technique*, Alan R. Liss Inc., New York, 1987

36. S. Gamwell Dawids, F. Christoffersen, and T. Elhauge, "Screening test for residual ethylene oxide on reference materials," *The Reference Materials of the European Communities*, Kluwer Academic Publishers, Dordrecht, The Netherlands, 107-112, 1992

37. R.E. Johnson Jr., and R.H. Dettre, "Wettability and contact angles," *Surface and Colloid Science*, Wiley Interscience, New York, 85-153, 1969

38. J.A. Schmidt, and A.F. von Recum, "Surface characterization of microtextured silicone," *Biomaterials*, **13**, 675-681 (1992)

39. C. Oakley, and D.M. Brunette, "The sequence of alignment of microtubules, focal contacts and actin filaments in fibroblasts spreading on smooth and grooved titanium substrata," *J. Cell Sci.*, **106**, 343-354 (1993)

40. P.B. Bell, Jr., "The preparation of whole cells for electron microscopy," presented at the 2nd Pfefferkorn Conference, Sugar Loaf Mountain Resort, Traverse City, MI, April 23-28, 1983

41. D.A. Lauffenburger, "Models for receptor-mediated cell phenomena: adhesion and migration," *Annu. Rev. Biophys. Chem.*, **20**, 387-414 (1991)

42. D.E. Ingber, "Cellular tensegrity; defining new rules of biological design that govern the cytoskeleton," *J. Cell Sci.*, **104**, 613-927 (1993)

43. M.D. Ward, and D.A. Hammer, "A theoretical analysis for the effect of focal contact formation on cell-substrate attachment strength," *Biophys. J.*, **64**, 936-959 (1993)

CHAPTER 3

Quantitative analysis of cell proliferation and orientation on substrata with uniform parallel surface micro grooves

E.T. den Braber[1], J.E. de Ruijter[1],
H.T.J. Smits[2], L.A. Ginsel[2], A.F. von Recum[3], and J.A. Jansen[1]

[1]University of Nijmegen, Dental School, Department of Oral Function, Laboratory of Biomaterials,
POB 9101, NL-6500 HB Nijmegen, The Netherlands.
[2]University of Nijmegen, Faculty of Medical Sciences, Department of Cell Biology and Histology,
POB 9101, NL-6500 HB Nijmegen, The Netherlands.
[3]Clemson University, Department of Bioengineering, College of Engineering,
301 Rhodes Research Center, Clemson SC 29634-0905, USA.

CHAPTER 3

Quantitative analysis of cell proliferation and orientation on substrata with uniform parallel surface micro grooves

INTRODUCTION

During the first part of this century several investigators discovered that cellular behaviour is affected by the topographical morphology of the underlying surface. In 1912 Harrison[1] reported that substrata with a specific linear arrangement, as with spider webs, influence the direction of the movement as well as the form and arrangement of the cells. This was later confirmed by the studies of Loeb and Fleisher[2]. They introduced the term stereotropism, which was described as the direction in which cells move, governed mainly by the contact with solids or very viscid bodies like fibres or fibrin. In 1945 Weiss[3] called this cellular response to the topography of a substratum surface `contact guidance', a term still in use today. Surprisingly, no further attention was paid to this guidance phenomenon until the early 70's. It was Rovensky et al.[4-5] and Maroudas[6-7] who rediscovered that cells are able to react on the topography of a substratum surface. From this moment on, research on this subject has expanded, resulting in many publications, which were thoroughly reviewed recently by Singhvi et al.[8].

Most of the studies are focused on the role of contact guidance in fundamental phenomena like embryogenesis and organogenesis. The possible effect of surface topography on the tissue response to implanted biomaterials has only been recognized for the last few years. Brunette[9-10] for example, suggested the application of microgrooved implant surfaces to prevent epithelial downgrowth around skin penetrating devices. Campbell and von Recum[11] described the use of surface micropatterns as a tool to reduce the inflammatory response at the implant-tissue interface. Although these studies have provided important information, the fundamental mechanism of, and optimal parameters for cell control by guidance are still unknown. In addition, the reported results are often based on subjective, qualitative observations. To surpass this lack of knowledge, it is evident that a systematic study of the influence of surface topography on the cellular behaviour is required. Therefore, the objective of our studies is to approach this guidance principle in a more orderly way.

In our first study[12], we reported on the effect of surface treatment on the wettability of surfaces and on the growth behaviour of cells cultured on various surfaces *in vitro*. These experiments revealed that fibroblast proliferation on UV treated surfaces was lower than on substrata treated with radio frequency glow discharge alone, or in combination with a UV treatment. The substrata that were used during these experiments also possessed parallel surfaces grooves. Scanning electron microscopic examination of fibroblasts on these microtextured surfaces suggested that parallel surface grooves of 2.0 μm and 5.0 μm were able to induce stronger cell orientation and alignment than grooves of 10.0 μm. Cellular orientation proved not to be affected by the various surface treatments. However, due to the number of substrata, only a qualitative conclusion regarding the cellular orientation could be formulated.

Based on the results of this first

study[12], the purpose of this study was to test the hypothesis whether microgeometrical surface patterns influence cellular behaviour only in terms of cell shape and orientation, or also alter the proliferation rate of the RDFs on these surfaces. In order to be able to quantify and test this hypothesis statistically, the experimental design of this study concerned a larger number of substrata than the first study to ensure good statistical power.

MATERIAL AND METHODS

The substrata

The experimental substrata were produced as described earlier by Schmidt and von Recum[13-14]. Briefly, photolithography was used to manufacture smooth and textured silicon wafers. These textured wafers possessed parallel surface grooves with a groove width of 2.0, 5.0, or 10.0 μm. All the grooves had a depth of 0.5 μm and were separated by a ridge, which had the same width as the groove. In order to obtain the final experimental substrata, these wafers or moulds were covered with polydimethylsiloxane (silicone elastomer MDX 4-4210, Dow Corning). After polymerization, the silicone rubber castings were removed from the wafers and cut into round discs with a diameter of 15 mm. These discs were then washed in a 10% Liquinox solution (Alconox Inc.), rinsed, cleaned ultrasonically for 30 minutes in a 1% Liquinox solution and given two 15 minute ultrasonic rinses in distilled, deionized water. Subsequently, they were given a Soxhlet rinse for 12 hours in distilled, deionized water. Finally, the substrata were air-dried and prepared for cell culture purposes by radio frequency glow discharge (RFGD) treatment (PDC-3XG, Harrick; Argon, 0.15 Torr, 5 minutes). After RFGD treatment, the surface geometrical properties of the microtextured substrata were characterized by Scanning Electron Microscopy (SEM-500, Philips) and Atomic Force Microscopy (AFM, SP300, Polaron).

Cell proliferation assay and digital image analysis

Rat dermal fibroblasts (RDFs) were isolated from ventral skin grafts, taken from male Wistar rats, 40 to 43 days of age (100-120 gram). After dissociation, these cells were incubated (37°C, 5% CO_2-95% air) in α-MEM with Earl's Salts and with L-glutamine (Gibco), supplemented with 15% (v/v) heat treated fetal calf serum (Gibco), 2.5 μg ml^{-1} amphotericin B (Gibco) and 50 μg ml^{-1} gentamicin (Gibco). After approximately 3 days of culturing the RDFs were rinsed with phosphate buffered saline without magnesium and calcium (PBS Dulbeco; pH 7.2), supplemented with 5 μg ml^{-1} amphotericin B and 100 μg ml^{-1} gentamicin to remove non-attached cells. Subsequently, new culture medium was added and replaced every two days. Upon confluence, the RDFs were detached by trypsinization [0.25% (w/v) crude trypsin and 1 mM EDTA (pH 7.2)] and resuspended at a lower cell concentration in new culture flasks (Nunc) in fresh growth medium. After identifying the cells as fibroblasts by phase contrast morphology analysis as described by Freshney[15], the fifth generation of these cells was used for all experiments.

Substrata with a smooth or microtextured surface were placed in culture wells of 24 well plates (tissue culture polystyrene, Greiner). Subsequently, approximately 1.0 $x10^4$ viable RDFs ml^{-1} suspended in sterile growth medium, were added to each substratum. In addition, cell suspension was also added to wells without substrata to serve as a control (CTRL). The cultures were incubated for 1, 2, 3, 5 and 7 days (37°C, 5% CO_2-95% air) under static conditions. The growth medium was changed every two days. At the end of the various incubation periods, the cultures were rinsed with PBS Dulbeco to remove non-attached cells. The remaining RDFs on the substrata were detached by trypsinization and counted in triplicate with a

Coulter Counter. After trypsinization, the substrata were observed routinely with a phase contrast microscope (Leitz DMIL) to check whether all cells were removed. This experiment was performed in tenfold.

The effect of the surface micro-geometry on the cellular morphology was quantified by digital image analysis (DIA). For DIA, the RDFs at six random evaluation areas (584.4 μm x 412.5 μm) were photographed by phase contrast microscopy during the cell proliferation assay on day 1, 2, 3, 5 and 7. The evaluation areas were selected by dividing the substratum surface in 740 possible fields of observation of 584.4 μm x 412.5 μm. Each field was given a number, which was entered in a randomization program. Thus, 5 randomly selected evaluation areas and the field at the centre of each substratum were photographed. Registration of the coordinates of these areas assured that the same areas were observed and photographed during the entire period of incubation.

After completion of the cell culture experiments these photographs were scanned digitally (400 dpi x 400 dpi) and analyzed with an Acorn R260 computer (RiSC processor), the ArcImage 5 for the HAWK V12 software package (Foster Findlay Associates, UK) and additional self programmed software. In short, the in-house written routines were used to trace all RDFs (approx. 50) in each digital phase contrast image and to prepare the resulting image for image analysis with the ArcImage program package. The ArcImage program measured several cell parameters, i.e. the cellular surface area, cellular perimeter, cellular circularity, maximum cell length, cell breadth perpendicular to the maximum length, and number of grooves spanned by a single cell. Furthermore, the angle of cellular orientation relative to the surface micro grooves was calculated. A diagram with the evaluated parameters, except circularity, can be found in Figure 1.

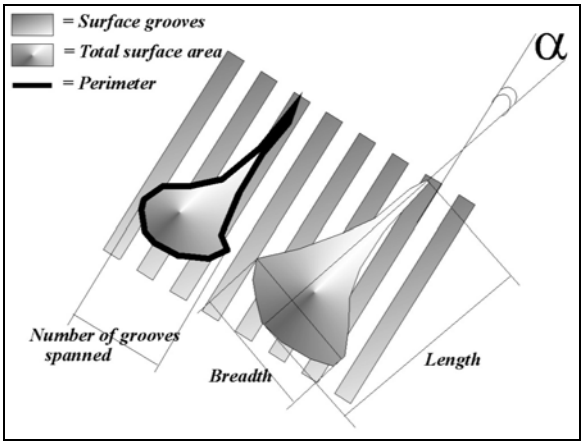

Figure 1 DIA parameters; α represents the angle of cellular orientation relative to the surface grooves.

Circularity is defined as

$$Circularity = \frac{4\pi(Area)}{(Perimeter)^2}$$

and ranges between 0 and 1. In the theoretical situation that circularity equals 0, the cell has a perfect linear shape. However, if circularity is 1, the cell is shaped as a perfect circle.

After gathering the numerical DIA data, these parameters were analyzed using univariate and general linear model procedures, including Scheffe's multi-comparison test.

TABLE I

Dimensions of the micro events on the silicone rubber substratum surface (Gd=groove depth, Gw=groove width, Rw=ridge width, and P=pitch).

Surface	***Actual values***			
	Gd (μm)	*Gw (μm)*	*Rw (μm)*	*P (μm)*
SilD00	± 0.02	----	----	----
SilD02	0.45	1.71	1.68	3.87
SilD05	0.45	4.65	4.98	9.49
SilD10	0.46	9.58	9.77	18.98

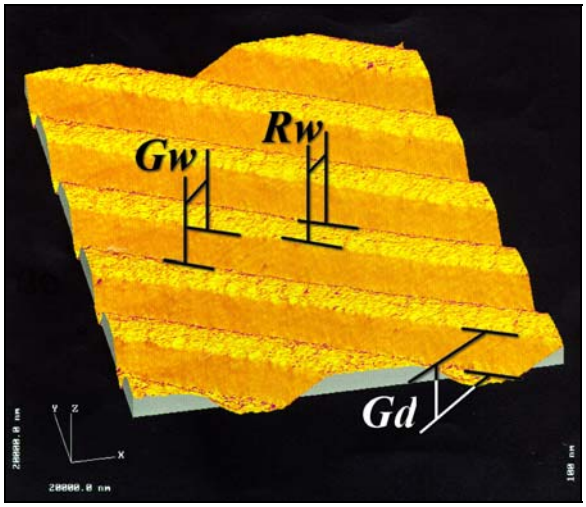

Figure 2 Three dimensional representation of the results of the AFM measurements on a SilD02 substratum. Different X- and Y-axis magnifications were used in this plot to clarify the conformation of the substratum surface. The codes in this image represent the ridge width (Rw), the groove width (Gw), and the groove depth (Gd).

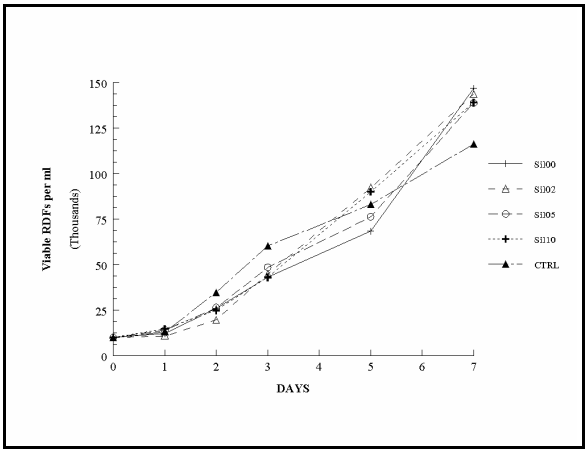

Figure 3 Proliferation of RDFs on substrata with different groove configurations (Average coefficient of variation= 14.76%), i.e. smooth silicone surfaces (SilD00), surfaces with 2 μm (SilD02), 5 μm (SilD05), and 10 μm grooves (SilD10). The proliferation data of the control group (CTRL) is also plotted (Average coefficient of variance= 7.04%). Statistical significant differences between CTRL and the silicone substrata were only found on day 7 ($0.0001 \leq p \leq 0.0103$).

RESULTS

Surface characterization

Surface inspection by SEM and AFM showed that the pattern of the parallel micro grooves on the substrata surfaces had no defects or irregularities (Figure 2). However, AFM measurements did show a slight deviation between the dimensions of the micro events on the silicone cast substrata and the designer values of the silicon moulds. These values can be found in Table I.

Cell proliferation assay

Figure 3 shows the proliferation curves of the RDFs cultured on surfaces with several parallel surface groove configurations. Statistical evaluation of the proliferation data produced no evidence for a constant significant influence of the surface topography on the RDF proliferation rate. For example, on day 2 cell proliferation on SilD00 substrata was significantly higher than on SilD02 substrata ($p=0.0001$), while on day 5 more RDFs were found on the SilD02 substrata than on the SilD00 surfaces ($p=0.0020$).

Digital Image Analysis (DIA)

Figures 4 to 7 show representative phase contrast images of the RDFs on the various surfaces after 3 days of incubation. On the smooth substrata the RDFs are well spread and orientated randomly (Figure 4). In contrast, the cells on the 2 μm grooved substrata appear to align in the direction of the grooves (Figure 5). Most of these RDFs have a highly elongated spindle shape. RDFs on the SilD05 and SilD10 substrata show a more complicated picture (Figure 6 and 7). On both substrata spindle shaped and flat, well spreaded RDFs can be seen. The cells on these surfaces are not aligned as strong as the RDFs on the SilD02 substrata.

DIA data confirmed this observed influence of the surface topography on the size, shape and orientation of the RDFs after the quantitative analysis of the measured cell parameters (Figure 1). RDFs were significantly smaller ($0.0002 \leq p \leq 0.0472$) on the SilD02 than on the other surfaces up to day 5 (Figure 8). Evaluation of the RDF perimeter showed that the size of the cell perimeter was not affected significantly by the surface topography.

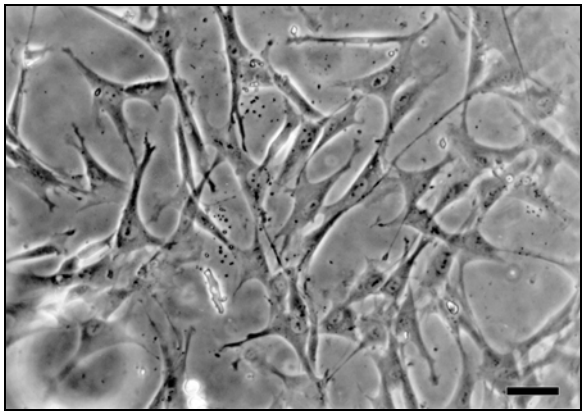

Figure 4 Phase contrast image of RDFs on a SilD00 substratum (bar=50 μm). The random cellular orientation is evident.

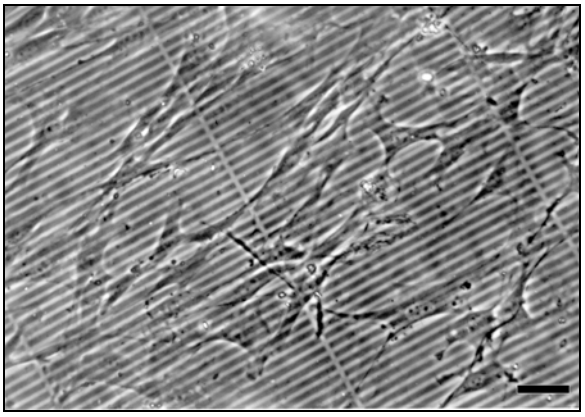

Figure 6 Phase contrast image of RDFs on a SilD05 substratum (bar=50 μm). The RDF orientation is not as clear as on the SilD02 surfaces.

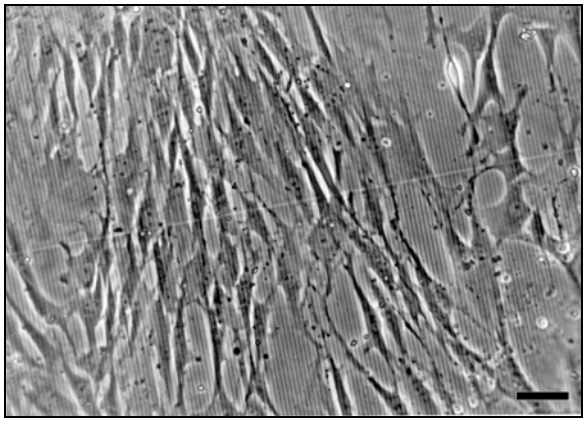

Figure 5 Phase contrast image of RDFs on a SilD02 surface (bar=50 μm). The cells are strongly aligned and elongated along the grooves.

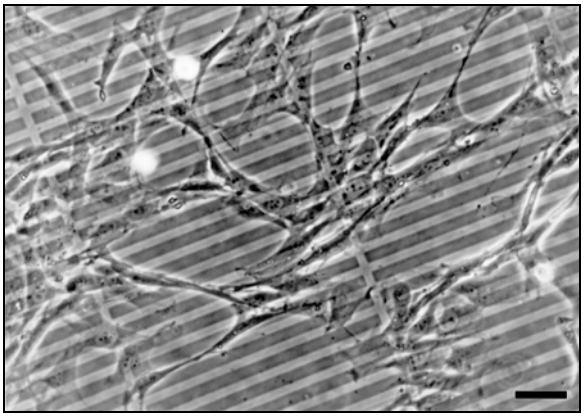

Figure 7 Phase contrast image of RDFs on a SilD10 surfaces (bar=50 μm). The orientation of the RDFs resembles that of the cells on the SilD00 substrata.

However, RDFs were more circular on the smooth substrata ($p_{day\ 3\text{-}7}$=0.001) and CTRL surfaces ($p_{day\ 1\text{-}7}$=0.001) than the cells on the textured substrata (Figure 9). In addition, RDFs on the grooved surfaces were significantly longer than the cells on the smooth substrata ($0.0001 \leq p_{day\ 2\text{-}7} \leq 0.0066$) and CTRL surfaces ($0.0001 \leq p_{day\ 2\text{-}7} \leq 0.0349$). The breadth of the RDFs on the SilD02 and SilD05 substrata was significantly smaller ($0.0001 \leq p_{day\ 1\text{-}7} \leq 0.0184$) than the breadth of the cells on the SilD00 and CTRL surfaces. The breadth of the RDFs on the SilD02 surfaces proved to be the smallest, while no difference in breadth was observed between the RDFs on the SilD10 substrata and the cells on the SilD00 and CTRL surfaces.

Quantitative digital image analysis also demonstrated that the angle of cellular orientation (α) relative to the surface grooves (Figure 1) was the smallest on the SilD02 surfaces during the first 5 days of incubation (Figure 10). This angle proved to be larger with the cells cultured on the SilD05 substrata, while the largest angle of orientation was found on the SilD10 surfaces. After 7 days of incubation the angles were comparable for the RDFs on the SilD02, SilD05, and SilD10 substrata. In

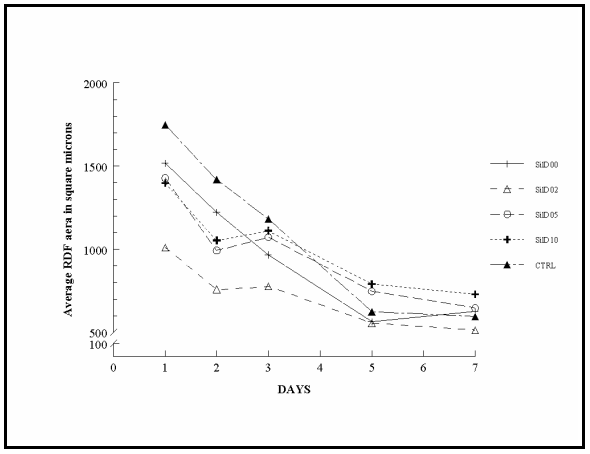

Figure 8 Average RDF surface area on the various surfaces in square microns ($CV_{average}$= 17.85%). The surface area of the cells on the SilD02 substrata is the smallest.

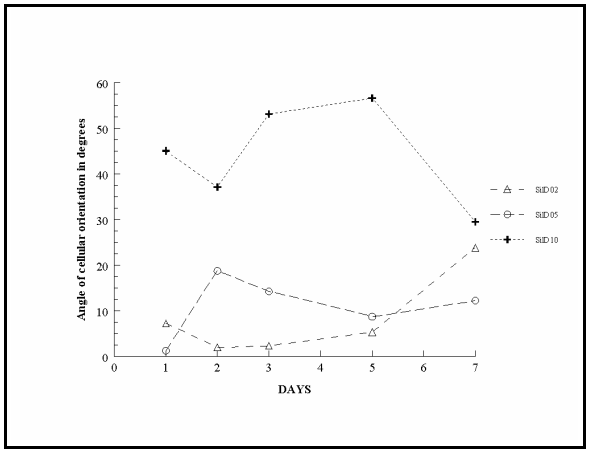

Figure 10 Average angle of RDFs orientation relative to the surface grooves. Especially the RDFs on the SilD02 substrata (1.67≤SD≤4.37), but also the cells on the SilD05 surfaces (3.02≤SD≤6.28) are orientated along the surface grooves. RDFs on the SilD10 substrata (3.76≤SD≤13.74) are randomly aligned considering the average angle of orientation of 45°.

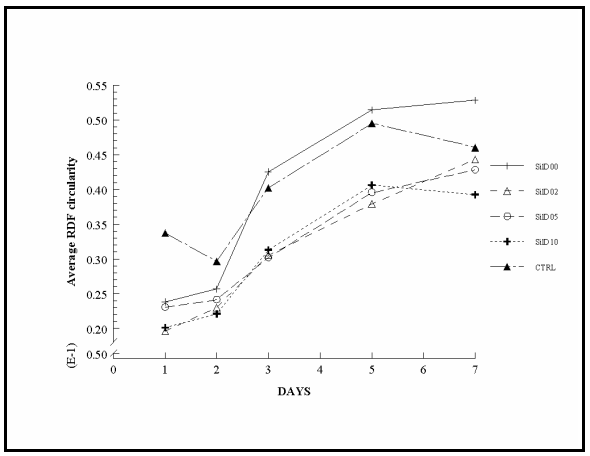

Figure 9 Average circularity of the RDFs on the various surfaces (Average coefficient of variance= 4.60%). The cells on the SilD00 and CTRL surfaces are rounder than the RDFs on the textured substrata.

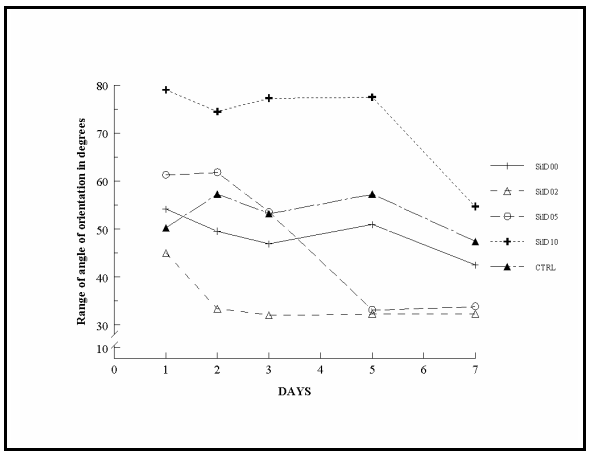

Figure 11 The range of the angle of RDF orientation. As a result of contact guidance, the range of cellular orientation is much smaller among RDF on the SilD02 substrata than on the SilD10 surfaces.

Figure 11 the range of the measured angle of cellular orientation relative to a virtual X-axis is plotted. This graph shows that the range of this angle is the smallest with the RDFs on the SilD02 substrata, while it is the largest with the cells cultured on the SilD10 surfaces.

Finally, the phase contrast images (Figure 4-7) also show that the RDFs were able to span the grooves on the textured surfaces. Apparently, the dimension of the grooves did not influence the ability of the RDFs to span these micro events. For example, on day 1 the RDFs on the SilD02, SilD05 and SilD10 substrata spanned an average of 7.10, 3.85, and 2.1 grooves respectively. Further evaluation of this data showed that the number of the grooves that were spanned decreased after more days of incubation. In order to compare this decrease of the cells on the various textured surfaces,

the grooves spanned on day 1 were defined as 100%. The number of grooves spanned on the following days was calculated as a fraction of this percentage (Figure 12). Although the dimension of the grooves on the various surfaces was different, the decrease of the number of spanned grooves did not differ significantly.

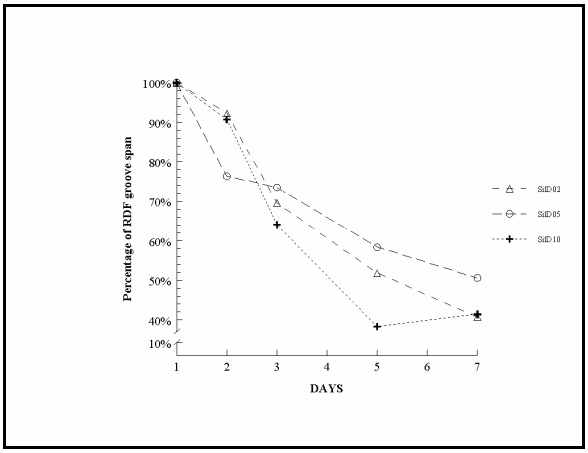

Figure 12 Percentage of RDF groove span. The total number of grooves spanned on day 1 is defined as 100%. The decrease of the number of grooves spanned by the cells is not significantly influenced by the dimension of the grooves.

CONCLUSIONS AND DISCUSSION

On basis of the results, it can be concluded that the dimensions of the parallel surface grooves as used in our experiments, did not result in a higher RDF proliferation rate. This observation is in contrast with the findings of Green et al., and Ricci et al. For example, Green et al.[16] reported that especially abdomen fibroblasts (CCD-969sk) cultured on surfaces with 2.0 and 5.0 μm square pillars showed increased proliferation rates. Ricci et al.[17] evaluated the *in vitro* growth of rat tendon fibroblasts and rat bone marrow colonies on unidirectional (grooved) surface micro geometries. They found that the overall colony growth rate was changed, and concluded that surface microgeometry could be used to control the growth rate at implant surfaces. However, this study by Ricci also showed that the response to surface topography is dependent on cell type, which could take account for the results in our present and earlier studies[12, 18-20], that show no correlation between microtextured surfaces and RDF proliferation.

With respect to our proliferation results it has to be mentioned that RFGD resulted in an optimal cell culture surface, since results proved to be comparable with tissue culture polystyrene. Nevertheless, it is still possible that, for instance the amount and composition of secreted proteins is different between cells cultured on smooth and textured surfaces, especially since DIA data showed a marked influence of the surface grooves on the shape, size, and orientation of the RDFs. In addition, stronger contact guidance was observed on the SilD02 and SilD05 substrata than on the SilD10 surfaces. This becomes even more evident when the alignment criteria that Clark et al.[21] suggested, are applied on the data plotted in Figure 10. These investigators defined a population of cells as highly aligned when the long axis of these cells makes an angle of <10° with the direction of the grooves. Review of the data in Figure 10 shows that the cells on the SilD02 substrata, and occasionally on the SilD05 surfaces, have an orientation which lies between 0° and 10°. Therefore, these cells have to be considered as highly aligned. These observations support the findings of other studies[12, 16, 18-19, 22], which conclude that surface features in the range of 1.0-5.0 μm have a high capability to induce cell guidance. Furthermore, it has to be noted that these findings were based on the result of a semi-automatic analysis procedure, which eliminates possible bias that could be present with an optical method as used by Clark et al.[21]. At this point, it is also appropriate to mention that the incubation period in our study ranged from 1 to 7 days, which is longer than in other studies. The significance of this prolonged incubation has been proven by the fact that all the data show that after 7 days the influence of the microtextured surfaces on

cellular behaviour decreases. This reduction might be caused by the formation of cell-cell contacts[23]. Consequently, it can be supposed that the observed guidance phenomenon is an initial response of cells to certain microtextured surfaces, which is gradually lost after prolonged incubation. Still, it should also be noted that the process of wound healing is a multi-factorial process in which many cell types and activation mechanisms play a role. This makes it difficult to apply the results of *in vitro* studies to *in vivo* studies. Therefore, the possible consequence of our finding for the final clinical use of surface micro geometry in the design of implants can only be questioned and has to be investigated in *in vivo* studies.

Comparison of our results with other studies[4, 7-8, 17, 21-22, 24-26] demonstrates that in most studies substrata were used with grooves of at least 1.0 μm deep, and not 0.45 μm. Despite this difference a similar influence on cellular alignment was found. This proves that the behaviour of RDFs can already be influenced by very shallow grooves. Unfortunately, no comparable numerical data are available from the other studies. This makes it impossible to investigate the existence of quantitative differences concerning the effect of the groove depth on the cellular interactions.

Our study confirmed the influence of surface microgeometry on fibroblast behaviour. The mechanisms of this phenomenon however, still remains unknown. As hypothesized by Meyle et al.[25], it is possible that the strong induction of contact guidance by 2.0, and to a lesser extent by 5.0 μm grooves, indicates at the need of cells for mechanical stabilization against interfacial motion and improved initial cell adhesion purely by mechanical interlocking. Another explanation could be that the orientation and alignment of cells on microtextured surfaces are a part of the cellular efforts to reach a biomechanical equilibrium with the net sum of forces minimized[27-28]. It is possible that the anisotropic geometry of the grooves and ridges establishes stresses and shear-free planes that influence the direction of microtubule growth[26] in order to create a force economic situation. Although economic force management is a common matter in nature, it does not explain the differences in susceptibility to topographical guidance that are found between different cell types[21]. This might be caused by functional differences between the cells in an *in vivo* situation, which can result in a difference in cytoskeleton organization[21]. This hypothesis needs to be investigated thoroughly in view of the recent findings which suggest that the altered cell-substratum interactions can be based on the resemblance of these surfaces with the topography of fibrillar extracellular matrix[23].

ACKNOWLEDGEMENT

This study is supported by the Technology Foundation (STW).

REFERENCES

1. Harrison RG. The cultivation of tissues in extraneous media as a method of morphogenetic study. *Anat Rec* 1912; **6:** 181-193

2. Loeb L, Fleisher MS. On the factors which determine the movements of tissues in culture media. *J Med Res* 1917; **37:** 75-99

3. Weiss P. Experiments on cell and axon orientation in vitro: the role of colloidal exudates in tissue organization. *J Exp Zool* 1945; **100:** 353-386

4. Rovensky YA, Slavnaya IL, Vasiliev JM. Behaviour of fibroblast-like cells on grooved surfaces. *Exp Cell Res* 1971; **65:** 193-201

5. Rovensky YA, Slavnaya IL. Spreading of fibroblast-like cells on grooved surfaces. *Exp Cell Res* 1974; **84:** 199-206

6. Maroudas NG. Growth of fibroblasts on linear and planar anchorages of limiting dimensions. *Exp Cell Res* 1973; **81:** 104-110

7. Maroudas NG. Anchorage dependence: correlation between amount of growth and diameter of bead, for single cells grown on individual glass beads. *Exp Cell Res* 1974; **74:** 337-342

8. Singhvi R, Stephanopoulos G, Wang DIC. Review: effects of substratum morphology on cell physiology. *Biotechology and Bioengineering* 1994; **43:** 764-771

9. Brunette DM, Kenner GS, Gould TRL. Grooved titanium surfaces orient growth and migration of cells from human gingival explants. *J Dent Res*, 1983; **62:** 1045-1048

10. Brunette DM. The effects of implant surface topography on the behavior of cells. *Int J Oral Maxillofac Implants*, 1988; **3:** 231-246

11. Campbell CE, von Recum AF. Microtopography and soft tissue response. *J Invest Surg*, 1989; **2:** 51-74

12. den Braber ET, de Ruijter JE, Smits HTJ, Ginsel LA, von Recum AF, Jansen JA. Effect of parallel surface micro grooves and surface energy on cell growth. *J Biomed Mater Res*, 1995; **29**: 511-518

13. Schmidt JA, von Recum AF. Texturing of polymer surfaces at the cellular level. *Biomaterials* 1991; **2:** 385-389

14. Schmidt JA, von Recum AF. Macrophage response to microtextured silicone. *Biomaterials* 1992; **13:** 1059-1061

15. Freshney RI. Culture of animal cells; a manual of basic technique, Alan R. Liss Inc., New York, 1987

16. Green AM, Jansen JA, von Recum AF The fibroblast response to microtextured silicone surfaces: texture orientation into or out of the surface *J Biomed Mater Res*, 1994; **28:** 647-653

17. Ricci JL, Charvet J, Chang R et al. In vitro effects of surface microgeometry on colony formation by fibroblasts and bone cells. *20th Annual Meeting of the Society for Biomaterials*, Boston, USA, April 5-9, 1994: 401

18. den Braber ET, de Ruijter JE, Smits HTJ, Ginsel LA, von Recum AF, Jansen JA. Effect of surface microgeometry and surface tension on cell growth. *20th Annual Meeting of the Society for Biomaterials*, Boston, USA, April 5-9, 1994: 170

19. den Braber ET, de Ruijter JE, Smits HTJ, Ginsel LA, von Recum AF, Jansen JA. Effect of parallel surface micro grooves and surface energy on cell growth. *11th European Conference on Biomaterials*, Pisa, Italy, September 10-14, 1994: 231-234

20. Singhvi R, Stephanopoulos G, Wang DIC. Effect of substratum morphology on animal cell adhesion and behavior. *Mater Res Soc Symp Proc*, 1992; **252:** 237-245

21. Clark P, Connolly P, Curtis ASG, Dow JAT, Wilkinson CDW. Topgraphical control of cell behaviour: II. multiple grooved substrata. *Development*, 1990; **108:** 635-644

22. Meyle J, Gültig K, Wolburg H, von Recum AF. Fibroblast anchorage to microtextured surfaces. *J Biomed Mater Res*, 1993; **27:** 1553-1557

23. Clark P, Connolly P, Curtis ASG, Dow JAT, Wilkinson CDW. Cell guidance by ultrafine topography in vitro. *J Cell Sci*, 1991, **99:** 73-77

24. Curtis ASG, Clark P. The effects of topographic and mechanical properties of materials on cell behaviour. *Critical Reviews in Biocompatibility*, 1990; **5:** 343-362

25. Meyle J, von Recum AF, Gibbesch B, Hüttemann W, Schlagenhauf U, Schulte W. Fibroblast shape conformation to surface micromorphology. *J Applied Biomat*, 1991; **2:** 273-276

26. Oakley C, Brunette DM. The sequence of alignment of microtubules, focal contacts and actin filaments in fibroblasts spreading on smooth and grooved titanium substrata. *J Cell Sci*, 1993; **106:** 343-354

27. Ingber DE. Cellular tensegrity; defining new rules of biological design that govern the cytoskeleton. *J Cell Sci*, 1993; **104:** 613-927

28. Ward MD, Hammer DA. A theoretical analysis for the effect of focal contact formation on cell-substrate attachment strength. *Biophys J*, 1993; **64:** 936-959

CHAPTER 4

Quantitative analysis of fibroblast morphology on microgrooved surfaces with various groove and ridge dimensions

E.T. den Braber[1], J.E. de Ruijter[1],
L.A. Ginsel[2], A.F. von Recum[3], and J.A. Jansen[1]

[1]University of Nijmegen, Dental School, Laboratory for Biomaterials,
POB 9101, NL-6500 HB Nijmegen, The Netherlands.
[2]University of Nijmegen, Faculty of Medical Sciences, Department of Cell Biology and Histology,
POB 9101, NL-6500 HB Nijmegen, The Netherlands.
[3]Clemson University, Department of Bioengineering, College of Engineering and Science,
301 Rhodes Research Center, Clemson SC 29634-0905, USA.

CHAPTER 4

Quantitative analysis of fibroblast morphology on microgrooved surfaces with various groove and ridge dimensions

INTRODUCTION

The field of biomaterials is slowly changing. Although biocompatibility is still defined as the ability of a material to perform with an appropriate host response in a specific application[1], recent research has shown that various physicochemical and geometrical material surface properties can be used to modulate the accompanying host response[2-5]. This makes it possible to engineer future biomaterials that provoke a specific biological response, resulting in an unique healing process. Physicochemical properties that have an effect on tissue behaviour are surface charge, surface energy, and surface oxidation[5-6]. Geometrical surface properties that can influence cellular interactions are shape, size, and topography of a surface. The latter is not only limited to surface conditions like roughness or curvature, but also includes microtextured surfaces with a standardized surface roughness. For example, in vitro experiments have already demonstrated that surfaces possessing micro grooves induce orientation of fibroblasts[3, 6-7]. This phenomenon is also known as "contact guidance"[8]. In two previous studies[6-7], we reported that especially surfaces with a 2.0 μm groove - 2.0 μm ridge configuration were able to induce strong orientation and elongation of the fibroblasts cultured on these substrata. Surfaces with 10.0 μm grooves and ridges however, did not orientate the cells. All the grooves in those experiments were 0.45 μm deep. Furthermore, we found that the proliferation rate of the rat dermal fibroblasts cultured on the microtextured surfaces was changed by the wettability of the surface[6], but not by the different micro events on the substratum surface[6-7].

Although the influence of microtextured surfaces on the cellular behaviour is evident, very little is known about the fundamentals and basic mechanisms of this phenomenon. Several hypotheses have been proposed to explain this specific cellular behaviour. Some investigators suggest that the fibroblasts not only orientate, but also conform to the topography of the biomaterial surface, thus leading to mechanical interlocking[9]. Others[6-7, 10-11] argue that cells on microtextured surfaces are able to rearrange their architecture in a three dimensional orientation to establish an equilibrium of internal and external forces. This could result in a relaxed cytoarchitecture, which favours cellular differentiation.

Considering these theories, it can be questioned whether cells react in a comparable way to surfaces with different geometrical compositions. By varying the groove width, ridge width, and groove depth of a standardized parallel groove pattern separately, it will be possible to determine which of these features induces the observed contact guidance. Furthermore, it will be possible to evaluate the impact and importance of the dimensional changes of specific surfaces features on the cellular behaviour. Therefore, the aim of this study was to quantify the possible changes in fibroblast morphology and orientation after culturing these cells on micro grooved surfaces with various dimensional configurations.

TABLE I
Dimensions of the micro features on the substrata surfaces (Gd=groove depth, Gw=groove width, Rw=ridge width, and P=pitch).

Surface	*Gd (μm)*	*Gw (μm)*	*Rw (μm)*	*P (μm)*
A	----	----	----	----
B	1.00	1.00	1.00	2.00
C	1.00	1.00	2.00	3.00
D	1.00	1.00	4.00	5.00
E	1.00	1.00	8.00	9.00
F	1.00	4.00	1.00	5.00
G	1.00	8.00	1.00	9.00
H	0.45	2.00	2.00	4.00
J	0.45	5.00	5.00	10.00
K	0.45	10.00	10.00	20.00
CTRL	----	----	----	----

MATERIALS AND METHODS

The substrata

The experimental substrata were produced as described earlier[3, 6, 12-13]. Briefly, photolithography was used to produce a total of 10 different textured silicon oxide wafers with different surface configurations (Table I).

In order to obtain the final experimental substrata, the smooth and grooved silicon oxide wafers were used as moulds, and covered with polydimethylsiloxane (silicone elastomer MDX 4-4210, Dow Corning) to produce a surface replica. After polymerization, the silicone rubber castings were peeled off the moulds and cut into small round discs of 175 mm^2. These substrata were then washed manually in a 10% Liquinox solution (Alconox Inc.), rinsed, cleaned ultrasonically for 30 minutes in a 1% Liquinox solution, and given two 15 minute ultrasonic rinses in distilled, deionized water. Subsequently, they were given a Soxhlet rinse for 12 hours in distilled, deionized water. Finally, the substrata were air-dried and prepared for cell culture purposes by radio frequency glow discharge (RFGD) treatment (PDC-3XG, Harrick; Argon, 0.15 Torr, 5 minutes). After RFGD treatment, the quality and dimensions of the micro features on the substrata were confirmed by scanning electron microscopy (SEM; JEOL 6310) and confocal laser scanning microscopy (CLSM; Zeiss LSM 410).

Cell culture

Rat dermal fibroblasts (RDFs) were isolated from ventral skin grafts, taken from male Wistar rats, 40 to 43 days of age (100-120 gram). After dissociation, these cells were incubated (37°C, 5% CO_2-95% air) in α-MEM with Earl's Salts and with L-glutamine (Gibco), supplemented with 10% (v/v) heat treated fetal calf serum (Gibco), 2.5 μg ml^{-1} amphotericin B (Gibco) and 50 μg ml^{-1} gentamicin (Gibco). After approximately 3 days of culturing the RDFs were rinsed with phosphate buffered saline without magnesium and calcium (PBS Dulbeco; pH 7.2), supplemented with 5 μg ml^{-1} amphotericin B and 100 μg ml^{-1} gentamicin to remove non-attached cells. Subsequently, the growth medium was added and replaced every two days by fresh growth medium. Upon confluence, the RDFs were detached by trypsinization [0.25% (w/v) crude trypsin and 1 mM EDTA (pH 7.2)] and resuspended at a lower cell concentration in fresh growth medium. After identifying the cells as fibroblasts by phase contrast morphology analysis[14], the fifth generation of these cells was used for all experiments.

Substrata with a smooth or microtextured surface were placed in the culture wells of 24 well plates (Greiner). After positioning the substrata, the surface grooves were examined with phase contrast micro-

scope (Leitz DMIL). Subsequently, approximately 1.0 x10^4 viable RDFs ml^{-1}, suspended in sterile growth medium, were added to each substratum. RDFs cultured in wells containing no substratum served as a control group (CTRL). The cells were incubated on a specific substratum for 5 days (37°C, 5% CO_2-95% air) under static conditions. Growth medium was changed every two days. Every substratum configuration was tested in quadruplicate.

Digital Image Analysis (DIA)

The effect of the surface microgeometry on the cellular morphology was quantified by digital image analysis (DIA) as described earlier by den Braber et al.[7]. In short, RDFs of six evaluation areas were photographed by phase contrast microscopy during incubation on day 1, 2, 3, 4 and 5. The evaluation areas were selected by dividing the substratum surface in 740 possible fields of observation of 584.4 μm x 412.5 μm. Each of these fields was given a number, which was entered in a randomization program. Thus, a total of 4 randomly selected evaluation areas and the field at the centre of each substratum were photographed. Registration of the coordinates of these areas assured that the same areas were observed and photographed during the entire period of incubation.

The phase contrast photographs were scanned digitally (400 dpi x 400 dpi) and analyzed with an Acorn R260 computer (RiSC processor), the ArcImage 5 for the HAWK V12 frame grabber software package (Foster Findlay Associates, UK) and additional self programmed software. In-house written routines were used to trace all RDFs in each digital phase contrast image and to prepare the resulting data for image analysis with the ArcImage software package. The ArcImage program measured several cell parameters, i.e. the cellular surface area, cellular perimeter, cellular circularity, maximum cell length, cell breadth perpendicular to the maximum length, the angle of cellular orientation relative to the

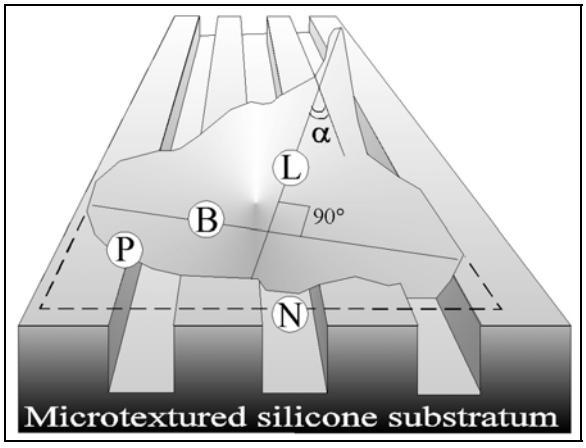

Figure 1 Schematic representation of a RDF on a microtextured substratum. The parameters measured during DIA were the RDF surface area (white area within perimeter), the longest length of the cell (L), the cellular breadth (B), perimeter (P), circularity (not shown), angle of cellular orientation (α), and the number of pitches spanned by the cell (N).

surface grooves, and number of pitches spanned by a single cell. A schematic representation of these parameters, with the exception of the parameter circularity, can be

$$Circularity = \frac{4\pi(Area)}{(Perimeter)^2}$$

found in Figure 1. This parameter is defined as

resulting in a number between 0 and 1. If this equation equals 0, the cell has a perfect linear shape, but when circularity is 1, the cell is shaped as a perfect circle.

After gathering the numerical DIA data, these parameters were analyzed using univariate, multiple regression, and the nonparametric Kruskal-Wallis models (SAS, release 6.03, SAS Institute Inc., USA).

RESULTS

Surface characterization

SEM investigations showed that the parallel grooved surfaces had no defects or irregularities.

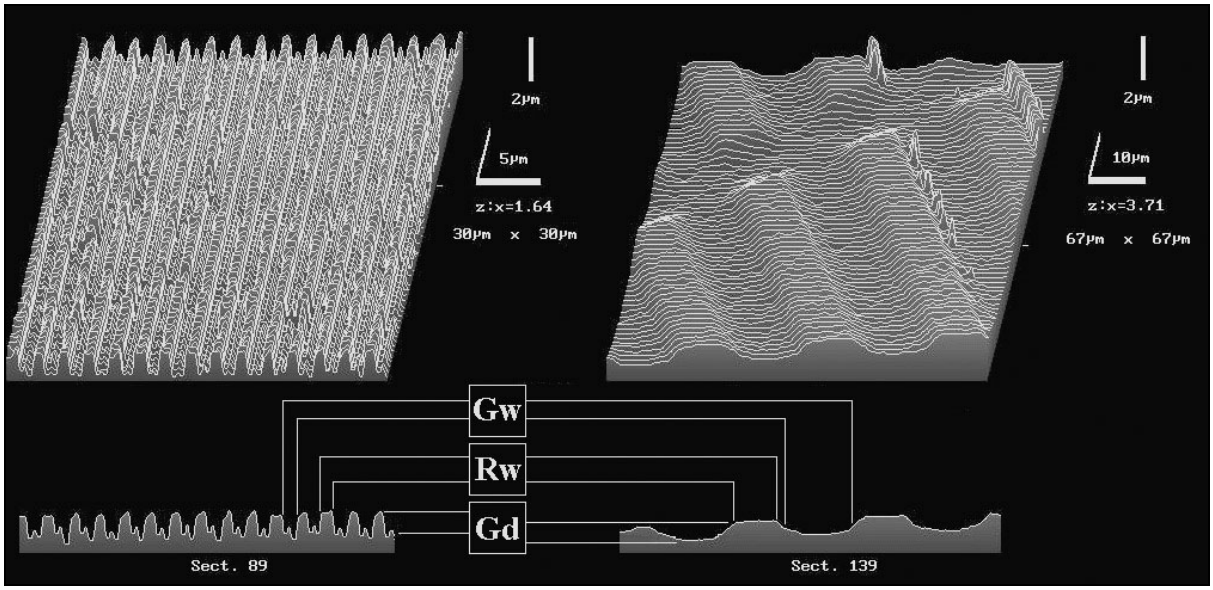

Figure 2 Results of the CLSM surface analysis of a B (left) and a K (right) substratum. Three dimensional surface representations are given, which are composed out of 256 optical Z sections. Right of the 3D surface profiles, the size of the scanned area (30 µm² and 67 µm² respectively) and difference in X vs. Z axis enlargement can be found (1:1.64 and 1:3.71). The codes accompanying the Z sections at the bottom represent the groove width (Gw), the ridge width (Rw), and the groove depth (Gd).

CLSM measurements demonstrated that the dimensions of the features on the substrata surfaces were well within tolerance levels (Figure 2). The dimensions of the specific micro features can be found in Table I. In addition, the optical Z sections showed that the walls of the grooves on the H, J, and K substrata were not as steep as on the other microtextured substrata. Also some small light diffraction peaks were observed on all the substrata. These artifacts were most prominent on the K substrata (Figure 2).

Digital Image Analysis (DIA)

Figures 3 to 7 show representative phase contrast images of the RDFs cultured on a smooth substrata and surfaces with different groove configurations. Figure 3 shows RDFs on a smooth (A) substratum surface. These cells were well spread, multipolar, orientated

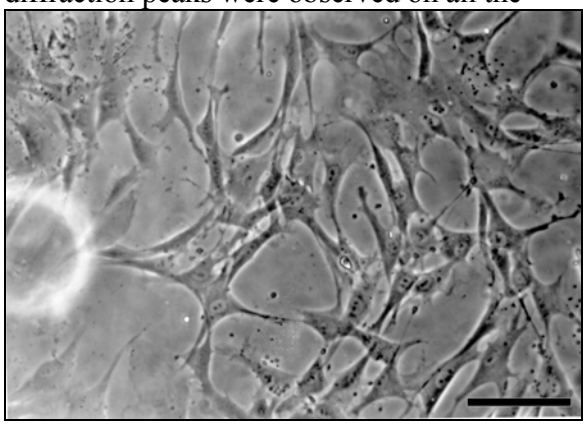

Figure 3 Phase contrast image of RDFs on a smooth substratum (A) after 2 days of incubation (bar=100µm). The cells are well spread and randomly orientated.

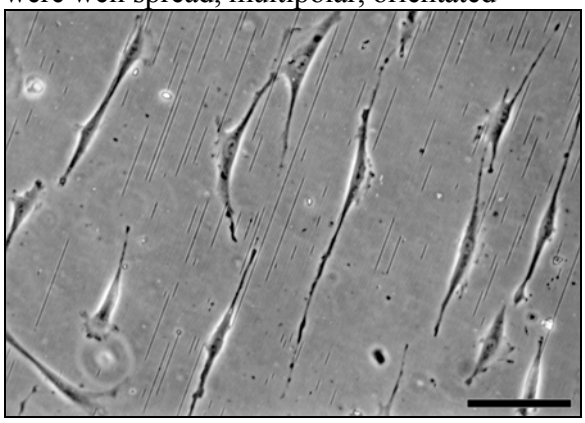

Figure 4 Phase contrast image of RDFs on a B substratum (Gw 1.0 µm, Rw 1.0 µm, Gd 1.0 µm, bar=100 µm) on day 1. The cells are highly aligned and elongated along the surface grooves.

randomly, and showed a morphology similar to the RDFs on the CTRL surfaces (data not shown). Fibroblasts on the grooved substrata showed a wide variety of shapes and angles of orientation relative to the surface grooves. For example, the cells on the B and C substrata appeared to be orientated strongly to the surface grooves. Most of these RDFs had a highly elongated spindle shape. RDFs on the F, G, and H substrata however, appeared to be orientated along the surface grooves, although these cells were not elongated as highly as those on the B and C surfaces. In contrast, the cellular orientation of the cells on the D, E, J, and K surfaces was less clear. Especially orientation of the RDFs on the E, J, and K substrata did not seem to be affected by the micro features on the substratum surface, while the cells on the D surface appeared to be orientated slightly by the grooves. The shape of the fibroblasts on these last substrata was quite diverse. Spindle shaped, elongated cells could be seen, but spread, multipolar fibroblasts were also present. Finally, careful examination of the phase contrast images also showed that the cells on the textured surfaces seemed to attach to the ridges of the micropattern. This is best demonstrated by the photographs of the RDFs on the G and H substrata (Figures 6 and 7). These cells possess several protrusions that end on the (darker coloured) ridges that are situated between grooves (Figure 2).

In order to quantify the DIA parameters (Figure 1), a total of 5217 cells were traced and evaluated. The quantitative analyses proved that the surface area of the RDFs on the B,C, and F substrata were significantly smaller ($0.0001 \leq p \leq 0.0449$) than the cells on the A, E, or CTRL surfaces (Figure 8). RDFs on the D, G, H, J, and K substrata did not show a clear difference in surface area, compared to the cells on the surfaces mentioned earlier. For example, the surface area of the RDFs on the G substrata was signifi cantly smaller ($0.0001 \leq p \leq 0.0127$)

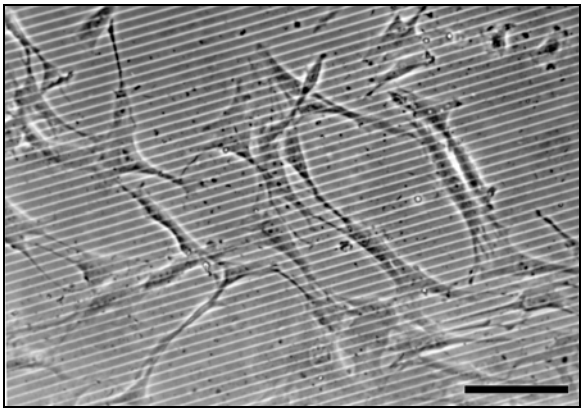

Figure 5 Phase contrast image of RDFs on an E substratum (Gw 1.0 μm, Rw 8.0 μm, Gd 1.0 μm, bar=100 μm) on day 2. Spreading and orientation are random.

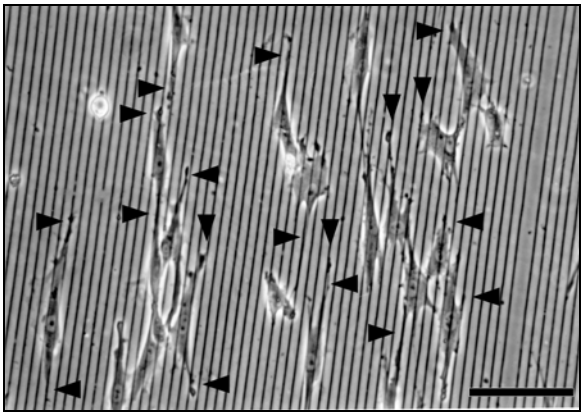

Figure 6 Phase contrast image of RDFs on a G substratum (Gw 8.0 μm, Rw 1.0 μm, Gd 1.0 μm, bar=100 μm) on day 1. These substrata are a negative replica of the E substrata (Figure 5). Although the cells are not as elongated as on the B (Figure 4) substrata, they are clearly orientated. Cell protrusions attach to the ridges (➢ ➢).

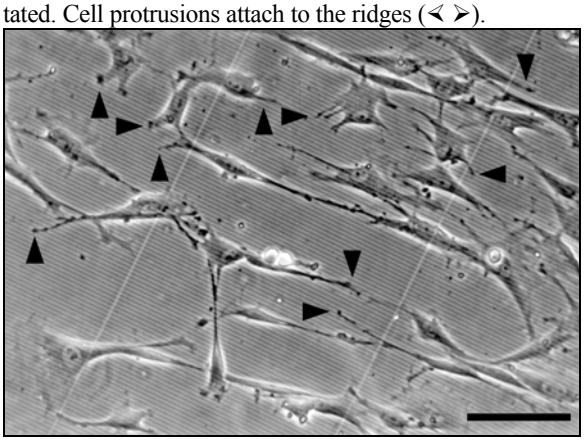

Figure 7 Phase contrast image of RDFs on an H substratum (Gw 2.0 μm, Rw 2.0 μm, Gd 0.45 μm, bar=100 μm) on day 1. Elongated, orientated RDFs can be seen, although Gd is smaller than on the B-G substrata. Ridge contacting cell protrusions can be seen (➢ ➢).

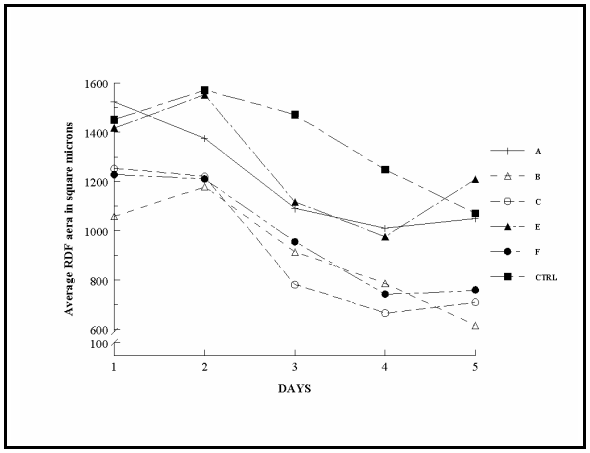

Figure 8 Average RDF surface area on the various surfaces in square microns. The area of RDFs on the B, C, and F substrata is significantly smaller compared to the area of the A, E, and CTRL surfaces (0.001≤p≤0.0449).

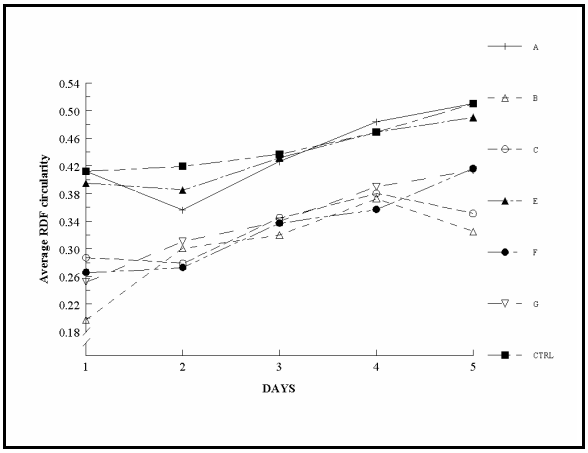

Figure 10 Average circularity of the RDFs on the various surfaces. The cells on the A, E, and CTRL surfaces are rounder than the RDFs on the B, C, F, and G substrata (0.0001≤p≤0.0469).

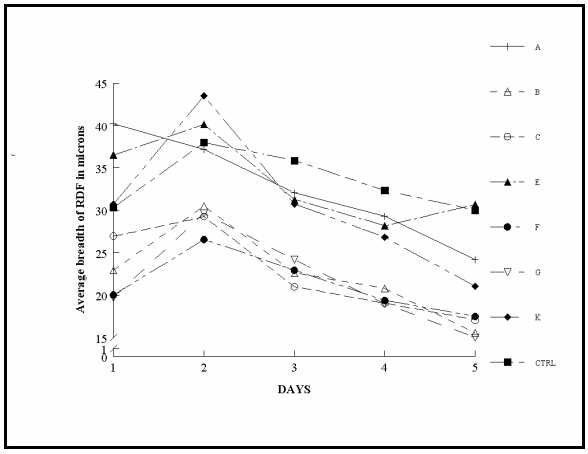

Figure 9 Average cell breadth of the RDFs on the various surfaces. The breadth of the RDFs on the B, C, F, and G substrata is significantly smaller than the breadth of the cells on the A, E, K, and CTRL surfaces (0.0001≤p≤0.0117).

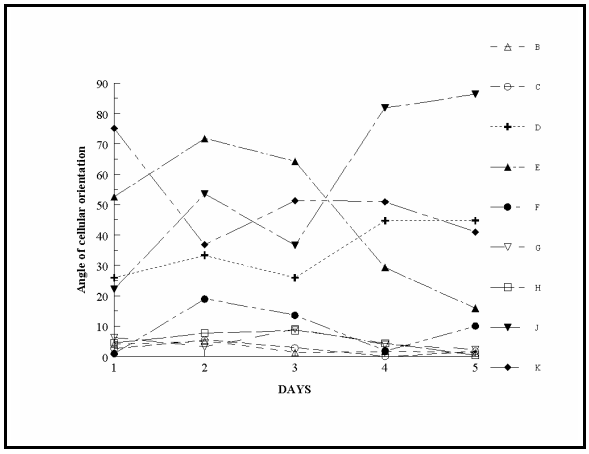

Figure 11 Average angle of RDF orientation relative to the surface grooves. Especially the RDFs on the B, C, G, and H substrata are orientated along the surface grooves (≤ 10°). The RDFs on the F substrata are not orientated as strongly as the cells on these surfaces. The cells on the D, E, J, and K substrata clearly have a cellular orientation of ≥ 10°.

on day 1 to 3 than the area of the cells on the A, E, and CTRL surfaces. The area of the cells on the G, and the B and C substrata did not differ significantly. However, on day 4 and 5 the opposite was found, since the area of the RDFs on the G, B, and C substrata did differ significantly, (0.0001≤p≤0.0263), while the cells on the G, A, E, and CTRL substrata did not.

Concerning the measured perimeter and (maximum) length of the RDFs (Figure 1) no continuous, strong significant differences were found (data not shown). For the parameter breadth however (Figure 9), it was found that the cell breadth of the RDFs on the B, C, F, and G substrata was significantly smaller (0.001≤p≤0.0117) than the breadth of the cells on the A, E, K, and CTRL surfaces. The plots

representing the breadth of the cells on the D, H, and J substrata (not shown) were positioned in an area between the cell breadth plots of the A, E, K, and CTRL surfaces and the B,C, F, and G substrata (Figure 9). The breadth of these cells did not differ significantly from the cell breadth plots of the upper (A, E, K, CTRL) or the lower margin (B, C, F, G).

Analysis of the RDF circularity (Figure 10) showed that the cells on the A, E, and CTRL surfaces were significantly rounder than the cells on the B, C, F, and G substrata ($0.001 \leq p \leq 0.0469$). The plots of the fibroblasts on the D, H, J, and K substrata (not shown) could be found in the area between these plots, with the A, E, and CTRL plots marking the upper margin,and the B, C, F, and G plots representing the lower margin of this area.

DIA also calculated the angle of cellular orientation relative to the surface grooves (α; Figure 1). The results of these computations (Figure 11) showed that the cells on the B, C, G, and H substrata were significantly stronger orientated ($0.001 \leq p \leq 0.0466$) along the surface grooves than the fibroblasts on the D, E, F, J, and K substrata.Orientation of the RDFs on the F substrata was more complex. On day 1, 3 and 4 the cellular orientation of these cells was not significantly different compared to the orientation of the RDFs on the B, C, G, and H substrata ($p \geq 0.1213$). On the other hand, the orientation of these cells did differ significantly from the orientation of the RDFs on the D, E, J, and K substrata on day 1, 2, 4, and 5 ($0.001 \leq p \leq 0.0122$).

The phase contrast images in Figure 3 to 7 also show that the RDFs were able to span several grooves and ridges on the textured surfaces. DIA counted the number of pitches spanned by a single cell. On day 1 for example, the RDFs on the B, C, D, E, F, G, H, J, and K substrata spanned 15.51, 12.66, 6.80, 3.94, 10.36, 1.16, 5.15, 2.30, and 1.89 pitches respectively. Additionally, the average

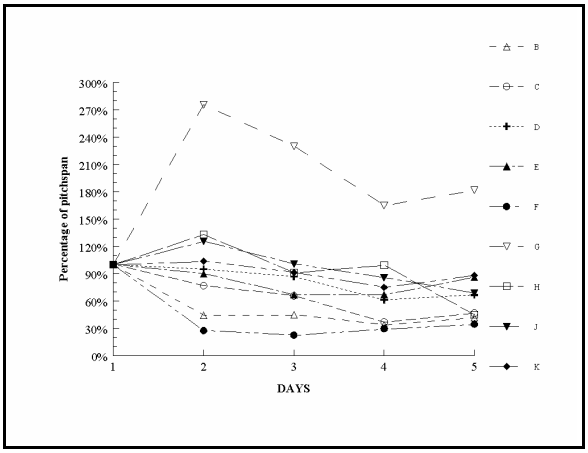

Figure 12 Percentage of RDF pitch span. The total number of pitches spanned on day 1 is defined as 100%. The number of pitches spanned by the RDFs is lower on the B and F surfaces than on the C, D, E, G, H, J, and K substrata. This is only significant for the cells on the F substrata up to day 3 ($0.0001 \leq p \leq 0.0369$).

number of pitches that were spanned by a single RDF on day 1 was defined as 100 percent, thus making comparison between the different textured surfaces possible. The results of these calculations are shown in Figure 12. Although this graph suggests that the number of pitches spanned by the RDFs is lower on the B and F surfaces than on the C, D, E, G, H, J, and K substrata, statistical evaluation proved that this difference was only significant for the cells on the F substrata up to day 3 ($0.0001 \leq p \leq 0.0369$). Furthermore, Figure 12 shows that pitches spanned by the RDFs on the G substrata increases on day 2 and remains on a high level. Since the patterns on the D and F substrata, and the E and G substrata were a direct negative replica of each other (Table I), direct statistical testing without a conversion to percentile values was possible. These evaluations showed that up to day 4 the pitch span of the RDFs on the F substrata was significantly lower ($0.0001 \leq p_{day\ 1\text{-}4} \leq 0.0004$) than on the D surfaces. Furthermore, this procedure showed that the pitch span by the cells was significantly lower ($0.0001 \leq p_{day\ 1\text{-}5} \leq 0.0122$) on the E substrata than on the G surfaces.

CHAPTER 4

DISCUSSION AND CONCLUSIONS

Results of this study confirm our earlier findings[6-7] that a microtextured surface can induce orientation of the RDFs cultured on these surfaces. DIA and statistical analysis demonstrate that the degree of cellular orientation relates to the dimensions of the micro features on the surface. This becomes even more evident when the alignment criteria that Clark et al.[15] suggested, are applied on the data plotted in Figure 11. These investigators defined a population of cells as highly aligned when the long axis of these cells makes an angle of <10° with the direction of the grooves. Review of the data in Figure 11, shows that the cells on the B, C, G, and H substrata, and occasionally on the F surfaces, have an orientation which lies between 0° and 10°. Therefore, these cells have to be considered as highly aligned.

Further review of the DIA results concerning RDF size and shape shows that cells cultured on surfaces with small grooves and especially small ridges like the B, C, and F substrata, have a significant smaller surface area and cell breadth, while no differences were found in cellular perimeter and length. These findings are supported by the measured parameter circularity, which shows that cells cultured on finely grooved surfaces are less circular than RDFs cultured on smooth surfaces. The correlation between these results is quite clear. Since more circular cells possess a cell breadth that is equal or almost equal to the maximum cell length, their area will be larger than the area of the elongated cells which possess a smaller cell breadth. This suggests that the elongated cells on microtextured surfaces change their size by reducing their cell breadth. Although these results are rather straightforward, it is important to note that phase contrast microscopy is a method that results in a two dimensional picture, not giving any information about the volume of the cell. Therefore, it is possible that the elongated RDFs are not as flat as the circular cells. This information could be important in determining whether the elongated cells reduce their size, or just change their shape. Size change would mean that the RDFs cultured on microtextured surfaces would actually have a smaller cell volume, where shape change suggests altered cell dimensions by an uniform cell volume. Recent reports by other authors[16] suggest that optical sectioning with a confocal laser scanning microscope (CLSM) could provide more information on this subject, i.e. cell volume.

Evaluation of the data retrieved during this study also clearly indicates that the width of the ridge is mainly responsible for the contact guidance of the RDFs on the microtextured surfaces. This corroborates the findings of Dunn et al.[17], Green et al.[18], and is supported by the following results of this study. First, the data plotted in Figure 11 shows that the average angle of cellular orientation (α) of RDFs cultured on the B, C, F, G, and H substrata is $\leq 10°$. The micropatterns on these substrata surfaces possess a ridge width of 1.0, 2.0, 1.0, 1.0 and 2.0 μm respectively, but have different groove width and depth. However, if the ridge is ≥ 4.0 μm, as with the D, E, J, and K surfaces (Figure 11), α results in an angle larger than 10°, even when the groove width and/or groove depth are identical to these dimensions on the "orientating" substrata (Table I). Slight orientation ($10° < \alpha < 45°$) can be found with the RDFs on the D substrata which possess a ridge width of 4.0 μm. In contrast with this, the cellular orientation on the surfaces with larger ridges like the E, J, and K substrata is random, which can be deduced from the fact that $\alpha \approx 45°$. Second, Figure 11 also demonstrates that the surface parameters groove width and groove depth are considerably less important for RDF orientation than the parameter ridge width. The data plotted in this graph shows that the RDFs on the B, C, F, G, and H substrata are orientated closely along the surface grooves, although the groove width measures 1, 2, 4, 8, and 2 μm

respectively. The same principle applies to the groove depth. Although the H substrata possess grooves of only 0.45 μm deep, no significant differences in RDF orientation were observed, when compared to the B, C, F, and G surfaces with 1.0 μm deep grooves. This is in accordance with reports by Dunn et al.[17], but differs from results published by Clark et al.[15-19], who concluded that groove depth is the most important dimension of parallel grooved substrata influencing the orientation of cells. However, Curtis and Clark[20] also concluded that these effects vary from one cell type to the other. Third, the phase contrast images show that RDFs probably attach specifically to the ridges of the surface pattern. This is particularly clear with the RDFs on the G (Figure 6) and H substrata (Figure 7). Careful examination of these photographs reveals that the RDFs on these substrata possess cell protrusions that end on, and seem to attach to the ridges. These possible attachments to the ridges could be associated with surface free energy changes caused by the manufactured, standardized roughness of the substratum surface[21-22]. If the surface energy is more preferable on the ridges, the deposition pattern of the substratum bound attachment proteins will be influenced[23-25]. This could result in the formation of cell-substratum bound contacts primarily on the ridges of the surface micropatterns. The significance of this finding is that surface free energy differences are produced on one and the same material by changing the surface topography. The surface free energy differences in the work of others[23-25] was achieved by differing the surface chemistry. Consequently, the effect of surface free energy and surface chemistry was separated here. This hypothesis is supported by the work of Meyle et al.[3], who reported numerous focal adhesion sites on the cellular periphery of gingival fibroblasts which were cultured on silicone surfaces with parallel surface micro grooves.

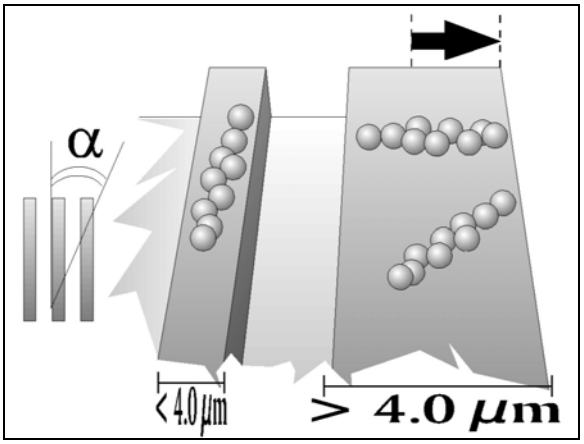

Figure 13 Schematic drawing showing that, on a ridge < 4.0 μm, a linear focal adhesion plaque can orientate only parallel to the surface groove/ridge. Hence, 0°<α<10°. However, if the ridge width >4.0 μm, the possible angles of orientation (α) increases, resulting in a random cellular orientation (α≈45°).

After producing a reflection contrast/fluorescence image by dual channel CLSM, it could be seen that the vinculin positive attachment sites were located on the ridges of the silicone microtextured substratum. Furthermore, Ohara and Buck[26] suggested that focal adhesion plaques are linear structures of 0.25-0.5 μm wide and 2.0-10.0 μm long. Since the geometrical dimensions of these plaques are so specific, only one major orientation of attachment is possible, which is parallel to the surface grooves and ridges (Figure 13). Accordingly, a cell attaching to a microtextured surface with small ridges will orientate itself parallel to these ridges. Still, it has to be noted that our results show a decrease of RDF orientation on substrata with a ridge size of ≥ 4.0 μm. This could be explained by the observation of Izzard and Lochner[27], that there is a possible minium length of 2.0 μm required for focal contacts to provide adhesion. Therefore, if the ridge width increases, the possible orientation of adhesion plaque attachment can increase, thus resulting in cell attachment with a larger angle of cellular orientation (Figure 13). Finally, reviewing the results of this study, it can not

be excluded that the observed cell-substratum interactions are based on the resemblance of these microtextured surfaces with the topography of the fibrillar extracellular matrix[28], causing the cell to transform and differentiate[5]. If this proves to be true, it is clear that these surfaces could contribute to the process of wound healing around implants surfaces.

ACKNOWLEDGEMENT

The help of F.A. Scholl (Carl Zeiss, The Netherlands) on the CLSM substratum surface analysis is greatly appreciated. The authors also would like to thank dr. J. Meyle for the donation of microtextured substrata produced in his laboratories. This study was supported by the Technology Foundation (STW).

REFERENCES

1. Definitions in biomaterials: Progress in biomedical engineering; 4, ed. D.F. Williams. Elsevier Science Publishers B.V., Amsterdam, 1987 pp 67

2. Ratner BD. New ideas in biomaterials science-a path to engineered biomaterials. *J Biomed Mater Res*, 1993; **27:** 837-850

3. Meyle J, Gültig K, Brich M, Hämmerle H, Nisch W. Contact guidance of fibroblasts on biomaterial surfaces. *J Mater Sci*, 1994; **5:** 463-466

4. Campbell CE, von Recum AF. Microtopography and soft tissue response. *J Invest Surg*, 1989; **2:** 51-74

5. Singhvi R, Stephanopoulos G, Wang DIC. Review: effects of substratum morphology on cell physiology. *Biotechology and Bioengineering* 1994; **43:** 764-771

6. den Braber ET, de Ruijter JE, Smits HTJ, Ginsel LA, von Recum AF, Jansen JA. Effect of parallel surface micro grooves and surface energy on cell growth. *J Biomed Mater Res*, 1995; **29:** 511-518

7. den Braber ET, de Ruijter JE, Smits HTJ, Ginsel LA, von Recum AF, Jansen JA. Quantitative analysis of cell proliferation and orientation on substrata with uniform parallel surface micro grooves. *Biomaterials*, 1996; **17:** 1093-1099

8. Weiss P. Experiments on cell and axon orientation in vitro: the role of colloidal exudates in tissue organization. *J Exp Zool* 1945; **100:** 353-386

9. Meyle J, von Recum AF, Gibbesch B, Hüttemann W, Schlagenhauf U, Schulte W. Fibroblast shape conformation to surface micromorphology. *J Applied Biomat*, 1991; **2:** 273-276

10. Ingber DE. Cellular tensegrity; defining new rules of biological design that govern the cytoskeleton. *J Cell Sci*, 1993; **104:** 613-927

11. Hohn HP, Steih U, Denker HW. A novel artifical substrate for cell culture: effects of substrate flexibility/malleability on cell growth and morphology. *In Vitro Cell Dev Biol*, 1995; **31A:** 37-44

12. Schmidt JA, von Recum AF. Texturing of polymer surfaces at the cellular level. *Biomaterials* 1991; **2:** 385-389

13. Schmidt JA, von Recum AF. Macrophage response to microtextured silicone. *Biomaterials* 1992; **13:** 1059-1061

14. Freshney RI. Culture of animal cells; a manual of basic technique, Alan R. Liss Inc., New York, 1987

15. Clark P, Connolly P, Curtis ASG, Dow JAT, Wilkinson CDW. Topgraphical control of cell behaviour: II. multiple grooved substrata. *Development*, 1990; **108:** 635-644

16. Chehroudi B, Soorany E, Black N, Weston L, Brunette DM. Computer-assisted three-dimensional reconstruction of epithelial cells attached to percutaneous implants. *J Biomed Mater Res*, 1995; **29:** 371-379

17. Dunn G, Brown AF. Alignment of fibroblasts on grooved surfaces described by simple geometric transformation. *J Cell Sci*, 1986; **83:** 313-340

18. Green AM, Jansen JA, von Recum AF The fibroblast response to microtextured silicone surfaces: texture orientation into or out of the surface *J Biomed Mater Res*, 1994; **28:** 647-653

19. Clark P, Connolly P, Curtis ASG, Dow JAT, Wilkinson CDW. Topgraphical control of cell behaviour: I. simple step cues. *Development*, 1987; **99:** 439-448

20. Curtis ASG, Clark P. The effects of topographic and mechanical properties of materials on cell behaviour. *Critical Reviews in Biocompatibility*, 1990; **5:** 343-362

21. Johnson Jr. RE, Dettre RH. Wettability and

contact angles. In: Surface and Colloid Science, vol. 2, Wiley-Inetrscience, New York, 1969 pp 85-153

22. de Jonghe V, Chatain D. Experimental study of wetting hysteresis on surfaces with controlled geometrical and/or chemical defects. *Acta metall mater*, 1995; **43:** 1505-1515

23. Baier RE. Surface properties influencing biological adhesion. In: Adhesion in biological systems, ed. R.S. Manly. Academic Press, New York, 1970

24. Schakenraad JM, Busscher HJ, Wildevuur CRH, Arends J. The influence of substratum surface free energy on growth and speading of human fibroblasts in the presence and absence of serum proteins. *J Biomed Mater Res*, 1986; **20:** 773-784

25. Altankov G, Groth TH. Reorganization of substratum-bound fibronectin on hydrophilic and hydrophobic materials is related to biocompatibility. *J Mater Sci*, 1994; **5:** 732-737

26. Ohara PT, Buck RC. Contact guidane in vitro. *Exp Cell Res*, 1979; **121:** 235-249

27. Izzard CS, Lochner LR. Cell-to-subtrate contacts in living fibroblasts: an interference reflexion study with an evaluation of the technique. *J Cell Sci*, 1976; **21:** 129-159

28. Clark P, Connolly P, Curtis ASG, Dow JAT, Wilkinson CDW. Cell guidance by ultrafine topography in vitro. *J Cell Sci*, 1991, **99:** 73-77

CHAPTER 5

Confocal laser scanning microscopical study of the fibroblast cytoskeleton, attachment complexes, and ECM protein deposition on silicone micro grooved surfaces

E.T. den Braber[1], J.E. de Ruijter[1],
L.A. Ginsel[2], A.F. von Recum[3], and J.A. Jansen[1]

[1]University of Nijmegen, Dental School, Laboratory of Biomaterials,
POB 9101, NL-6500 HB Nijmegen, The Netherlands.
[2]University of Nijmegen, Faculty of Medical Sciences, Department of Cell Biology and Histology,
POB 9101, NL-6500 HB Nijmegen, The Netherlands.
[3]Clemson University, Department of Bioengineering, College of Engineering and Science,
301 Rhodes Research Center, Clemson SC 29634-0905, USA.

CHAPTER 5

Confocal laser scanning microscopical study of the fibroblast cytoskeleton, attachment complexes, and ECM protein deposition on silicone micro grooved surfaces

INTRODUCTION

The role of the texture of materials in inducing cell and tissue responses is still unclear. In spite of the fact that several publications and reviews[1-7] do report on the effects of microtextured surfaces, little is known about the exact mechanism whereby surface topography exerts its effects. Several theories have been suggested however. First, it has been hypothesized that wettability plays a role in these phenomena. A microtextured surface could possess local differences in surface free energy, which promote a specific deposition pattern of the substratum bound attachment proteins[2-3, 8-10]. In addition, the spatial arrangement of the adsorbed proteins[11-13] and the conformation of these proteins[14-15] would be influenced by these substratum surface properties. Second, it has been suggested that the specific geometrical dimensions of the focal adhesion plaques force a cell on a surface with small grooves and ridges to orientate itself parallel to these ridges[16-17]. This hypothesis is based on the observation that a minium length of 2.0 μm is required for focal contacts to establish adhesion[18]. This implies that, if the ridge width increases, multiple vectors of adhesion plaque orientation are possible, enabling less orientated cell attachment. Finally, a third hypothesis[19-20] supposes that the orientation and alignment of cells on microtextured surfaces are a part of the cellular efforts to reach a biomechanical equilibrium with the net sum of forces minimized. This phenomenon has for instance been described extensively in the so-called tensegrity models[19-21]. According to these models, it is possible that the anisotropic geometry of substratum surface grooves and ridges establishes stresses and shear-free planes that influence the direction of microtubule[22] and microfilament growth[23-24] in order to create a force economic situation.

Given the current available information, it is impossible to express an opinion on which or whether one of these hypotheses is true. On the other hand, several separately performed studies report that surface microtextures can have a profound effect on specific elements of the cytoskeleton like for example the microfilament bundles[23-26], focal contacts[16], and microtubules[22]. Although these separate studies provide a very useful insight on these specific cellular components, none of these reports combine the findings on the cytoskeletal components, attachment complexes, and extracellular matrix (ECM) proteins in a general overall analysis to investigate the interaction of these individual components in the process of cellular orientation, elongation, and attachment on microtextured surfaces. Still, such a study appears to be mandatory, since one of the future goals in the biomaterials research area is to apply topographical surface mechanisms on implants to manipulate the healing response of regenerating tissues[1-3]. Therefore, rat dermal fibroblasts (RDFs) were cultured on microgrooved silicone rubber substrata during this study. After incubation, confocal laser scanning microscopy and several digital techniques were used to investi-

gate the relationship between the microfilament bundles, attachment complexes with vinculin as a marker, ECM proteins fibronectin and vitronectin, and the underlying microgrooved surface.

MATERIAL AND METHODS

Substrata production and characterization

Smooth and microgrooved silicone rubber substrata were produced, as described before[5-6, 27-28], by first making silicon oxide moulds with photolithography. These silicon oxide moulds possessed parallel surface grooves with a groove width of 2.0, 5.0, or 10.0 μm. All the grooves had a depth of 0.5 μm and were separated by a ridge, which had the same width as the groove. For the production of the substrata for *in vitro* purposes, the smooth and microgrooved silicon moulds were covered with polydimethylsiloxane (silicone elastomer MDX 4-4210, Dow Corning). After polymerization, the silicone rubber negative surface replicas were removed, cut into an appropriate circular shape and size (175 mm^2), mounted on glass microscopic slides (76 x 26 mm; Knittel, Germany), cleaned ultrasonically with Liquinox and by Soxhlet rinsing as described before[4-6], and prepared for cell culture purposes by radio frequency glow discharge (RFGD) treatment (PDC-3XG, Harrick; Argon, 0.15 Torr, 5 minutes).

Cell culture

Primary culture rat dermal fibroblasts (RDFs), taken from abdominal skin grafts of male Wistar rats as described earlier[4-6], were used for incubation on the smooth and microgrooved substrata. Briefly, the silicone rubber substrata on their supporting microscopic slides were placed in the wells of Quadriperm® culture plates (Heraeus Instruments GmbH, Germany), and examined routinely with a phase contrast microscope (Leitz DMIL). A total of 16 substrata, four per specific texturing group were processed during a single experiment.

After identifying the fifth generation of primary culture cells as (myo)fibroblasts[29], approximately 1.0 $x10^4$ viable RDFs ml^{-1}, suspended in α-MEM with Earl's Salts and with L-glutamine (Gibco), supplemented with 10% (v/v) heat treated fetal calf serum (Gibco), were added to each substratum. RDFs cultured in wells containing a microscopic slide without a silicone substratum served as a control group. The cells were incubated on a specific substratum for 1, 3, 5, and 7 days (37°C, 5% CO_2-95% air) under static conditions. Growth medium was changed every two days. This experiment was performed in quadruple.

Fluorescent staining of attached RDFs

Before staining the attached RDFs on the silicone substrata, the substrata were first rinsed in phosphate buffered saline without magnesium and calcium (PBS; pH 7.3) to remove non attached cells. After this first rinse, the cells were fixed with 2.0% paraformalin (Merck) in PBS for 15 minutes. After rinsing the samples twice in PBS, the RDFs were permeabilized in 1.0% Triton X-100 for 5 minutes. Following permeabilization, the specimens were washed in PBS three times for 5 minutes.

For visualizing specific cytoskeletal components and proteins interacting in the attachment of the RDFs, the following monoclonal and polyclonal antibodies were used:

-1- The mouse monoclonal antibody hVIN-1, specific for vinculin[30], purchased from Sigma Chemical Company, St. Louis, MO, USA.

-2- The rabbit monoclonal anti-fibronectin antibody FN-3E2[31] (Sigma).

-3- A rabbit polyclonal antiserum raised against bovine fibronectin[32], purchased from Life Technologies Inc., Grand Island, NY, USA.

-4- The rabbit polyclonal antiserum

against bovine vitronectin[33] (Life Technologies).

-5- A polyclonal antiserum raised against human vitronectin in rabbits, which has been shown to have a good cross reactivity with rat vitronectin (Life Technologies), but not with bovine vitronectin[34].

After incubation for 30 minutes with these primary antibodies, the specimens were washed three times in PBS for 5 minutes, and incubated with the appropriate secondary antibody, i.e. fluorescein *iso*-thiocyanate (FITC) conjugated goat anti-mouse IgG (dilution 1:30 in 1% BSA/PBS; Sigma) or FITC-conjugated goat anti-rabbit IgG (dilution 1:30 in 1% BSA/PBS; Sigma). For the staining of the RDF filamentous actin no antibodies were used, since F-actin was visualized with thio-rhodamine *iso*-thiocyanate (TRITC) labelled phalloidin (Sigma). Double staining procedures were performed, i.e. F-actin and vinculin, F-actin and bovine fibronectin (FNb), F-actin and rat fibronectin (FNr), F-actin and bovine vitronectin (VTNb), and F-actin and rat vitronectin (VTNr). Due to the nature of the silicone substrata the stained specimens were not covered with a coverslip. First, because the thickness of the silicone substrata prohibits a solid seal between the coverglass and the substrata surface, enabling movement between the coverglass and the substratum surface, which will result in disruption of the stained objects. Second, the light refraction characteristics of sealing medium and silicone rubber are almost identical, thus making it impossible to retrieve reflection microscopical data of the substratum surface. Therefore, the samples were air-dried slowly in a dark humid environment and viewed immediately after preparation.

Confocal Laser Scanning Microscopy (CLSM) and digital image analysis (DIA)

Immediately after staining, the RDFs were examined with a Bio-Rad MRC 1000 confocal laser scanning microscope (CLSM, Bio-Rad Laboratories). This CLSM was equipped with a krypton/argon mixed gas laser (Ion Laser Technology, Salt Lake City, UT, USA), which was mounted on a Nikon Diaphot microscope with non-cover glass (NCG) objectives (Nikon). This type of laser offers separate, well spaced wavelengths for the excitation of FITC (λ=488 nm) and TRITC (λ=568 nm)[35]. Next to the fluorescence mode, the reflection mode (λ=488 nm) of the CLSM was used to visualize the underlying substratum surface. Under this condition, special filters were used, since the specimen was illuminated at an excitation wavelength of 488 nm, which also excitated the fluorescent FITC conjugate. Furthermore, the laser gain voltage and pinhole were adjusted properly to eliminate any information originating from the FITC labelled secondary antibodies in the reflection image.

The resulting digital images were captured with a Sprynt frame grabber (Synoptics) and stored on a 1 GB optical disk cartridge (LM-D702W, Panasonic) with a optical disk drive (LF7010E, Panasonic). By using the Confocal Assistant V3.10 for Windows™ 3.1x program (available at FTP.GENETICS.BIO-RAD.COM; copyright Todd Clark Brelje, 1995) overlay images were created, thus making it possible to capture the fluorescent and

TABLE I

Dimensions of the micro events on the silicone rubber substratum surface as measured by AFM (Gd=groove depth, Gw=groove width, Rw=ridge width).

Surface	*Gd (µm)*	*Gw (µm)*	*Rw (µm)*
SilD00	± 0.02	----	----
SilD02	0.45	1.71	1.68
SilD05	0.45	4.65	4.98
SilD10	0.46	9.58	9.77

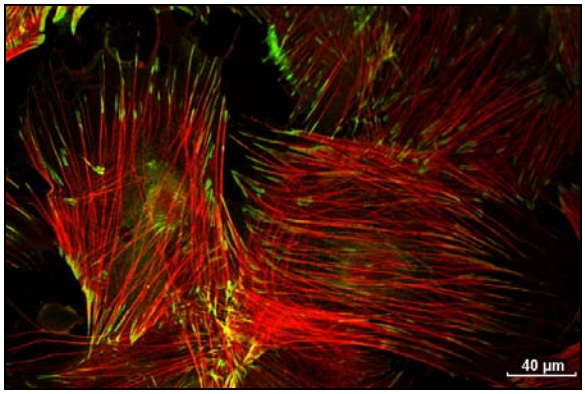

Figure 1 CLSM image of a fluorescent double labelling of RDFs on a smooth silicone rubber substrata (SilD00) after 3 days of incubation. Although the microfilaments (RED) show a high degree of orientation within a single RDF, their main directional orientation varies between cells. The vinculin aggregates (GREEN) are linear and are located at the end of the actin filaments. The yellow colour indicates at an overlap of the red actin and green vinculin data. Except from single vinculin staining streaks, larger complexes can be seen.

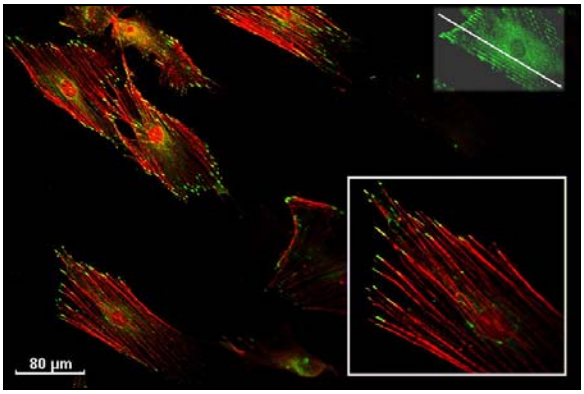

Figure 2 Confocal micrograph of a fluorescent labelling of RDFs on a SilD02 surface after an incubation of 3 days. The highlighted rectangle in the top right hand corner reveals the groove direction (white line) by enhancing the aspecific FITC background fluorescence. The main image shows the orientation of the microfilaments (RED) and vinculin containing attachment complexes (GREEN). The inset displays a part of one of the orientated RDFs in the main image at higher magnification.

reflection data in one 24 bits RGB (**R**ed-**G**reen-**B**lue) picture. These RGB images were transferred to CD-ROM by using a CD-ROM writer (CDD2000, Philips) for permanent storage and further analysis.

DIA of the digital RGB images was performed with the PC_Image V2.1 for Windows™ 3.1x software package (Foster Findlay Associates, UK). By isolating the different components, several parameters were investigated. First, the (acute) angle of orientation of F-actin, vinculin, fibronectin (FNr and FNb), vitronectin (VTNr and VTNb), and the surface grooves relative to a virtual X-Y axis were measured. Second, the relative position and the angle of the linear components of vinculin, fibronectin (FNr and FNb), and vitronectin (VTNr and VTNb) were compared with the position and angle of orientation of the actin filaments. Finally, the location of vinculin relative to the grooves and ridges of the microtextured surface was charted and analyzed. After transferring the results of the DIA through a DDE (Dynamic Data Exchange) link, the data were analyzed with SAS™ (release 6.03, SAS Institute Inc., USA), using univariate, multiple regression, and nonparametric Kruskal-Wallis models.

RESULTS

Confocal laser scanning microscopy (CLSM)

A total of 616 digital overlay images were acquired as a result of the CLSM observation of the RDFs on the smooth and microtextured silicone substrata. A small, but representative selection of these CLSM images can be found in the Figures 1 to 10. The dimensions of the various surface grooves and ridges can be found in Table I.

On the smooth substrata, the RDFs were arranged in monolayers. The cells had a well spread, multipolar appearance (Figure 1), and the microfilaments possessed no main direction of orientation when compared between cells. Most observed actin fibres ended at the vinculin containing attachment complexes, while the latter generally possessed an elongated elliptic shape. The microfilaments and elliptic vinculin aggregates of the RDFs on the SilD02 substrata all appeared to be orientated along the surface grooves after 1, 3, and 5 days of incubation (Figure 2). After 7 days of incubation,

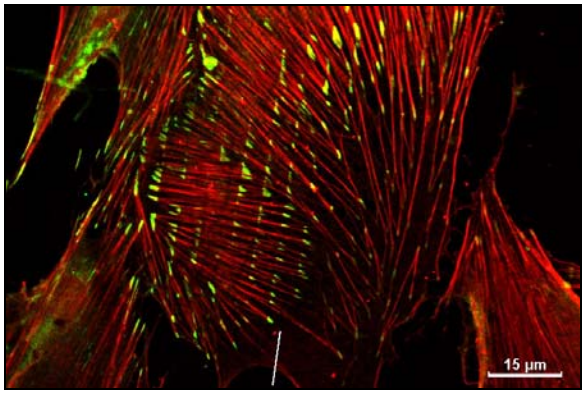

Figure 3 Fluorescent double staining of RDFs on a 5.0 µm grooved surface (SilD05) after 3 days of incubation. The microfilaments (RED) and vinculin aggregates (GREEN) are not orientated exclusively in the direction of the surface pattern (white line). Vinculin seems to attach specifically to a particular surface feature with regular intervals.

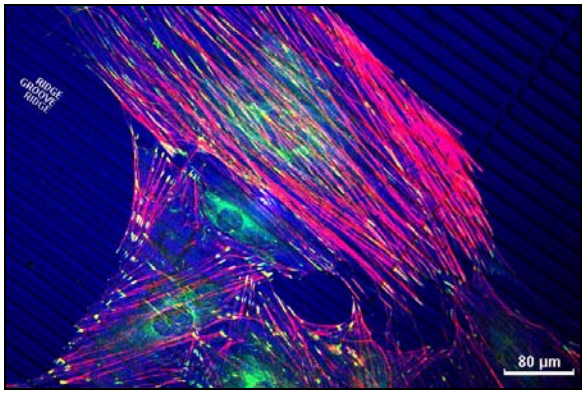

Figure 4 Overlay image composed out of a reflection microscopical image of the SilD10 substrata surface (BLUE) and the actin (RED) and vinculin (GREEN) fluorescence data. RDFs were incubated for 3 days. As with the cells on the SilD05 surfaces, various angles of microfilament and vinculin orientation can be seen. Vinculin is located mainly on the ridges of the surface pattern.

frequent cell-cell contact was seen, resulting in less orientated/elongated cells and less orientated cytoskeletal components. Furthermore, it was striking that the vinculin stains displayed a repetitive pattern and that the linear aggregates were orientated parallel to the direction of the 2.0 µm surface grooves (Figure 2). The presence of vinculin at regular intervals was seen even clearer on the SilD05 and SilD10 substrata (Figures 3 and 4). In contrast with the vinculin aggregates on the SilD02 surfaces, it was observed that the linear vinculin stains on the SilD05 and SilD10 substrata were not all orientated in the direction of the surface pattern. Also, in contrast with the SilD02 substrata, the microfilaments of the fibroblasts on the SilD05 and SilD10 surfaces were not orientated solely along the surface grooves. Finally, addition of the corresponding reflection microscopical image to the fluorescent data showed that vinculin tended to be located mainly on the surface ridges of all the microtextured surfaces (Figures 4 and 5).

For the incubation periods up to 3 days, FNr, FNb, VTNr, and VTNb were found on all surfaces. After longer incubation periods, the amount of VTNb decreased rapidly, and had almost completely disappeared after 7 days. Such a decrease was also observed for FNb, but the reduction of this protein was more gradual, since FNb was still present on all surfaces after 7 days of incubation. Furthermore, FNr was seen in larger quantities than VTNr. While VTNr remained present in the same amounts throughout the different incubation periods, FNr increased during the first 3 days of this study. After these 3 days the FNr quantity on the surfaces remained stable.

Figure 6 shows FNr on a smooth silicone rubber substratum after an incubation

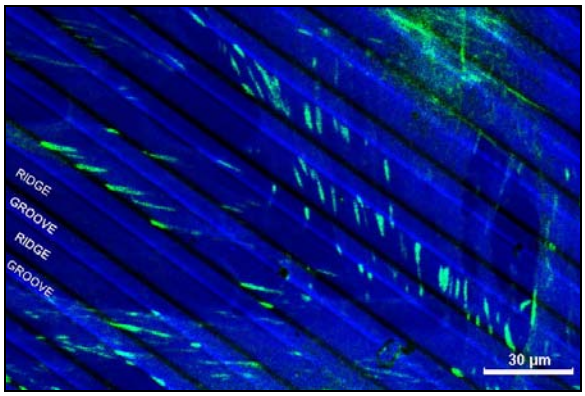

Figure 5 Overlay image of the location of vinculin (GREEN) in relation to the SilD10 surface features (BLUE) after a incubation of 5 days. Vinculin is located mainly on the surface ridges and often attaches to the edges of these ridges.

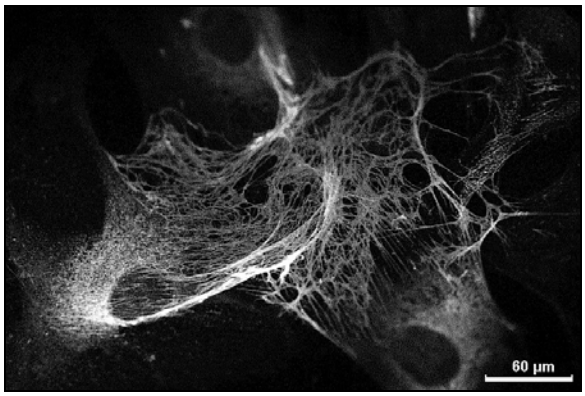

Figure 6 Immunofluorescence micrograph of a fibronectin (FNr) staining on a SilD00 surface (incubation period of 3 days). Filaments in a web-like conformation at a point of cell-cell contact and positive FNr dots are visible. Some details are out of focus due to variations in the substratum thickness.

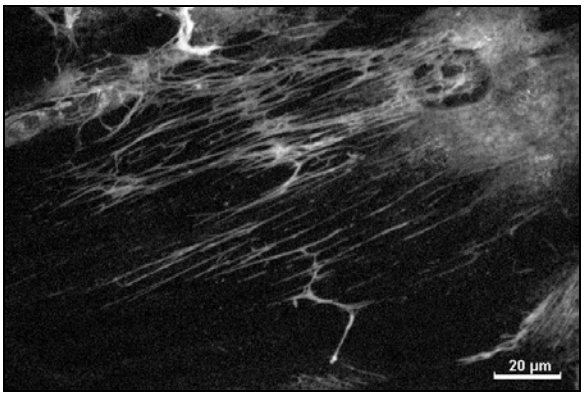

Figure 7 Immunofluorescence micrograph of rat fibronectin (FNr) staining on a SilD05 surface (incubation period of 3 days) shows thin FNr filaments at the leading edge of the cell. The location of the nucleus is clearly visible. The main FNr filaments possess similar orientational vectors.

period of 3 days. Observation of FNr, FNb, VTNr, and VTNb on the smooth surfaces learned that some protein depositions had a web-like structure, and were localized mainly at the ventral side of the fibroblasts near the nucleus. If linear filaments were found, RGB overlay images showed a large similarity with the orientation of the microfilaments and vinculin containing attachment complexes for a single RDF. However, if the orientation of the extra- and intracellular proteins was compared between different cells, various angles of orientation were found, designating the orientation of FN and VTN filaments on the SilD00 surfaces as random. Finally, FN and VTN were also found on the smooth substrata in areas where no RDFs were present.

On the microtextured surfaces FNr, FNb, VTNr, and VTNb were found mainly at the ventral side of the leading edge of the RDFs (Figures 7 to 9). RGB overlay images revealed that most of these protein filaments were located on, or originated at the surface ridges (Figures 7 and 9). Moreover, these filaments at the leading edge were orientated in the direction of the surface pattern. They did not seem to be hindered by the surface grooves, since many groove spanning filaments were found on all textured surfaces (Figures 7 to 10). These groove spanning filaments were also found when the RDFs established cell-cell contact (Figures 9 and 10). Finally, it was observed that the orientation of many microfilaments of the RDFs on the SilD02 and SilD05 surfaces were comparable to the orientation of the deposited ECM proteins (Figure 8 and 9). At the caudal side of the cells very little filaments, but a lot of protein spots or dots were found (Figure 9). These dots were located in the grooves as well as on the surface ridges.

Digital image analysis (DIA)

By analyzing the 616 digital overlay images with the PC_Image V2.1 for Windows™ 3.1x software package, a total of 326669 observations for statistical analysis were retrieved. Analysis of this data first of all showed that the RDF actin fibres were significantly more orientated on the SilD02 surfaces than on the SilD00, SilD05, and SilD10 substrata ($0.0001 \leq P_{DAY\ 1\text{-}7} \leq 0.0269$; Figure 11). In addition, a cumulative frequency distribution showed that 70.52% of all the microfilaments of the cells on the SilD02 surfaces had an angle of orientation smaller than, or equal to 10°, compared to cumulative percentages of 28.25 and 26.98 on the SilD05 and SilD10

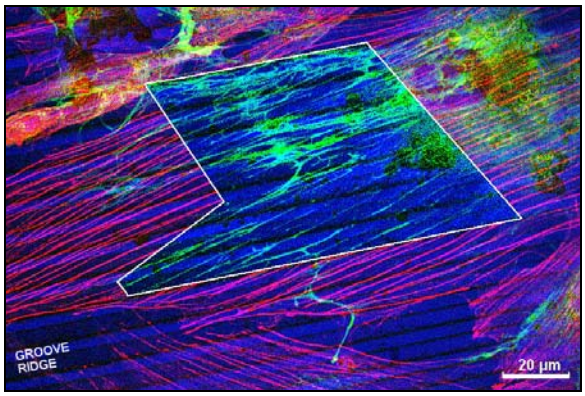

Figure 8 Digital overlay image of a reflection micrograph of a SilD05 surface (BLUE) and the corresponding actin (RED) and FNr (GREEN) fluorescence data after a RDF incubation of 3 days. The FNr data is shown separately in Figure 7. The window at the centre of the picture, created by eliminating the actin data, allows clear observation of the orientated FNr filaments at the ventral side of the fibroblast. These filaments are located and/or originate mainly at the surface ridges and span the grooves. Note the similarity in the orientation of these protein filaments and the microfilaments of the overlaying RDF.

substrata respectively. For the vinculin containing attachment complexes a similar pattern of orientation was detected (Figure 12). Statistical analysis showed that the linear vinculin complexes on the SilD02 substrata were significantly stronger orientated parallel to the surface grooves (69.19%≤10°) than those on the SilD05 and SilD10 surfaces

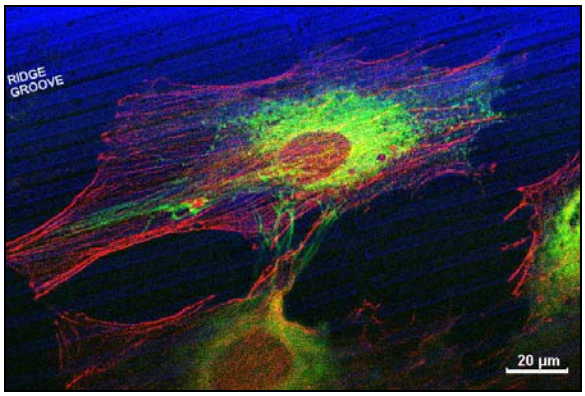

Figure 9 Digital overlay image of a reflection micrograph of a SilD05 substrata (BLUE) and the corresponding actin (RED) and FnB (GREEN) fluorescence data after a RDF incubation of 1 day. Some orientation of the microfilaments and FNb is visible. Note the groove spanning of the FNb, the FNb spots at the caudal side of the RDF, and the similarity in stress fibre and FNb location/orientation.

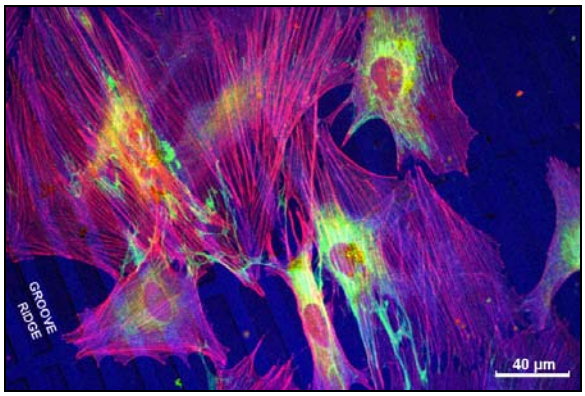

Figure 10 RGB overlay image of a SilD10 surface (BLUE) and fluorescent labelled microfilaments (RED) and FNb (GREEN) after a RDF incubation of 3 days. Although not all the microfilaments are orientated, large orientated deposits of FNb are located mainly on the surface ridges. Groove spanning FNb filaments are clearly visible.

(0.0001≤$P_{DAY\ 1\text{-}7}$≤0.0096). Statistical testing also confirmed that the vinculin aggregates of the RDFs on the microtextured surfaces were located mainly (≥69.49%) on the ridges. No significant differences for ridge located vinculin were detected between the different surface textures (Figure 13). Comparison of the angle of orientation of the microfilaments

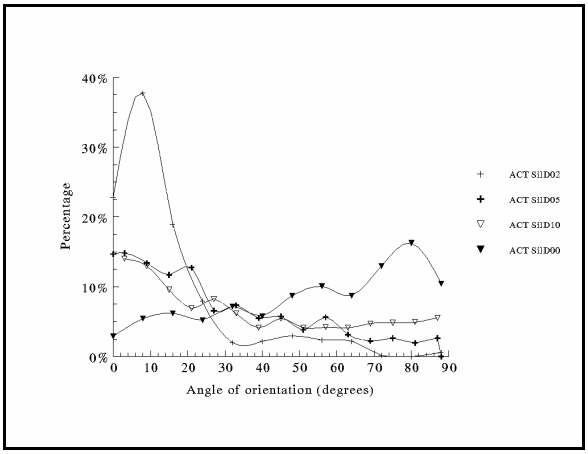

Figure 11 Orientation of the RDF microfilaments on smooth and microtextured silicone rubber surfaces. Analysis of the data in this percentile frequency plot showed a significantly stronger orientation of microfilaments on the 2.0 µm grooved surfaces (SilD02). The high percentage of microfilaments with an angle ≤10° on the SilD02 surfaces is clearly visible.

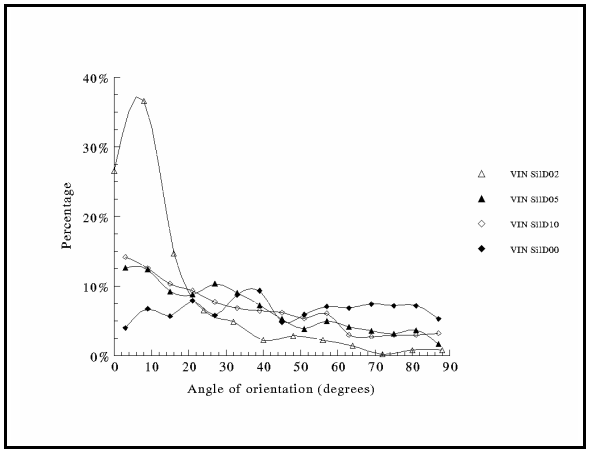

Figure 12 Percentile frequency plot of the angles of orientation of the vinculin containing attachment complexes on all silicone rubber surfaces. Statistics showed a significantly stronger orientation of these vinculin aggregates on the SilD02 surfaces. Note the high percentage of ≤10° orientated vinculin stains on the SilD02 surfaces.

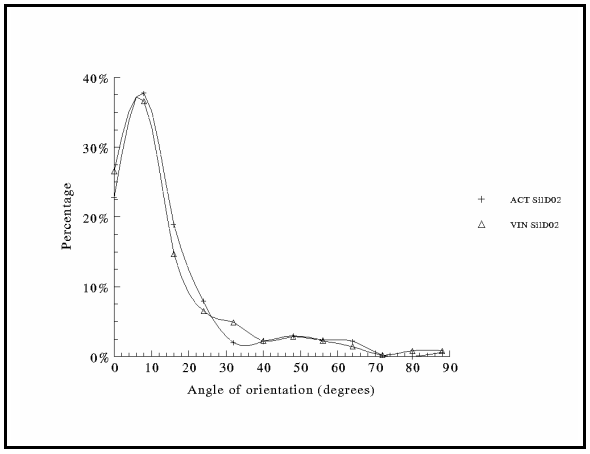

Figure 14 Percentile frequency plot of the angles of orientation of the microfilaments and vinculin containing attachment complexes on the SilD02 surfaces. The similarity between the orientation of these intracellular proteins is evident.

and vinculin stains showed that there was no significant difference for cells cultured on the smooth or microtextured substrata ($P \geq 0.4115$; Figure 14).

Concerning FNr, FNb, VTNr, and VTNb, statistical analysis showed that the protein depositions on the SilD00 substrata were orientated randomly. When the angles of orientation of these proteins were compared to each other or correlated with the angles of the microfilaments or the vinculin stains on the smooth surfaces, no significant differences were found. On the other hand, when the orientation of these ECM proteins on the microtextured surfaces was compared to the orientation of actin and vinculin, it was found that the orientation differed significantly on the 5.0 μm ($P_{\text{DAY 1-5}} \leq 0.0373$) and 10.0 μm grooved surfaces ($P_{\text{DAY 1-5}} \leq 0.0394$), while no significant differences were found on the SilD02 substrata. Review of frequency distribution for the angle of orientation revealed that these significant differences on the SilD05 and SilD10 surfaces were caused by variations in the measure of orientation, since FNr, FNb, VTNr, and VTNb on the 5.0 and 10.0 μm grooved surfaces were orientated more strongly to the surface grooves than for example the microfilaments (Figure 15). This discrepancy in the degree of orientation was not observed on the SilD02 surfaces.

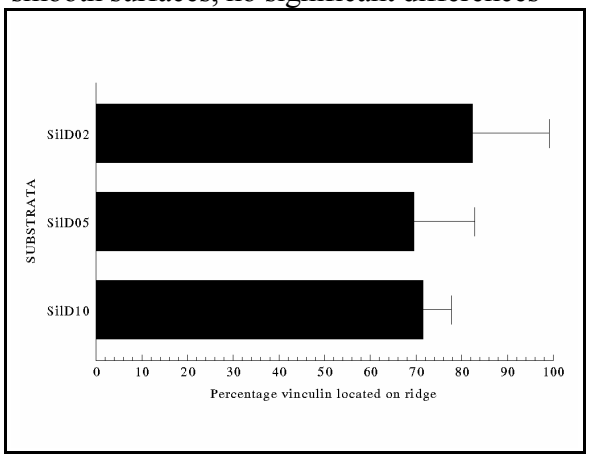

Figure 13 Graph showing the percentage of vinculin aggregates that were located on the ridges of the various microtextured surfaces. No significant differences were found between the various textured surfaces. On all surfaces the percentage of vinculin located on the ridges was ≥50%.

DISCUSSION AND CONCLUSIONS

The term contact guidance can be used to describe not only the movement of a cell according to a topographical cue on a substratum surface, but also for the orientation of a cell to certain features of that microtextured surface[1]. The results of this study first of all show that CLSM and DIA make it possible to visualize, combine, and analyze several speci-

fic components that play a role in the process of contact guidance. Especially the composition of a digital overlay image out of several fluorescence and reflection microscopical images in any desired combination and the analysis of this image by computer presents a powerful tool in this field of research. Further development of these techniques, the availability of (fluorescent labelled) antibodies, modifications of both the CLSM and the supporting image analysis software, and even the development of three dimensional reconstruction software should therefore be followed with scrutiny.

In addition, the findings of this study make it possible to extend the results of our earlier studies, which reported on the orientation of RDFs on silicone rubber surfaces with ridges ≤4.0 µm[5, 36]. By correlation of all these results, we can conclude that the microfilaments and the vinculin containing attachment complexes exhibit similar angles of orientation to the same surface patterns. This becomes even more evident when the alignment principle that Clark et al.[37] suggested, is applied. They defined a population of cells as highly aligned when the long axis of these cells makes an angle of ≤10° with the grooves. Implementation of this alignment criterion in one of our previous studies showed that RDFs orientated strongly on 2.0 µm grooved surfaces, and less on the 5.0 and 10.0 µm grooved surfaces[5, 36]. If we use this criterion on the data of this study, we can conclude that the alignment of the cytoskeletal and attachment complex elements is in agreement with these earlier observations. We showed that the microfilaments possessed the highest degree of orientation on the SilD02 surfaces (70.52%≤10°), while the orientation of vinculin was also the strongest on the SilD02 surfaces (69.19%≤10°). Finally, earlier phase contrast and electron microscopical observations[5-6, 36] suggested specific fibroblast attachment to the surface ridges of microtextured silicone surfaces.

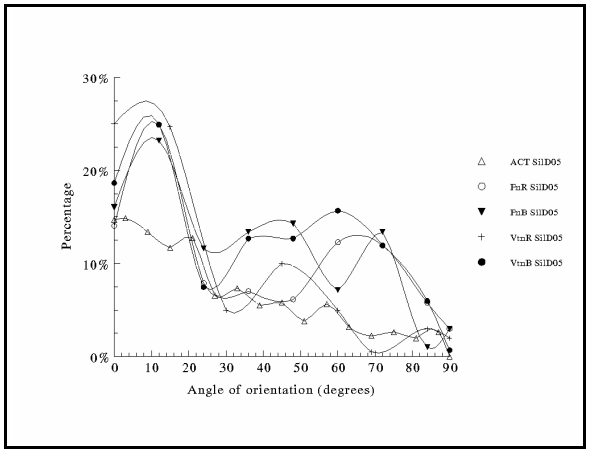

Figure 15 Percentile frequency distribution of the microfilaments, FNr, FNb, VTNr, and VTNb on SilD05 surfaces. Statistical analysis of the data showed a significantly higher degree of alignment of FNr, FNb, VTNr, and VTNb on these surfaces.

The high incidence of vinculin on the ridges found in this study confirms these earlier observations. As shown in Figure 3, this ridge related localization of vinculin made it possible to determine the localization, pitch, and orientation of the 5.0 µm surface ridges even without adding the reflection data of the surface pattern to the resulting overlay image. Furthermore, the orientation of these vinculin containing attachment complexes corroborate with the earlier mentioned hypothesis by Ohara and Buck[16]. According to this hypothesis, the focal adhesion complexes can have several angles of orientation on the 5.0 and 10.0 µm, but not on the 2.0 µm surfaces, since the ridges of the latter do only provide the area for attachment and orientation in the direction of the surface ridge. If the size of the surface ridge increases, like with the 5.0 and 10.0 µm grooved surfaces, more vectors of orientation for these adhesion complexes are possible. This is in agreement with the orientation of the vinculin stains in Figures 2 to 5.

Concerning the extracellular matrix proteins FNr, FNb, VTNr, and VTNb, no significant differences were found between the orientation of these proteins and the microfilaments and the vinculin containing

attachment complexes of the RDFs on the smooth surfaces. CLSM observation learned that, if a single RDF was observed, the intra- and extracellular proteins possessed comparable angles of orientation. This corroborates with earlier observations and has been generally recognized and described by for instance Alberts et al.[38]. Concerning the microtextured surfaces, fibronectin and vitronectin were found to be aligned along the surface grooves and ridges. This could indicate that the properties of the substrata surface play a major role in the distribution and deposition of these proteins on these surfaces. For example, bovine fibronectin and vitronectin were found mainly on and aligned along the ridges during this study. In contrast with the endogenous (rat) fibronectin and vitronectin, the bovine ECM proteins, which originated from the FCS which was supplemented to the culture medium, had to be distributed passively along the surface. This could mean that surface properties like for instance surface charge and surface free energy had a profound influence on the specific ridge related deposition that was found on all textured surfaces. However, until techniques and models have been developed to measure these and other surface properties and their effects on the protein distribution and deposition, this can only be considered as an educated guess.

In consequence, we have to conclude that the current study does fail to explain completely how substratum surface features influence cellular behaviour. Nevertheless, by combining our results with generally accepted concepts and results of other investigators, it is possible to speculate on a possible working mechanism. For example, we observed the specific deposition and orientation of fibronectin and vitronectin on the smooth and microtextured silicone rubber substrata. It is generally recognized that these two proteins are heavily involved in cell-substratum interactions, including cell attachment and cell movement[10, 33, 38-42]. The process of attachment results generally in a clustering of integrins and an assembly of multi-molecular focal complexes associated with the actin cytoskeleton[38, 41-42]. These focal complexes contain a large number of cytoplasmatic-derived proteins like for instance $p125^{FAK}$, src, and tensin that are assumed to play an active role in the signalling pathway with the intracellular environment[41]. Others like for example talin, α-actinin and vinculin, appear to be mainly structural[41, 43]. Although the nature of the various interactions between these and other components of the focal complexes is too voluminous to describe here in full, it is valid to mention that it has been shown that vinculin binds to α-actinin, talin and actin[44-45]. Moreover, it is also generally accepted that both α-actinin and talin bind to actin and the cytoplasmatic domains of integrin[46-47]. Integrin matrix interactions have been shown to have a significant effect on the overall cell behaviour by activating intracellular transduction pathways[38, 41, 48-49]. Therefore, it can be supposed that integrin, which is the receptor for fibronectin (integrin $\alpha_5\beta_1$)[50] and vitronectin (integrin $\alpha_v\beta_3$)[50], induces orientation of the cell (components) through its binding to the orientated fibronectin and vitronectin on microtextured surfaces. The topographical cue of the orientated fibronectin and vitronectin could then be transferred by integrin to the total focal adhesion point. Orientation of the focal adhesion point would result in the orientated vinculin stains as seen during this study, since vinculin is a component of these focal adhesion points[41, 43]. Furthermore, we know through the results of this and other studies[44-47], that several proteins in the focal adhesion complex, including vinculin, bind to actin, enabling a possible transduction of the topographical cue to the microfilaments.

If the above mentioned is related with other findings, some interesting similarities can be detected. For example, Singer et al.[42]

showed that, as fibronectin containing extra cellular matrix filaments accumulated beneath the cell, the fibronectin receptors became concentrated at contacts with these filaments. Similar events occurred with the fibronectin and vitronectin receptors on vitronectin coated surfaces. Co-accumulation of fibronectin and vitronectin receptors in focal contacts was seen after 2-6 hours incubation in serum containing cultures. These results by Singer et al.[42], together with those of others[10, 33, 38-43, 50], show that cells recruit and cluster transmembrane integrin, form vinculin containing focal contacts, and attach to fibronectin and vitronectin. Based on their results, Singer et al. suggested that the fibronectin receptor might also function in the process of cellular migration along the fibronectin containing matrix cables. If this is true, orientated fibronectin filaments could very well take account for the directed locomotion of cells on microtextured surfaces. In addition, this corresponds with the frequently described migration behaviour of fibroblasts on ECM matrices[38].

Considering this, many questions remain unanswered. For instance, our results show a significant reduction of the orientation of the microfilaments and vinculin containing attachment complexes on the SilD05 and SilD10 surfaces, while DIA shows that the ECM proteins on these surfaces are highly aligned with the surface patterns. This seems to be in contradiction with the generally accepted model of the interaction between the ECM matrix and the cytoskeleton. This model[38, 41, 46, 48, 51] states that there are reciprocal interactions between extracellular fibronectin and intracellular microfilaments that are mediated mainly by integrins. Through this mechanism, cytoskeletons of cells can exert forces that orientate the matrix macromolecules that the cells secrete, while the matrix molecules can in turn organize the cytoskeletons of cells that contact them, thus propagating order from cell to cell in tissues. The fact that this model does not seem to apply to our microgrooved substratum surfaces, suggests that specific properties of microtextured surfaces alter this intricate interaction between the intracellular and extracellular proteins. Close observation of the CLSM images shows large ECM deposits on the ridges of especially the SilD10 surfaces (Figure 10). According to DIA, these deposits possess a linear shape, since their length is longer than their width. But microscopical investigation shows that their appearance is notably different from the deposits that were often seen on the SilD02 and SilD05 surfaces (Figures 7 to 9). ECM deposits like in Figure 10 cover a large area of the surface ridge, enabling multiple angles of orientation for the focal contacts attaching to these ECM proteins. Whether these deposits consist out of smaller ECM components that possess a particular orientational vector, remains unclear due to the limitations of CLSM concerning magnification and resolution.

In conclusion, it can be said that microtextured surfaces influence the orientation of the intracellular and extracellular proteins. Although our results do corroborate with all three hypotheses that were described earlier, they do not justify a specific choice for one of these hypotheses. The differences in deposition patterns and the appearances of the ECM proteins during this study for example, make it possible to suggest that surface properties like surface free energy have an influence on the displayed cellular behaviour. The vinculin location and orientation however, pleas in favour of the "ridge width" theory. Finally, whether the cells orientate to the microtextured surfaces as a result of the force distribution that is created by these surfaces and the cells cultured on them, is impossible to determine with the results of this study. Recognizing the fact that these three hypothesis can even be integrated into one overall model, contributes to the intriguing phenomena of cellular behaviour on microtextured surfaces.

ACKNOWLEDGEMENT

This study is supported by the Technology Foundation (STW).

REFERENCES

1. A.S.G. Curtis, and Clark P, "The effects of topographic and mechanical properties of materials on cell behavior," *Critical Reviews in Biocompatibility,* **5,** 344-362 (1990)

2. R. Singhvi, G. Stephanopoulos, and D.I.C. Wang, "Effects of Substratum Morphology on Cell Physiology - Review," *Biotechnol. Bioeng.,* **43,** 764-771 (1994)

3. A.F. von Recum and T.G. van Kooten, "The influence of micro- topography on cellular response and the implications for silicone implants," *Journal of Biomaterials Science - Polymer Edition,* **7,** 181-198 (1995)

4. E.T. den Braber, J.E. de Ruijter, H.T.J. Smits, L.A. Ginsel, A.F. von Recum, and J.A. Jansen, "Effect of parallel surface micro grooves and surface energy on cell growth," *J. Biomed. Mater. Res.* **29,** 511-518 (1995)

5. E.T. den Braber, J.E. de Ruijter, L.A. Ginsel, A.F. von Recum, and J.A. Jansen, "Quantitative analysis of cell proliferation and orientation on substrata with uniform parallel surface micro grooves," *Biomaterials* **17,** 1093-1099 (1996)

6. E.T. den Braber, J.E. de Ruijter, H.J.E. Croes, L.A. Ginsel, and J.A. Jansen, "Transmission electron microscopical study of fibroblast attachment to microtextured silicone rubber surfaces," *Cells and Materials* accepted 1997

7. J.A. Hubbell, "Biomaterials in tissue engineering," *Biotechnology,* **13,** 565-576 (1995)

8. R.E. Baier, "Surface properties influencing biological adhesion," *Adhesion in biological systems*, R.S. Manly (ed.) Academic Press, New York, 1970, 15-48

9. J.M. Schakenraad, H.J. Busscher, C.R.H. Wildevuur, and J. Arends, "The influence of substratum surface free energy on growth and spreading of human fibroblasts in the presence and absence of serum proteins," *J. Biomed. Mater. Res.,* **20,** 773-784 (1986)

10. G. Altankov and T.H. Groth, "Reorganization of substratum-bound fibronectin on hydrophillic and hydrophobic materials is related to biocompatibility," *J. Mater. Sci.,* **5,** 732-737 (1994)

11. R.L. Williams and D.F. Williams, "The spatial resolution of protein adsorption on surfaces of heterogeneous metallic biomaterials," *J. Biomed. Mater. Res.*, **23,** 339-350 (1989)

12. M.L. Rudee and T.M. Price, "The initial stages of adsorption of plasma derived proteins on artificial surfaces in a controlled flow environment," *J. Biomed. Mater. Res.*, **19,** 57-66 (1985)

13. H.M.W. Uyen, J.M. Schakenraad, J. Sjollema, J. Noordmans, W.L. Jongbloed, I. Stokroos and H.J. Busscher, "Amount and surface structure of albumin adsorbed to solid substrata with different wettabilities in a parallel plate flow cell," *J. Biomed. Mater. Res.*, **24,** 1599-1614 (1990)

14. R.J. Rapoza and T.A. Horbett, "Postadsorptive transitions in fibrinogen: influence of polymer properties," *J. Biomed. Mater. Res.*, **24,** 1263-1287 (1990)

15. E. Shiba, J.N. Lindon, L. Kushner, G.R. Matsueda, J. Hawiger, M. Kloczewiak, B. Kudryk, and E.W. Salzman, "Antibody detectable changes in fibrinogen adsorption affecting platelet activation on polymer surfaces," *Am. J. Physiol.*, **260,** C965-974 (1991)

16. P.T. Ohara and R.C. Buck, "Contact guidance in vitro," *Exp. Cell. Res.,* **121,** 235-249 (1979)

17. G.A. Dunn and A.F. Brown, "Alignment of fibroblasts on grooved surfaces described by a simple geometric transformation," *J.Cell Sci.*, **83**, 313-340 (1986)

18. C.S. Izzard, and L.R. Lochner, "Cell-to-substrate contacts in living fibroblasts: an interference reflection study with an evaluation of the technique," *J. Cell Sci.,* **21,** 129-159 (1976)

19. D.E. Ingber, "Cellular tensegrity; defining new rules of biological design that govern the cytoskeleton," *J. Cell Sci.*, **104**, 613-927 (1993)

20. M.D. Ward, and D.A. Hammer, "A theoretical analysis for the effect of focal contact formation on cell-substrate attachment strength," *Biophys. J.*, **64**, 936-959 (1993)

21. N. Wang, J.P. Butler, and D.E. Ingber, "Mechanotransduction across the cell surface and through the cytoskeleton," *Science*, **260,** 1124-1127 (1993)

22. C. Oakley and D.M. Brunette, "The sequence of alignment of microtubules, focal contacts and actin filaments in fibroblasts spreading on

smooth and grooved titanium substrata," *J. Cell Sci.,* **106,** 343-354 (1993)

23. C. O'Neill, P. Jordan, P. Riddle, and G. Ireland, "Narrow linear strips of adhesive substratum are powerful inducers of both growth and total focal contact area," *J. Cell Sci.*, **95,** 577-586 (1990)

24. C. Oakley, and D.M. Brunette, "Topographic compensation: Guidance and directed locomotion of fibroblasts on grooved micromachined substrata in the absence of microtubules," *Cell Motility and the Cytoskeleton,* **31,** 45-58 (1995)

25. A. Ben-ze'ev, "The role of changes in cell shape and contacts in the regulation of cytoskeleton expression during differentiation," *J. Cell Sci. Suppl.,* **8,** 293-312 (1987)

26. G.A. Dunn and J.P. Heath, "A new hypothesis of contact guidance in tissue cells," *Exp. Cell Res.,* **101,** 1-14 (1976)

27. J.A. Schmidt and A.F. von Recum, "Macrophage response to microtextured silicone," *Biomaterials* **13,** 1059-1061 (1992)

28. J.A. Schmidt and A.F. von Recum, "Texturing of polymer surfaces at the cellular level," *Biomaterials* **2,** 385-389 (1991)

29. G. Gabbiani, "Modulation of fibroblastic cytoskeletal features during wound healing and fibrosis," *Pathol. Res. Pract.*, **190,** 851-853 (1994)

30. R. Benori, D. Salomon, and B. Geiger, "Identification of two distinct domains on vinculin involved in its association with focal contacts," *J. Cell. Biol.,* **108,** 2383-2393 (1989)

31. C. Garbarsch, M.E. Matthiessen, B.E. Olsen, D. Moe, "Immunohistochemistry of the intercellular matrix components and the epithelio-mesenchymal junction of the tooth germ," *Histochem. J.,* **26,** 110-118 (1994)

32. E.G. Hayman, A. Oldberg, G.R. Martin, and E. Ruoslahti, "Co-distribution of heparan sulfate proteoglycan, laminin, and fibronectin in extra cellular matrix of normal rat kidney cells and their coordinate absence in normal cells," *J. Cell. Biol.,* **94,** 28-35 (1982)

33. E.G. Hayman, M.D. Pierschbacher, S. Suzuki, and E. Ruoslahti, "Vitronectin; a major cell attachment-promoting protein in fetal bovine serum," *Exp. Cell. Res.,* **160,** 245-258 (1985)

34. E.G. Hayman, M.D. Pierschbacher, Y. Ohgren, and E. Ruoslahti, "Serumspreading factor (vitronectin) is present at the cell surface and in tissues," *Proc. Natl. Acad. Sci.,* **80,** 4003-4007 (1983)

35. G. Cox, "Trends in Confocal Microscopy," *Micron,* **24,** 237-247 (1993)

36. E.T. den Braber, J.E. de Ruijter, L.A. Ginsel, A.F. von Recum, J.A. Jansen, "Quantitative analysis of fibroblast morphology on microgrooved surfaces with various groove and ridge dimensions," *Biomaterials*, **17,** 2037-2044 (1996)

37. P. Clark, P. Connolly, A.S.G. Curtis, J.A.T. Dow, C.D.W. Wilkinson, "Topographical control of cell behaviour: II. multiple grooved substrata," *Development*, **108,** 635-644 (1990)

38. B. Alberts, D. Bray, J. Lewis, M. Raff, K. Roberts, and J.D. Watson, *Molecular biology of the cell*, Third edition, Garland Publishing Inc., New York, 1994, 984-999

39. L.S. Chou, J.D. Firth, V.J. Uitto, and D.M. Brunette, "Substratum surface topography alters cell shape and regulates fibronectin mRNA level, mRNA stability, secretion and assembly in human fibroblasts," *J. Cell Sci.,* **108,** 1563-1573 (1995)

40. P.A. Underwood, J.G. Steele, and B.A. Dalton, "Effects of polystyrene surface chemistry on the biological activity of solid phase fibronectin and vitronectin, analyzed with monoclonal antibodies," *J Cell Sci,* **104,** 793-803 (1993)

41. N.A. Hotchin and A. Hall, "The assembly of integrin adhesion complexes requires both extracellular matrix and intracellular rho/rac GTPases," *J. Cell Biol.*, **131,** 1857-1865 (1995)

42. I.I. Singer, S. Scott, D.W. Kawka, D.M. Kazazis, J. Gailit, and E. Ruoslahti, "Cell surface distribution of fibronectin and vitronectin receptors depends on substrate composition and extra cellular matrix accumulation," *J. Cell Biol.*, **106,** 2171-2182 (1988)

43. E.J. Luna and A.L. Hitt, "Cytoskeleton-plasma membrane interactions," *Science,* **258,** 955-964 (1992)

44. A.P. Gilmore, and K. Burridge, "Cell adhesion-cryptic sites in vinculin," *Nature*, **373,** 197 (1995)

45. R.P. Johnson and S.W. Craig, "F-actin binding site masked by the intramolecular association of vinculin head and tail domains," *Nature*, **373,** 261-264 (1995)

CHAPTER 6

Transmission electron microscopical study of fibroblast attachment to microtextured silicone rubber surfaces

E.T. den Braber[1], J.E. de Ruijter[1],
H.J.E. Croes[2], L.A. Ginsel[2], and J.A. Jansen[1]

[1]University of Nijmegen, Dental School, Laboratory of Biomaterials,
POB 9101, NL-6500 HB Nijmegen, The Netherlands.
[2]University of Nijmegen, Faculty of Medical Sciences, Department of Cell Biology and Histology,
POB 9101, NL-6500 HB Nijmegen, The Netherlands.

CHAPTER 6

Transmission electron microscopical study of fibroblast attachment to microtextured silicone rubber surfaces

INTRODUCTION

Various research reports have been published on the effect of microtextured surfaces on many cellular processes like morphology, orientation, attachment, differentiation, DNA/RNA transcription, cell metabolism, and protein production[11-13, 22]. In addition, it has even been suggested that surface microtexturing could benefit the clinical success of skin penetrating devices by prevention of epithelial downgrowth[4-5, 7], and of subcutaneous implants by reduction of the inflammatory response[6] and fibrous capsule formation at the implant-tissue interface[8].

Reviewing the literature on this topic, it is possible to deduce that the changes in cellular response originate at the interface between the microtextured surface and the contacting cells or tissues. However, it is not sufficient to examine the interface exclusively. Information concerning the conditions and mechanisms relevant to cell-substratum reactions can also be obtained from the degree of differentiation of the cells attached to this substratum, as well as the presence and orientation of cytoskeletal filaments. Therefore, a detailed study on the morphology of cells cultured on microtextured implant surfaces seems justified.

Although new techniques, like confocal laser scanning microscopy (CLSM) and digital three dimensional reconstruction, have made other approaches possible, transmission electron microscopy (TEM) still seems to be the appropriate choice for this particular type of research. For example, the resolution and magnification factor of CLSM are relatively low, and 3D reconstruction of complex structures is not yet fully developed and applicable[9]. On the other hand, TEM study of the biomaterial/cell interface is often impeded by difficulties like obtaining intact ultrathin sections without disruption of the bond between the substratum and the cells. This problem can be solved by selecting the proper technique of sample preparation. In view of this, several solutions have been found in the past for the TEM examination of metallic[3, 16] and ceramic[16] implants. However, in our studies we use silicone rubber replicas of microtextured silicon moulds to investigate the effects of parallel surface microgrooves on the cellular behaviour[11-13]. Due to the specific properties of these replicas, TEM sample preparation presents a lot of problems. For example, silicone rubber does not allow specific dehydration procedures or the use of several resin agents. In addition, ultrathin sectioning is impossible because of the elastic and thermodynamic properties of this elastomer.

Therefore, the aim of this study was to develop a technique that allows TEM observation of cells incubated on (microtextured) silicone rubber substrata, and to use this method to study the interaction of primary culture rat dermal fibroblasts (RDFs) with the grooves and ridges on these substrata.

MATERIALS AND METHODS

Production and characterization of the microtextured substrata

Surface textured experimental substrata were

TABLE I
Dimensions of the micro events on the silicone rubber substratum surface as measured by AFM (Gd=groove depth, Gw=groove width, Rw=ridge width, and P=pitch).

Surface	***Actual values***			
	Gd (μm)	*Gw (μm)*	*Rw (μm)*	*P (μm)*
SilD00	± 0.02	----	----	----
SilD02	0.45	1.71	1.68	3.87
SilD05	0.45	4.65	4.98	9.49
SilD10	0.46	9.58	9.77	18.98

produced by first making silicon oxide moulds in a class 100 clean room using photolithography[24-25]. In short, these mould surfaces were produced by coating silicon oxide masks with high reflective chrome, after which the chrome was coated with a thin (0.5 μm) layer of positive photoresist (PR). Subsequently, the PR was exposed and developed, uncovering the underlying chrome, which was etched. Finally, the unexposed PR was stripped off, thus creating a parallel groove pattern with grooves of 0.5 μm deep. The mould was then covered with an additional layer of PR and hardened by baking for 30 minutes at 150°C.

The substrata for *in vitro* purposes were obtained by covering the moulds with polydimethylsiloxane (silicone elastomer MDX 4-4210, Dow Corning), thus producing negative surface replicas, which possessed parallel surface grooves with a groove and ridge width of 2.0 (SilD02), 5.0 (SilD05), and 10 μm (SilD10). Groove depth was approximately 0.5 μm. After polymerization, these silicone rubber castings were removed, cut into their appropriate circular shape and size (175 mm^2), and washed manually in a 10% Liquinox solution (Alconox Inc.). Subsequently, these substrata were rinsed, cleaned ultrasonically for 30 minutes in a 1% Liquinox solution, given two 15 minute ultrasonic rinses in distilled, deionized water and a Soxhlet rinse for 12 hours in distilled, deionized water. Finally, these experimental substrata were prepared for cell culture purposes by radio frequency glow discharge (RFGD) treatment (PDC-3XG, Harrick; Argon, 0.15 Torr, 5 minutes). The quality and dimensions of the micro features on the substrata were investigated by scanning electron microscopy (SEM; JEOL 6310; 20kV) and atomic force microscope (AFM; Polaron SP300). The dimensions of these grooves can be found in Table I.

Cell culture

Ventral skin grafts taken from male Wistar rats (100-120 gram) were used for harvesting rat dermal fibroblasts (RDFs). After dissociation, these cells were incubated (37°C, 5% CO_2-95% air) in α-MEM with Earl's Salts and with L-glutamine (Gibco), supplemented with 10% (v/v) heattreated fetal calf serum (Gibco), 2.5 μg ml^{-1} amphotericin B (Gibco) and 50 μg ml^{-1} gentamicin (Gibco). Following approximately 3 days of culturing, the RDFs were rinsed with phosphate buffered saline without magnesium and calcium (PBS; 0.1M; pH 7.2), supplemented with 5 μg ml^{-1} amphotericin B and 100 μg ml^{-1} gentamicin to remove non-attached cells. Subsequently, the growth medium was replaced every two days by fresh growth medium. Upon confluence, the RDFs were detached by trypsinization [0.25% (w/v) crude trypsin and 1 mM EDTA (pH 7.2)] and resuspended at a lower cell concentration in fresh growth medium. The fifth generation of these cells was used for incubation on the microtextured silicone substrata after identifying them as (myo)fibroblasts by phase contrast morphology analysis[14].

After positioning the smooth and microtextured substrata in the culture wells of 24 well plates (Greiner), approximately 1.0 $x10^4$ viable RDFs ml^{-1} were added to each substratum. The cells were incubated on a

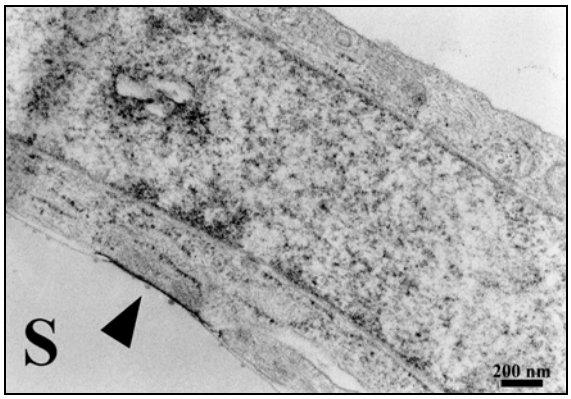

Figure 1 TEM micrograph of a RDF on a smooth (SilD00) silicone rubber surface (S=substratum). The arrowhead shows a focal adhesion point, which attaches the cell with the underlying silicone surface. The cell possesses a normal appearance. No fibrilar ECM material was found.

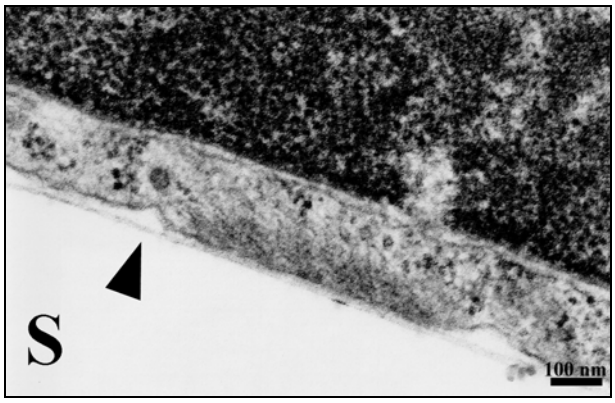

Figure 2 High magnification TEM image of a mature focal adhesion point (S=substratum). Except from the adhesion point, the electron dense layer (⅄) is clearly visible.

specific substratum for 3 and 5 days (37°C, 5% CO_2-95% air) under static conditions. Growth medium was changed every two days.

Transmission Electron Microscopy (TEM)

At the end of the incubation period, the cultures were rinsed with PBS to remove non-attached cells, and fixed with 2% glutaraldehyde (Merck) in 0.1 M phosphate buffer (pH 7.3) for 2 hours at 4°C. After fixation, the samples were rinsed twice with 0.1 M phosphate buffer for 30 minutes and postfixed with a 1% OsO_4 (Merck) - 0.1M phosphate buffer solution for 1 hour. The substrata with the RDFs were then dehydrated using a graded ethanol series and covered with a 50% (w/v) Epon - 100% ethanol solution for at least 2 hours. Subsequently, this solution was replaced by 100% Epon and were left to polymerize for 24 hours at 60°C. Following polymerization, the Epon covered silicone rubber samples were soaked in ethyl - acetate (Merck) to facilitate the removal of the silicone substrata. After removal of the silicone, some semithin sections were cut of these Epon blocks, which contained the RDFs and a cast of the microgrooved silicone surface. These sections were stained with toluidine blue in order to determine the original groove orientation of the substrata surface. Thereafter, these Epon casts were reembedded in Epon, and ultrathin sections perpendicular or longitudinal to the surface grooves were cut on a Reichert OMU-3 ultramicrotome with a diamond knife (DRUKKER International, the Netherlands). Sections were collected on Formvar-coated copper grids and stained with saturated uranyl acetate[27] (20 minutes) and lead citrate[21] (10 minutes) for contrast enhancement. All specimens were observed with a JEOL 1010 transmission electron microscope at 60 kV.

RESULTS

Transmission electron microscopy of the RDFs on the microtextured surfaces

Figures 1 to 10 show some transmission electron microscopical images of the RDFs on smooth (SilD00) and microtextured (SilD02, SilD05, SilD10) substrata. Although the silicone substrata were removed during the preparation of the samples, differences in electron density showed their former location. Furthermore, a narrow, electron dense film with a thickness varying between 8 and 36 nm separated the supra-substratum compartment and the compartment that was formerly oc-

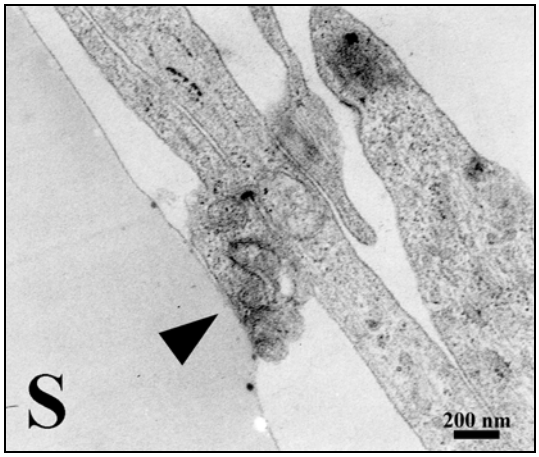

Figure 3 TEM image of multiple cell layers on a SilD00 substratum (S=substratum). A cell protrusion (⮜) seems to limit the contact of the cell with the substratum surface.

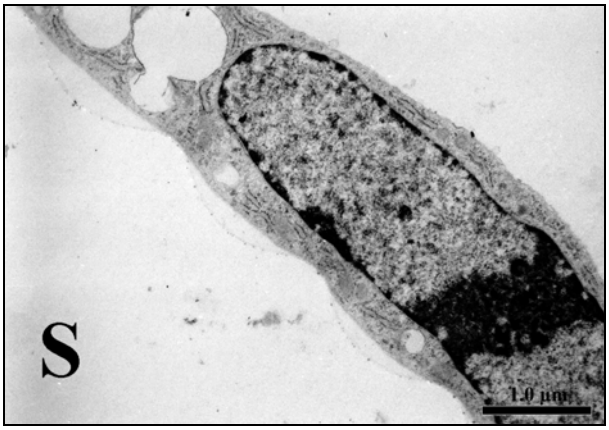

Figure 4 TEM photograph of a fibroblast on a substratum with 2.0 µm grooves (SilD02; S=substratum). The cell does not contact with, or attaches to the bottom of the surface grooves.

by the silicone microtextured substrata. This layer was seen in all the TEM images, and probably existed out of adsorbed proteins.

On the smooth substrata (Figures 1 to 3), RDFs were seen to grow in multilayers. Except from the electron dense layer at the interface between the supra-substratum compartment and the substratum, no extracellular matrix (ECM) material in the form of collagen fibres was observed. The fibroblasts, attached to neighbouring cells or to the substrata (Figure 1), showed a normal distribution of endoplasmatic reticulum and mitochondria. Often it was seen that the RDFs avoided extensive membrane contact with the substratum surface and formed small protrusions, which contacted directly with the substratum surface (Figure 3). These protrusions varied in size (200-600 nm) and seemed "to lift" the main cell body from the surface of the substratum.

Figures 4 to 6 show micrographs of RDFs incubated on 2 µm grooved (SilD02) surfaces. The fibroblasts on these substrata attached exclusively to the ridges, and were seen to bridge the intermittent spaces of the surface grooves (Figure 4). Although the slope of the ridges was gradual and the grooves possessed a wavy appearance, the cells did not contact the bottom of the grooves. In some instances cell protrusions extended into the grooves, but none of these cell extensions were found to contact or attach to the bottom of the surface grooves. Cell attachment to the surface ridges was observed regularly. An example is the RDF in contact with the substratum in Figure 5,

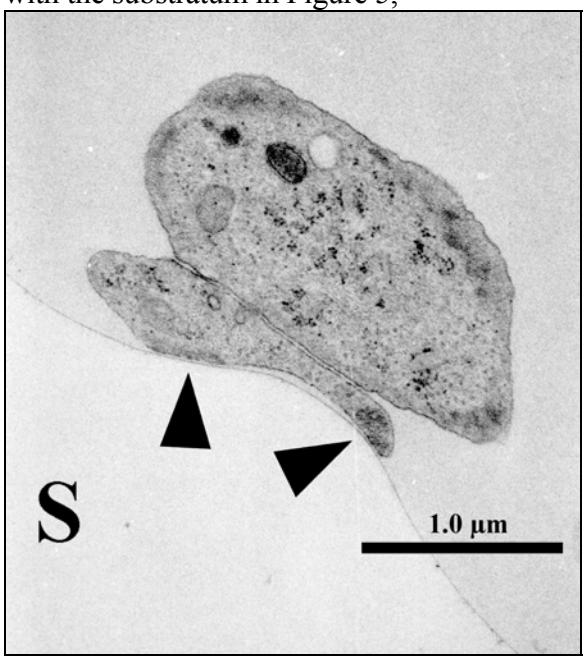

Figure 5 TEM micrograph of a perpendicular section of fibroblasts on a SilD02 surface (S=substratum). The dense areas indicating the presence of (immature) focal adhesion points (⮜ ⮞) are located at the edge of the surface ridge.

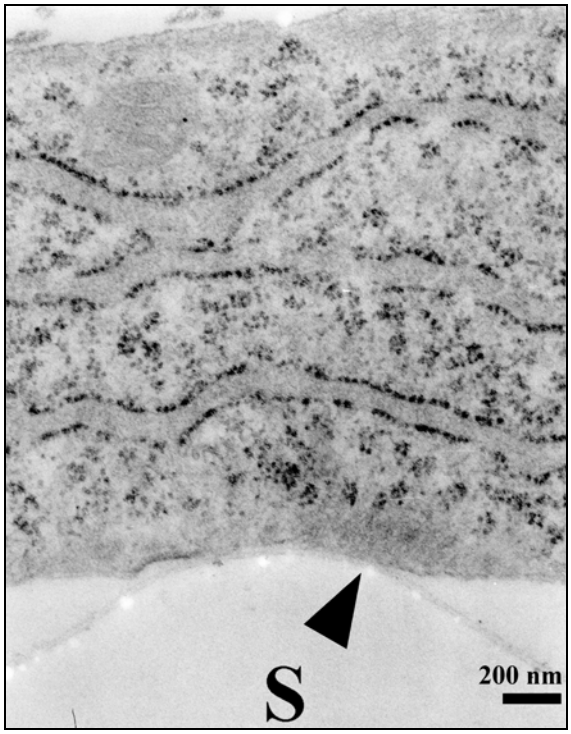

Figure 6 Detail of an immature focal adhesion point (⮜) forming at the edge of a ridge of a SilD02 substratum (S=substratum).

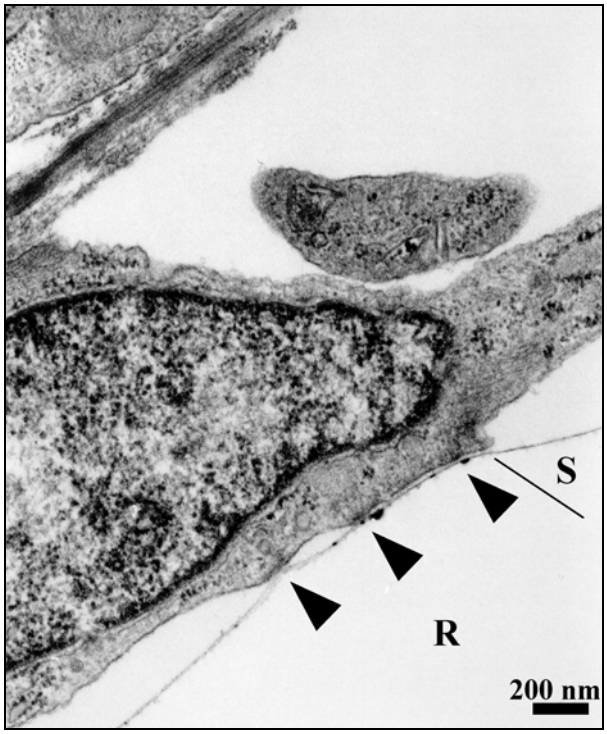

Figure 7 TEM image of a RDF on a 5.0 μm grooved silicone rubber surface (SilD05), showing a surface ridge (R) and the slope (S) leading to the bottom of the surface groove. Except from the dense plaque near the ridge edge, more focal adhesion points were seen towards the centre of the ridge area (⮜).

which possessed two dense areas on the two opposite sides of the surface ridge. Close observation at higher magnifications learned that (pre-stages of) focal adhesion points tended to centrifugal attachment to the surface ridges of the SilD02 surfaces (Figures 5 and 6).

Focal adhesion points were also observed in RDFs on the SilD05 and SilD10 substrata. Although these cells also attached to the ridges, close to the slope that separated the ridge from the surface groove, additional focal adhesion points were seen towards the centre of the ridge area (Figures 7 and 8). Furthermore, RDFs on the SilD10 substrata were occasionally seen to attach to the bottom of a surface groove (Figure 8).

In the sections made of the RDFs on the SilD02 and SilD05 substrata perpendicular to the surface grooves (Figures 4 to 7), no cytoskeletal structures could be observed that corresponded with the observed dense plaques. However, if the samples were not sectioned in a perpendicular but in a longitudinal direction parallel to the surface grooves, filamentous structures were seen near the cell membrane (Figure 9). Furthermore, focal adhesion points and close contacts were seen with a higher frequency in these longitudinal sections than in the perpendicular sections, although this was only the case if a surface ridge was captured in the longitudinal section. This was in contrast with the (ridge) sections of the SilD10 substrata, which showed focal adhesion points, close contacts, and cytoskeletal filaments in both perpendicular and longitudinal sections (Figure 10).

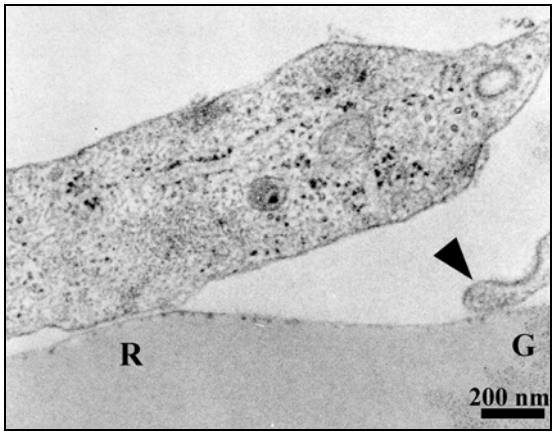

Figure 8 TEM photograph of fibroblasts on a 10.0 μm grooved silicone surface (SilD10). Focal adhesion points are present on the edge, and more towards the centre of the surface ridge (R). In addition, a contact of a cell extension with the bottom of the groove (G) can be seen (⮜).

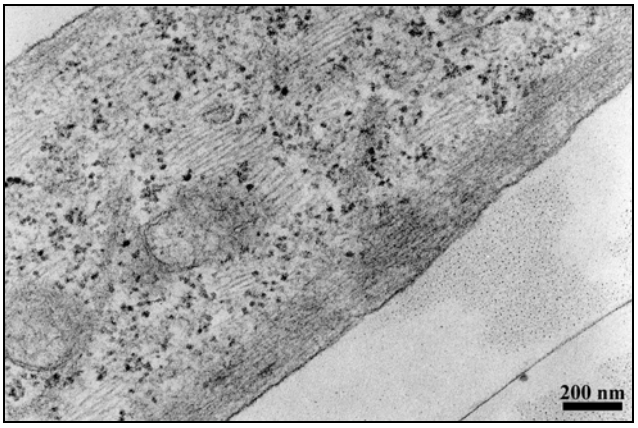

Figure 9 TEM image of a longitudinal section of a RDF on a SilD05 substratum. The filamentous structures near the cells membrane suggest orientation of the cytoskeletal components of the fibroblast on this microtextured surface.

Finally, no fibrous ECM material was found in either the perpendicular or the longitudinal sections of the smooth and microtextured substrata.

DISCUSSION AND CONCLUSIONS

Results demonstrate that the described method allows the preparation of ultrathin sections of cells cultured on (microtextured) silicone rubber substrata. Although ultrathin sections, containing both the cells and substratum is of course desirable, our technique offers a possibility to harvest TEM sections with a very limited effect on the sample and the quality of the sections made. The ability of an apolar liquid like ethylacetate to detach the silicone substrata from the Epon is based on the distribution of ethylacetate at the interface between the silicone substrata and the Epon through capillary force. As a result, ethylacetate increases the distance between these two components, thus reducing the van der Waals forces that bind the Epon to the silicone rubber substrata. This process transpires without affecting the integrity of the Epon and its contents. Because the Epon polymer matrix is more closely packed and possesses more covalent bound chain cross-links, the effect of ethylacetate on Epon is negligible. This is in contrast with the effect of ethylacetate on silicone rubber, since silicone swells because of the penetration of ethylacetate in the polymer chain matrix.

Focal adhesion points have been recognized as the points of adhesion of fibroblasts and their substratum[1-2] and have been studied extensively. A number of studies have revealed that particular ECM proteins like fibronectin[23, 26], vitronectin[26], laminin[17], fibrinogen[28], and even collagen[15] collaborate in the processes of cell attachment and cell movement. It is possible, that the electron

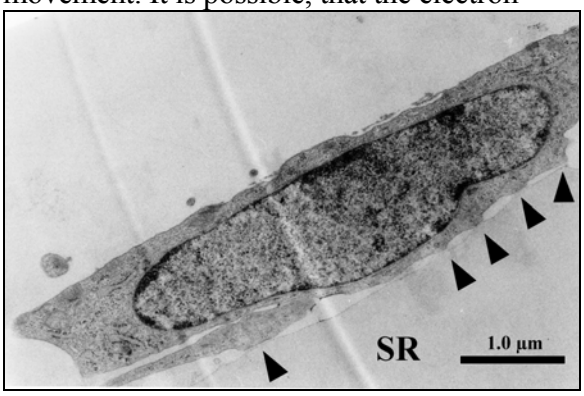

Figure 10 TEM micrograph of a longitudinal section of a RDF on a SilD10 surface. Multiple cellular attachment sites (⮜) can be seen on the surface ridge (SR).

dense layer that was observed (Figures 1 to 10) consisted of these adsorbed proteins. Future investigations with other techniques like CLSM could reveal the intricate interaction of the attachment mechanisms of the cells contacting this protein layer.

The formation of protrusions, as shown in Figure 3, has also been observed in a TEM study by Meyle et al.[18]. In agreement with Meyle and co-workers, we found that the cells did not contact with the bottom of the grooves, and appeared to attach to the ridges of the surface patterns (Figures 4 to 7). These specific attachments of the cells to the surface ridges was also observed by Meyle et al.[18-19] and in our previous studies[13]. For example, by using fluorescence microscopy Meyle et al.[19] demonstrated that gingival fibroblasts cultured on microgrooved silicone rubber substrata possessed vinculin-positive focal contacts that were localized specifically on the surface ridges. Furthermore, using low magnification phase contrast microscopy, we observed that cellular protrusions of fibroblasts cultured on microgrooved silicone substrata attached specifically to the ridges of the surface pattern[13]. On the other hand, Meyle et al.[18] also described many "grip-like" protrusions with the surface ridges. Consequently, they concluded that such an intimate interdigitation of the cell body with the surface contours would increase the shear strength up to the point of cell rupture. Such protrusions were not observed in our TEM study. An explanation could be that the surface profile of the surface ridges in our study was significantly different (rounded) from that used in the experiments of Meyle et al. (i.e. rectangular). In sum, all these studies lead to the conclusion that the ridges (≤ 5.0 μm) of the surface pattern seem to be the preferential sites for cell attachment. Although the causing effect for the specific localization of the focal adhesion points still is not clear, this conclusion supports the hypothesis by Clark et al.[10]. They suggested that the altered cell-substratum interactions are based on the resemblance of these surfaces with the fibrillar extracellular matrix.

Finally, for the cells cultured on the SilD02 and SilD05 surfaces, microfilaments were observed only in the longitudinal sections of these substrata. In contrast, cytoskeletal components were observed in both longitudinal and perpendicular sections made of the RDFs on the SilD10 surfaces. This observation suggests an alignment effect of the 2.0 and 5.0 μm ridges on the cytoskeletal components. This is in corroboration with our earlier findings, which were observed on similar surfaces by using different microscopic techniques[12-13]. Although, it has been suggested that orientation of the cytoskeletal components is responsible for cellular alignment along surface microgrooves[20], further investigations are required to clarify the role of the cytoskeleton.

ACKNOWLEDGEMENT

The authors would like to thank prof. dr. A.F. von Recum (Clemson University, USA) for the microtextured silicon wafers that were produced under his supervision in his laboratories. In addition, the authors would like to thank dr. P.H.K. Jap for his help on the analysis of the TEM images. This study is supported by the Technology Foundation (STW).

REFERENCES

1. Abercrombie M and Ambrose EJ. Interference microscope studies of cell contacts in tissue culture. *Exp Cell Res*, 1958; **15:** 332-345

2. Ambercombie M. The crawling movement of metazoan cells. In *Cell Behaviour*, R. Bellairs, ASG Curtis, and GA Dunn eds., Cambridge University Press, Cambridge, 1982

3. Bjursten LM, Emanuelsson L, Ericson LE, Thomson P, Lausmaa J, Mattsson L, Rolander U, Kasemo B. Method for ultrastructural studies of the intact tissue-metal interface. *Biomaterials*, 1990; **11:** 596-601

4. Brunette DM, Kenner GS, Gould TRL. Grooved titanium surfaces orient growth and migration of cells from human gingival explants. *J Dent Res*, 1983; **62:** 1045-1048

5. Brunette DM. The effects of implant surface topography on the behavior of cells. *Int J Oral Maxillofac Implants*, 1988; **3:** 231-246

6. Campbell CE, von Recum AF. Microtopography and soft tissue response. *J Invest Surg*, 1989; **2:** 51-74

7. Chehroudi B, Gould TR, Brunette DM. Effects of a grooved epoxy substratum on epithelial cell behavior in vitro and in vivo. *J Biomed Mater Res*, 1988; **22:** 459-473

8. Chehroudi B, Gould TRL, and Brunette DM. A light and electron microscope study of the effects of surface topography on the behavior of cells attached to titanium-coated percutaneous implants. *J Biomed Mater Res*, 1991; **25:** 387-405

9. Chehroudi B, Soorany E, Black N, Weston L. Computer-assisted three-dimensional reconstruction of epithelial cells attached to percutaneous implants. *J Biomed Mater Res,* 1995; **29:** 371-379

10. Clark P, Connolly P, Curtis ASG, Dow JAT, Wilkinson CDW. Cell guidance by ultrafine topography in vitro. *J Cell Sci*, 1991, **99:** 73-77

11. den Braber ET, de Ruijter JE, Smits HTJ, Ginsel LA, von Recum AF, Jansen JA. Effect of parallel surface micro grooves and surface energy on cell growth. *J Biomed Mater Res*, 1995; **29:** 511-518

12. den Braber ET, de Ruijter JE, Smits HTJ, Ginsel LA, von Recum AF, Jansen JA. Quantitative analysis of cell proliferation and orientation on substrata with uniform parallel surface micro grooves. *Biomaterials*, 1996; **17:** 1093-1099

13. den Braber ET, de Ruijter JE, Ginsel LA, von Recum AF, Jansen JA. Quantitative analysis of fibroblast morphology on microgrooved surfaces with various groove and ridge dimensions. *Biomaterials*, 1996; **17:** 2037-2044

14. Freshney RI. Culture of animal cells; a manual of basic technique, Alan R. Liss Inc., New York, 1987

15. Hotchin NA and Hall A. The assembly of integrin adhesion complexes requires both extracellular matrix and intracellular rho/rac GTPases. *J Cell Biol*, 1995; **131:** 1857-1865

16. Jansen JA, de Wijn JR, Wolters-Lutgerhorst JM, van Mullem PJ. Ultrastructural study of epithelial cell attachment to implant materials. *J. Dent. Res.*, 1985; **64:** 891-896

17. Mercurio AM. Laminin receptors: achieving specifity though cooperation. *Trends Cell Biol*, 1995; **5:** 419-423

18. Meyle J, Gültig K, Wolburg H, von Recum AF. Fibroblast anchorage to microtextured surfaces. *J Biomed Mater Res*, 1993; **27:** 1553-1557

19. Meyle J, Gültig K, Brich M, Hämmerle H, Nisch W. Contact guidance of fibroblasts on biomaterial surfaces. *J Mater Sci*, 1994; **5:** 463-466

20. Ohara PT, Buck RC. Contact guidance in vitro. *Exp Cell Res*, 1979; **121:** 235-249

21. Reynolds EA. The use of lead citrate at high pH as an electron opaque stain in electron microscopy. *Cell Biol*, 1963; **17:** 208-212

22. Singhvi R, Stephanopoulos G, Wang DIC. Review: effects of substratum morphology on cell physiology. *Biotechology and Bioengineering* 1994; **43:** 764-771

23. Schaller MD and Parsons JT. Focal adhesion kinase and associated proteins. *Curr Opin Cell Biol*, 1994; **6:** 705-710

24. Schmidt JA, von Recum AF. Texturing of polymer surfaces at the cellular level. *Biomaterials*, 1991; **12;** 385-389

25. Schmidt JA, von Recum AF. Surface characterization of microtextured silicone. *Biomaterials*, 1992; **13;** 675-681

26. Uitto VJ, Larjava H, Peltonen J, and Brunette DM. Expression of fibronectin and integrins in cultured periodontal ligament epithelial cells. *J Dent Res*, 1992; **71:** 1203-1211

27. Watson ML. Staining of tissue section for electron microscopy with heavy metals. *Biophys Biochem Cytol*, 1958; **4:** 475-478

28. Williams RL, Hunt JA, and Tengvall P. Fibroblast adhesion onto methyl-silica gradients with and without preadsorbed protein. *J Biomed Mater Res*, 1995; **29:** 1545-1555

CHAPTER 7

The effect of a subcutaneous silicone rubber implant with shallow surface micro grooves on the surrounding tissues in rabbits

E.T. den Braber, J.E. de Ruijter, and J.A. Jansen

University of Nijmegen, Dental School, Laboratory of Biomaterials,
POB 9101, NL-6500 HB Nijmegen, The Netherlands.

CHAPTER 7

The effect of a subcutaneous silicone rubber implant with shallow surface micro grooves on the surrounding tissues in rabbits

INTRODUCTION

The interaction between an implant material and the surrounding tissues can be considered vital for the final clinical performance of implanted artificial medical devices. For example, the promotion of tissue attachment and the concomitant reduction of the highly undesirable chronic inflammatory response and fibrosis around implant materials are of central importance for the biocompatibility of biomaterials[1]. Since various surface properties[2] of an implant material determine the biocompatibility of these materials, surface modifications based on the most recent technologies are being explored in search for the ideal implant surface[3]. This study will focus on one of these modifications, i.e. implant surface texturing on a micrometer scale.

Earlier studies have shown that microgeometrical patterns on substratum surfaces have a high potential in provoking specific cellular reactions by influencing basic cellular mechanisms like DNA/RNA related processes, cellular attachment, and cell locomotion[1-2]. This led to the idea that surface microtexturing could be used deliberately to achieve certain desired end results in processes, like morphogenesis, cell invasion, repair, and regeneration[4]. If this hypothesis proves to be true, it is obvious that surface texturing can be a very important tool in designing a successful implants[1, 4]. Unfortunately, most of the currently available information on microtextured related cellular behaviour is derived from *in vitro* experiments. *In vivo* studies with microtextured implants are scarce. Moreover, review of these *in vivo* studies shows that the design of the used textured implants is very diverse. But even with this large diversity, it is possible to perceive the possible potential of microtextured implant surfaces on several implant related processes. For example, some studies[5-6] have reported on the reduction of epithelial downgrowth with microgrooved skin penetrating devices. Other investigators, which implanted microporous or pillared surfaces subcutaneously, found tightly adherent fibrous capsules without inflammatory cells[7], reduced fibrosis[8], and improved blood vessel proximity[8]. These results, together with the fact that our laboratory has been involved in the development of a new, subcutaneous anchored, percutaneous device for more than 10 years[9-13], suggested evidently a study of the tissue response to standardized surface patterns. Therefore, the specific aim of this study was to evaluate the effect of a subcutaneous implant with a standardized pattern of shallow surface micro grooves on the surrounding tissues in rabbits.

MATERIALS AND METHODS

Production and characterization of the microtextured substrata

Surface textured experimental substrata were produced by first making silicon oxide moulds with photolithography[14-15]. These moulds were covered with silicone elastomer (MDX 4-4210, Dow Corning) and after polymerization the silicone rubber surface replica was removed from the mould. The final experimental implants were obtained by cutting the silicone

TABLE I

Designer values of the micro grooves on the silicon mould surface (Gd=groove depth, Gw=groove width, Rw=ridge width, and P=pitch).

	Designer values			
Surface	*Gd (μm)*	*Gw (μm)*	*Rw (μm)*	*P (μm)*
SilD00	----	----	----	----
SilD02	0.50	2.00	2.00	4.00
SilD05	0.50	5.00	5.00	10.00
SilD10	0.50	10.00	10.00	20.00

rubber castings into round discs. All implants had a diameter of 15.0 mm, were 1.45 mm thick, and had one smooth and one textured side. Subsequently, the implants were cleaned as described before[16] and prepared for implantation by radio frequency glow discharge (RFGD; PDC-3XG, Harrick; Argon, 0.15 Torr, 5 minutes). After RFGD treatment the implants were stored in sterile 6 well cell culture plates (Greiner) for transport to the operation theatre.

Additional implants were produced to enable surface characterization. The production process and post production treatment of these implants was identical to those produced for implantation. The surfaces of the implants were investigated by scanning electron microscopy (SEM; JEOL 6310) and atomic force micro-

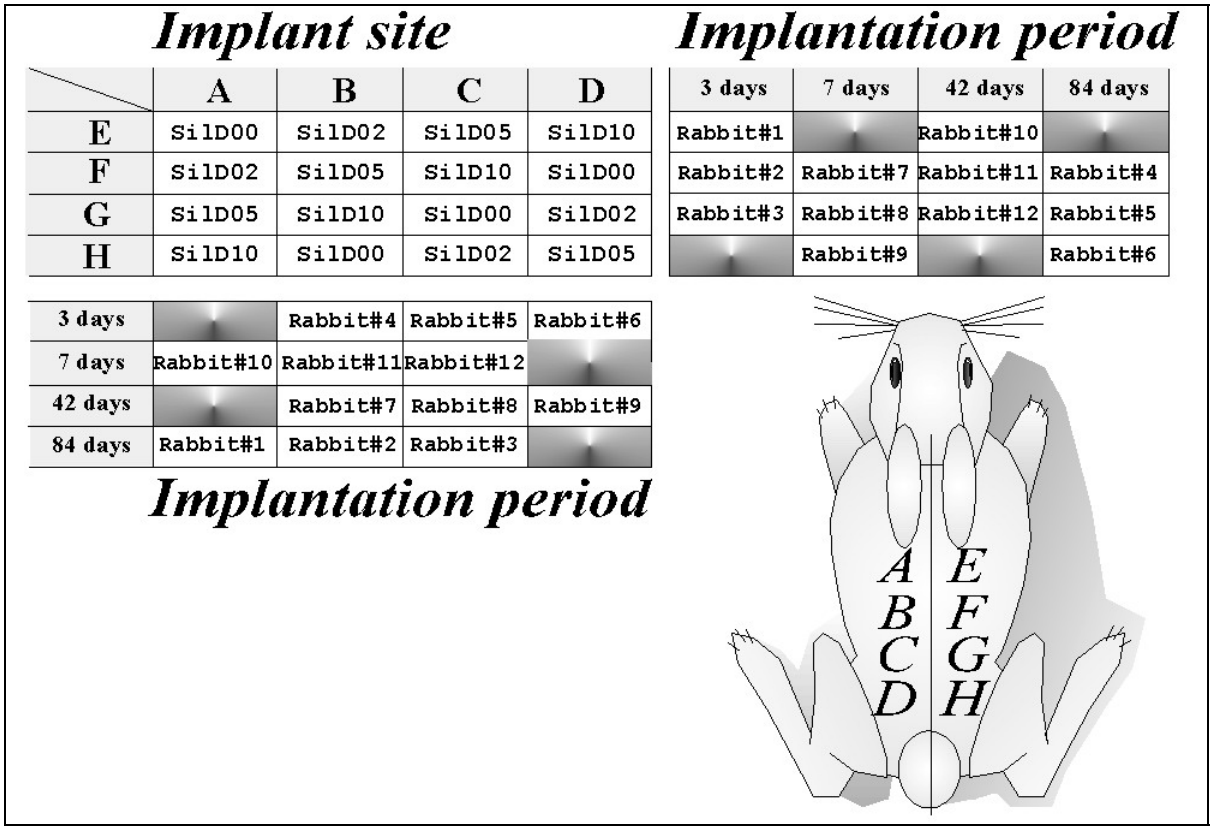

Figure 1 The schematic drawing of the rabbit shows the sites of implantation. The letters of these sites (A to D, and E to H) correspond with the letters in the upper left hand table. This table, together with the two additional tables make it possible to determine which implant (smooth or textured) was implanted at which specific site. For example, the implantation periods for rabbit #8 were 7 (top right hand table) and 42 (bottom table) days. During the 7 day period, the SilD10 implant was located on site B and the SilD02 implant on site D (read upper left hand table from left to right), while during the 42 day period the SilD00 implant was located at site G (read upper left hand table from top to bottom). Implant textures are given in Table I.

scope (AFM; Polaron SP300). The designer dimensions of the surface patterns can be found in Table I.

Animal model and implantation

For implantation, a total of 12 female New Zealand White rabbits, 3 months of age (2-6 kg), were used. The smooth and textured implants were inserted for periods of 3, 7, 42, and 84 days (Figure 1), and were placed in four separate surgical sessions, set up according to the split plot design[17]. During every surgical session, the implants were placed on either the left or right side of the spinal column, enabling the evaluation of two implantation periods within a single rabbit. Randomization of the site of implantation for the various types of implant texture and length of implantation period was achieved with a Latin square implantation schedule (Figure 1). For every period of implantation, six implants with an identical surface texture were used. In total, 96 implants were evaluated during this study.

Before surgery, the skin was shaved, washed and disinfected with iodine. The actual surgical procedures were performed under general anaesthesia, induced by intramuscular injection of Hypnorm™ (0.5 ml/kg) and atropine (0.5 mg/animal). After orotracheal intubation, anaesthesia was maintained by ethrane (2.0-3.0%) through a constant volume ventilator. During each surgical session, four paravertebral incisions of approximately 15 mm were made. Lateral to these incisions small subcutaneous pockets were created by blunt dissection with scissors. The implants were inserted in the pockets (textured side medial), but were not fixed with sutures. Finally, the wounds were closed intracutaneously with Vicryl™ 3-0. To reduce the perioperative infection risk, prophylactic antibiotic Terramycine™ was administered postoperatively. After surgery, the animals were placed in a cage and allowed to move

TABLE II

Parameters used in the statistical analysis of the soft tissue microtextured silicone rubber implants

GENERAL

--- Section# [independent]
--- Animal# [independent]
--- Side [L/R]
--- Site [1/2/3/4]
--- Implantation period [3/7/42/84]
--- Implant texture [0/2/5/10]

CAPSULE, LOCALISATION

--- No capsule present [1]
--- Capsule on 1 (dermis) side [2]
--- Capsule on 1 (medial) side [3]
--- Capsule on 2 sides present [4]

CAPSULE, FORMATION

--- No capsule present [1]
--- Loose, fibro-elastic [2]
--- Loose, adipose [3]
--- Loose, fibro-adipose [4]
--- Less dense [5]
--- Dense [6]

CAPSULE, CELLULAR

--- Fibroblast thickness
[1=0, 0<2<5, 5<3<10, 10<4<30, 5>30]
--- Fibroblasts contacting surface [1=YES, 2=NO]
--- Acute/chronic inflam. process [1=AC, 2=CHR]
--- Severity inflammatory process [1=none, 4=severe]
--- Inflammatory cells location
[1=non, 2=end, 3=middle, 4=2+3]
--- Inflam. cells contacting surface [1=YES, 2=NO]
--- macrophages [1=YES, 2=NO]
--- giant cells [1=YES, 2=NO]
--- PMNs [1=YES, 2=NO]
--- plasma cells [1=YES, 2=NO]
--- Blood vessels present [1=YES, 2=NO]
--- mature/new vessels [1=MAT, 2=NW]

CAPSULE SURROUNDING TISSUES

--- Acute/chronic inflam. process [1=AC, 2=CHR]
--- Severity inflammatory process [1=none, 4=severe]
--- macrophages [1=YES, 2=NO]
--- giant cells [1=YES, 2=NO]
--- PMNs [1=YES, 2=NO]
--- plasma cells [1=YES, 2=NO]
--- Blood vessels present [1=YES, 2=NO]
--- mature/new vessels [1=MAT, 2=NW]

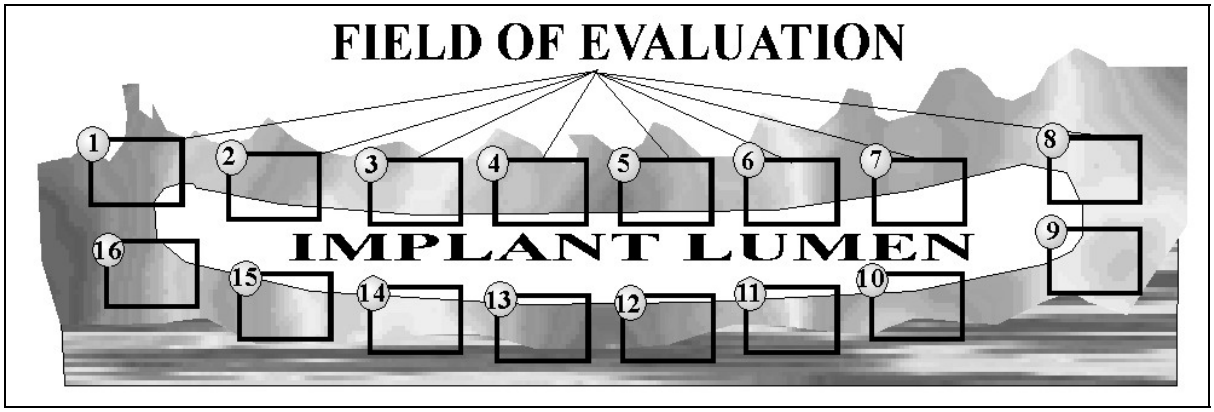

Figure 2 Schematic drawing representing a section. The implant lumen is clearly visible. For histomorphometric evaluation a total of 16 evaluation areas were used.

unrestricted at all times. Normal tap water and standard rabbit chow were provided ad libitum.

Histological evaluation

At the end of the implantation periods, the animals were killed with an overdose Nembutal™ (i.v., 150 mg/kg). The skin was shaved and the implants with the surrounding tissues were excised immediately. A patch of tissue, containing one implant only, was labelled with an unique code, linking it directly to an implant with a specific surface texture, test animal, the date of removal, and the site of implantation. After fixing the specimens with 10% buffered formalin solution through immersion for 72 hours, the tissue patch with the embedded implant was cut into two equally large pieces. Subsequently, the implant became visible and was removed from the tissue capsule with tweezers. These removed halves of the silicone rubber implants were prepared for SEM examination as described earlier[18]. In short, these samples were dehydrated by rinsing with 100% methanol for 5 minutes, air dried, sputter coated with gold and investigated by SEM (JEOL 6310).

After removal of the silicone implants, the tissue specimens were prepared for observation with confocal laser scanning microscopy (CLSM) and normal light microscopy (LM). Therefore, the samples were dehydrated through a series of graded alcohol and Histoclear™, and embedded in Paraplast™. Subsequently, 5.0 µm sections were cut with a Leitz microtome and stained with haematoxylin eosin (Mayer), Azan, May-Grünwald-Giemsa, trichrome (Goldner) and Picro-Sirius Red stains[19]. Since the Picro-Sirius Red stain exhibits auto-fluorescent properties when excited at λ=568 nm, observation with a CLSM (Bio-Rad MRC 1000, Bio-Rad Laboratories) was possible. Subsequently, the Picro-Sirius Red sections were viewed with normal and oil objectives, mounted on a Nikon Diaphot microscope. Digital images were captured and stored as described earlier[20], and additional 3 dimensional reconstruction of the stained tissues was performed by using the Confocal Assistant V3.10 for Windows™ 3.1x program (available at FTP.GENETICS.BIO-RAD.COM; copyright Todd Clark Brelje, 1995).

In short, the histological assessment parameters for LM were:

-1- the general appearance of the tissues surrounding the implant.
-2- the presence and number of inflammatory cells, i.e. macrophages, giant cells, polymorphonuclear granulocytes (PMNs), and plasma cells.
-3- the number and status of blood vessels in the surrounding fibrous capsule.

For the analyses of all the stained sections a refined histomorphometric grading scale[17, 21] was used (Table II). Per examined section, the implant surrounding tissues were evaluated by gathering the scores of the histomorphometric parameters in Table II for 16 predetermined fields (Figure 2). After scanning six sections of each implant, the results of the light microscopical evaluation were evaluated with SAS™ (release 6.03, SAS Institute Inc., USA), using univariate tests, Fisher Exact tests, and Spearman correlation models.

RESULTS

Macroscopic findings

Eight days after the start of the experiment, one of the 12 animals died due to pneumonia. This animal was replaced by a new rabbit, which received identical treatment and completed the initial implantation period. Except from this incident, all the experimental animals appeared to be in good health throughout the test period, and none of the rabbits had any wound complications. At sacrifice, all silicone rubber implants were surrounded by a thin, reaction-free fibrous capsule. Macroscopically, there were no indications of differences in capsule thickness between the various implantation periods.

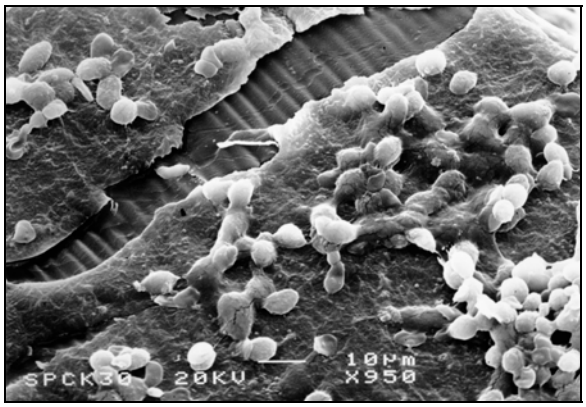

Figure 3 SEM micrograph of the surface of a 2.0 µm grooved implant after a 3 day implantation period. Underneath the dense layer with fibroblasts, the original grooved silicone surface is visible. On top of this layer erythrocytes and inflammatory cells can be seen.

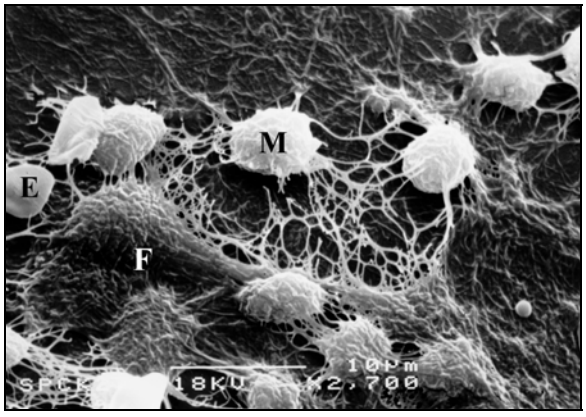

Figure 4 SEM image of 5.0 µm grooved implant after 3 days of implantation. The silicone surface is totally covered and the surface grooves are not visible. Fibroblasts (F), macrophages (M), erythrocytes (E), and many fibrin fibres are present.

SEM observation of the excised implants

SEM examination revealed that, after an implantation period of 3 and 7 days, the surface of all implants was covered with a dense layer. Fibroblasts proved to be embedded in this layer, while erythrocytes, lymphocytes, and macrophages were seen on top of this layer (Figures 3 and 4). Furthermore, large quantities of fibrin (Figure 4) and collagen (Figure 5) were seen. The collagen fibres were located on top of the dense layer or directly in contact with the silicone surface. These fibres appeared to be orientated randomly on all textured surfaces.

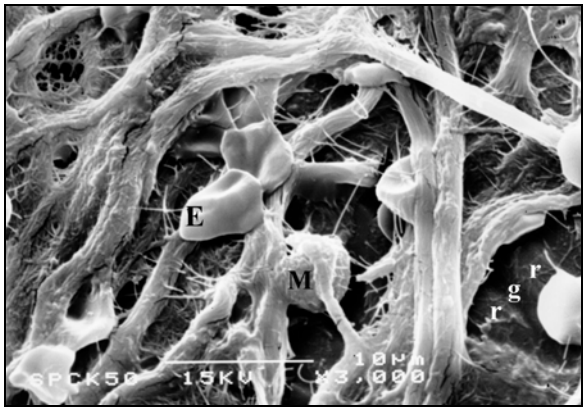

Figure 5 On this SEM image (3 days of implantation), the 2.0 µm grooved silicone surface (g=groove, r=ridge) is visible underneath the collagen fibres. Several punctured erythrocytes (E) and a macrophage (M) are located within the collagen matrix.

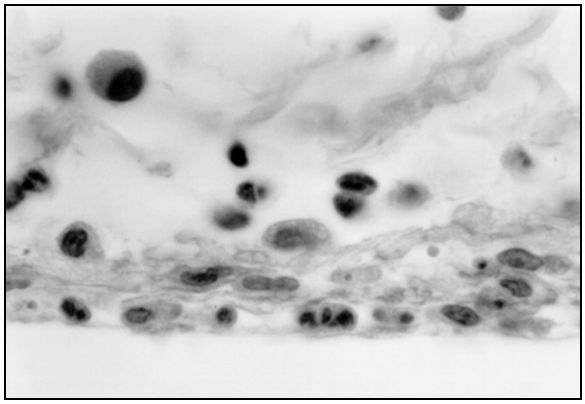

Figure 6 Detail of the inflammatory cell accumulation at the interface after 3 days of implantation. (10.0 µm grooved implant; HE stain; original magnification 400x)

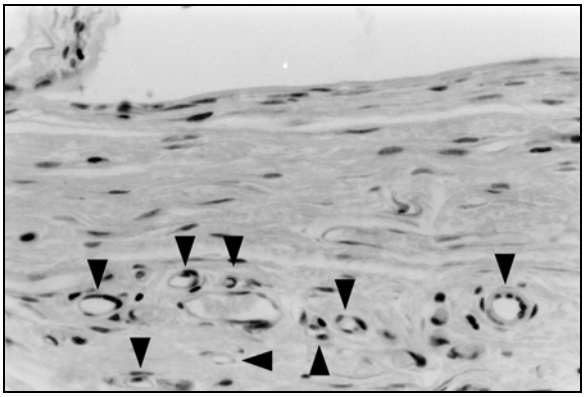

Figure 8 After 7 days implantation many blood vessels (⮝⮟) can be seen in the capsule. The more tightly packed capsule possessed several layers of flattened fibroblasts. (2.0 µm grooved implant; original magnification 160x)

After 42 and 84 days of implantation, only few collagen fibres were observed on the surfaces of the retrieved silicone implants. On most of the implant surfaces only a dense deposit was visible. Occasionally, fibroblasts were seen, but these cells did not show any signs of alignment to the surface pattern. As with the various textured implants after an implantation period of 3 and 7 days, no differences were found in the number of cells or the amount of ECM material on the smooth and textured surfaces.

Descriptive LM and CLSM evaluation of the implant surrounding tissues

Gross evaluation of the differently stained sections revealed that the tissue reaction to all implants appeared to be relatively uniform. After a 3 day implantation period, LM showed that the implants were surrounded by a loose collagen matrix, containing fibroblasts and many inflammatory cells, i.e. granulocytes, macrophages, and monocytes (Figure 6). At the interface between implant and the surrounding tissues, these inflammatory cells had accumulated, while very few fibroblasts were seen at this location. In addition to the LM observation, 3 dimensional reconstruction of loose collagen matrix surrounding the implants after 3 days revealed that very long collagen fibres were present, following the surface of the implant (Figure 7). More or less perpendicular to these long fibres, smaller collagen fibres were seen, forming a type of lattice. Finally, many globular structures were observed, which appeared to be attached to this loose collagen lattice.

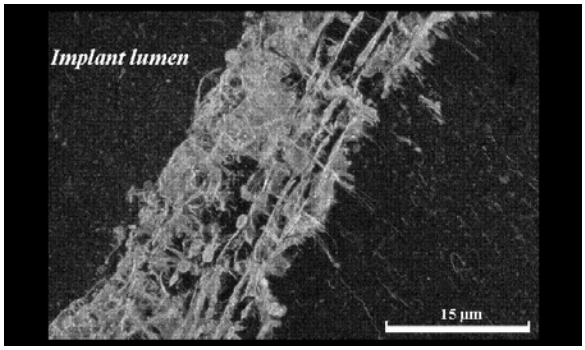

Figure 7 Three dimensional reconstructed CLSM image of the collagen fibres in the implant surrounding capsule after 3 days of implantation (5.0 µm grooved implant). The collagen fibres are orientated parallel and perpendicular to the implant surface. In addition, small globular collagen concentrations can be seen.

CLSM observation of the tissues after an implantation period of 7 days showed a transition of the implant surrounding capsule from a loose collagen matrix to a more densely packed capsule. The collagen fibres in these capsules were much thicker. In addition, all fibres seemed orientated parallel to the initial implant surface. LM investigation showed several layers of fibroblasts, which appeared

as either active cells with a round nucleus or as highly elongated cells with a flattened nucleus. Very often these flat, elongated fibroblasts were found in or close to the surface layer of the tissues bordering the implant lumen. In addition, many sections showed newly formed vessels (Figure 8). All sections displayed a large decrease of the number of inflammatory cells. This decrease was seen most clearly at the interface between the tissues and the implant lumen, where no or little inflammatory cells were observed after 7 days (Figure 9).

The histological appearance of the tissues after the 42 and 84 day implantation periods was highly comparable. With both implantation periods, implant surrounding capsules were seen to consist out of tightly packed, mature collagen. Embedded in this matrix, flat elongated fibroblasts were observed. At the interface between the tissues and the lumen of the removed implant flattened fibroblasts, but no inflammatory cells were seen (Figure 10).

Histomorphometric evaluation of the implant surrounding tissues

Statistical analysis with the Spearman correlation model showed that there was no correlation between the location of a specific implant type (Figure 1) and the values of investigated parameters (Table II) for each of the implantation periods ($0.10052 \leq r_s \leq 0.31569$). However, high correlation was found when parameter scores were compared for the same evaluation fields (Figure 2) of identical textured implants within a single implantation period ($0.88941 \leq r_s \leq 0.96923$). In contrast, the correlation between fields 10 to 15 (smooth side implant; Figure 2) of the different textured implants within a single implantation period proved to be relatively low ($0.19560 \leq r_s \leq 0.37317$).

Statistical evaluation of parameters mentioned in Table II with a Fisher Exact test

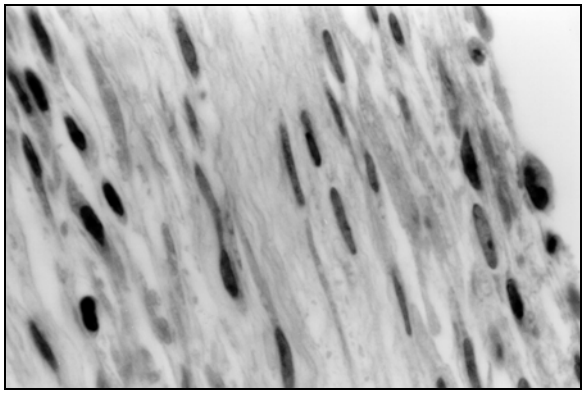

Figure 9 Magnification showed the decrease of the number of inflammatory cells at the interface, and the various nucleus shapes of the fibroblasts in the capsule after 7 days of implantation. (2.0 μm grooved implant; Mason Trichrome stain; original magnification 400x)

showed that the capsule surrounding all implants became significantly more dense with increasing length of the implantation period ($2.17 \times 10^{-5} \leq P_{3\text{-}84\ days} \leq 0.0241$). Furthermore, the thickness of this capsule, measured by counting the layers of fibroblasts, proved to increase significantly over time ($7.36 \times 10^{-8} \leq P_{3\text{-}84\ days} \leq 0.0054$). On the other hand, no significant differences in capsule density or thickness were detected between the smooth and the textured implant surfaces for all implants during all implantation periods (Figure 11).

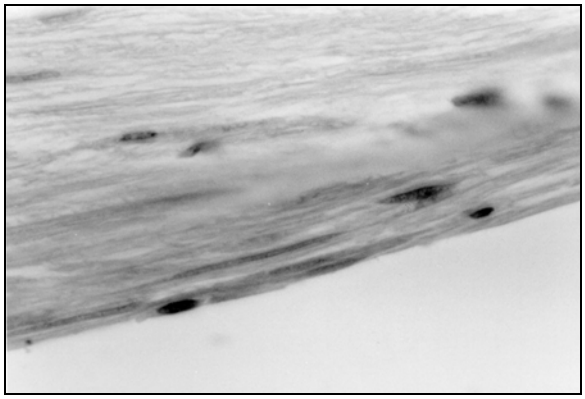

Figure 10 High magnification of the fibroblasts at the interface of capsule and implant lumen after 84 days of implantation. The fibroblasts are flattened and arranged parallel to the implant surface. No inflammatory cells are present. (5.0 μm grooved implant; Mason Trichrome stain; original magnification 400x)

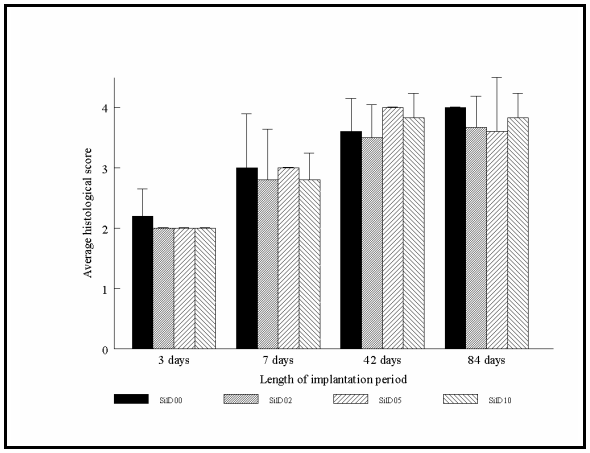

Figure 11 Average histological scores for capsule thickness (Table II). No significant differences were detected between the various textured implants with identical implantation periods.

In contrast, differences were found for the number of inflammatory cells that were present at the interface between the implant lumen and surrounding tissues (Figure 12). It proved that after an implantation period of 42 and 84 days, significantly more inflammatory cells ($0.0018 \leq P \leq 0.026$) were present at the interface with the SilD00 implant lumen than at the SilD02, SilD05, and SilD10 implant lumen interface. No significant differences in the number of inflammatory cells were detected between the smooth and textured side of the SilD02, SilD05, and SilD10 implants. More-

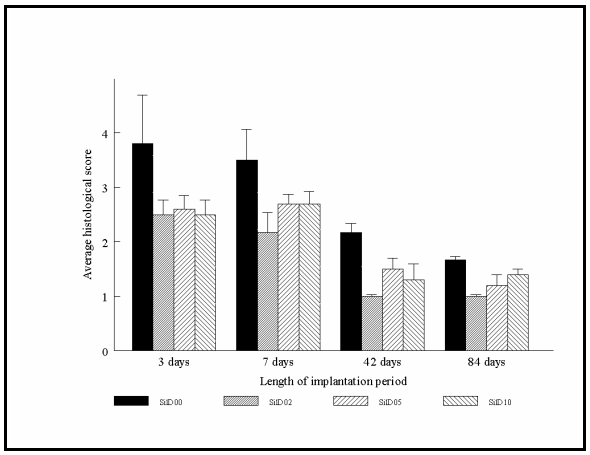

Figure 12 Average histological scores for the severity of the inflammatory process (Table II). Significant differences were detected between the smooth and the textured implants for all implantation periods.

over, significantly more inflammatory cells were present in the SilD00 implant capsules than in SilD02, SilD05, and SilD10 implant capsules during all the incubation periods ($0.00625 \leq P_{3\text{-}84\ days} \leq 0.0158$). During these implantation periods, it was found that the various types of inflammatory cells in the tissues surrounding the smooth and textured implants did not differ ($P_{3\text{-}84\ days} \geq 0.122$). Finally, no significant differences concerning the presence, position, or type of inflammatory cells were found for the SilD02, SilD05, and SilD10 implants ($P_{3\text{-}84\ days} \geq 0.211$).

For the presence and location of blood vessels, it was found that the number of vessels that were present in the capsules of all implants did differ significantly. After 7 days of implantation, small vessels were present in the capsule of all implants. Statistical testing showed that the number of vessels in the capsule was significantly lower with the SilD00 implants than with the SilD02, SilD05, and SilD10 implants ($0.00293 \leq P_{7\text{-}84\ days} \leq 0.0272$). No significant differences in the number of vessels were detected between the SilD02, SilD05, and SilD10 implants and the textured and smooth side of the these implants. Finally, the number of vessels that was observed in the capsule of all implants was the highest after 7 days of implantation, and significantly decreased with longer implantation periods ($P \leq 0.0469$).

DISCUSSION AND CONCLUSIONS

The results of this study did not show significant differences in capsule thickness between smooth and textured implant surfaces (Figure 11). Although the CLSM images made it possible to observe the development of the collagen matrix in the capsule over time, no differences could be detected that might have been caused by the texture of the implant surfaces. In addition, the histological evaluation combined with the statistical analysis showed that after 84 days of implantation the

capsules surrounding all implants were at least 20 fibroblasts thick. These findings do not support the hypothesis that microtextured implant surfaces reduce the size of the capsule surrounding these implants[1-2]. According to this hypothesis, the size of the capsule is reduced by mechanical interlocking between the implant and the surrounding tissues. The interlocking would reduce the stress and movement at the implant interface and limit the consequential "mechanical irritation" of the surrounding tissues, which is supposed to induce tissue damage, fibrosis, and severe inflammatory responses[1-2, 7-8]. Other investigators indeed have reported reduction of the capsule size due to microtextured surfaces. However, review of these studies[7-8, 22-23] shows that the surface texture of the implants in these studies differs significantly from our implants, both in terms of microfeature appearance (pores, pillars, tapered pits, or V-shaped grooves) and dimensions (feature depth, size, and pitch). These considerable differences make it possible to suggest that the dimensions of our grooves and ridges were not sufficient to facilitate mechanical interlocking. As a result, the "mechanical irritation" of the smooth and grooved surfaces would be comparable, resulting in capsules of equal thickness. Furthermore, our textured implants possessed one smooth and one textured side. Although this opened up the possibility for intra-implant evaluation, it did not enhance possible mechanical interlocking between the implant and the surrounding tissues. Therefore, it can be questioned whether the capsule thickness would have been less, if both sides of the implant would have been textured.

Considering the results found for the capsule thickness, it is remarkable that significantly more inflammatory cells were present in the smooth implant capsules than in the capsule surrounding the textured implants (Figure 12). In addition, it is surprising that these differences were not found between the smooth and textured side of the SilD02, SilD05, and SilD10 implants. This suggests that the influence of the textured implant surface on the surrounding tissue transcends the area directly in contact with these surfaces. Several hypotheses apply as possible explanations for the observed discrepancies. For instance, it is suggested that mechanical interlocking could reduce the interfacial shear forces which are supposed to induce severe inflammatory responses. However, considering the thickness of the implant surrounding capsule, it remains doubtful whether mechanical interlocking did occur. Another possibility could be that direct attachment of fibroblasts to the implant surface promotes implant immobilization and therefore prevents or diminishes the presence of inflammatory cells at the implant/tissue interface[5]. That fibroblasts attach to the implants was observed with SEM, while LM showed that fibroblasts were present at the interface between tissues and implant lumen after prolonged implantation (Figure 10). The question remains however, if this direct attachment of fibroblasts to the implant surface is strong and durable enough to induce the observed differences in inflammatory response.

Our SEM observations also showed that the fibroblasts on the textured implant surfaces did not orientate themselves parallel to the surface grooves. This is not in agreement with the findings of earlier *in vitro* studies[1-2, 4, 16, 18, 26-28]. In addition, our previous CLSM study[20] with RDFs on microtextured surfaces showed that intracellular components were aligned along SilD02 grooves and ridges. A possible explanation for these differences between *in vitro* and *in vivo* orientational cell behaviour could be that the cells that are used in *in vitro* studies are isolated cells, which have no contact with other cells, cell types, or ECM. Previous studies[4, 26-27] show that prolonged *in vitro* incubation on microtextured surfaces results

in the formation of cell-cell contacts, an increase of the spread area, and a decrease of the orientation of the cells on these surfaces. Consequently, it was supposed that the observed guidance phenomenon is an initial response of cells *in vitro* to certain microtextured surfaces, which is lost gradually after cell-cell contacts are formed[4, 26-27]. In tissues, these contacts with other cells are already present, which could mean that the orientational effect of the textured surfaces is overruled by stronger tissue related signals or cues.

Concerning the vascularity of the capsules, we observed that significantly more blood vessels were present in the capsules of the microgrooved implants after 7 days of implantation. Although other studies[8, 24] also reported a higher incidence of blood vessels in the capsules surrounding textured implants, the validity of a comparison can be questioned. Indeed, in both studies microtextured silicone rubber implants were used, but the textures of the surfaces were considerably different. In one study[24], an aspecific, non characterized, rough surface was used, while in the other[8] a pillared surface was implanted with pillars 10,000 times higher as the ridges in this study. Furthermore, the latter only reports an improved blood vessel proximity, and does not issue any statements on the origin or status of these vessels. In our study, the observed vessels after 7 days of implantation appeared to be newly formed, but their numbers decreased with longer implantation periods. This could indicate that the formation and presence of these vessels were part of the proliferation phase of the woundhealing process[29]. This proliferation phase is a part of the formation of granulation tissue, which is characterized by high fibroblast densities, the formation of new blood vessels, and a new connective tissue matrix[29]. After repair, the number of the vessels decreases generally, marking the end of the woundhealing process and the start of a steady state. The fact that more vessels were observed around the textured implants during our study could indicate at a higher rate of tissue repair.

In conclusion, it can be said that our study did not show any changes in thickness of the implant surrounding capsule due to the shallow implant surface grooves. As mentioned before, deeper grooves could perhaps improve the mechanical interlocking between the tissues and the implant, thereby reducing the thickness of the capsule. If such a reduction could be achieved, this would enhance the performance of many soft tissue implants. In addition, differences were observed in inflammatory response and the number of bloodvessels. Further research could perhaps clarify what mechanisms cause these phenomena and whether the observed differences change if the depth of the surface grooves increases.

ACKNOWLEDGEMENT

The authors would like to thank prof. dr. A.F. von Recum (Clemson University, USA) for the microtextured silicon wafers that were produced under his supervision. In addition, the help of dr. P.H.K. Jap and H.A.L. van der Lee with the histological staining procedures was greatly appreciated. This study is supported by the Technology Foundation (STW).

REFERENCES

1. A.F. von Recum and T.G. van Kooten, "The influence of micro- topography on cellular response and the implications for silicone implants," *Journal of Biomaterials Science - Polymer Edition,* **7,** 181-198 (1995)

2. R. Singhvi, G. Stephanopoulos, D.I.C. Wang, "Review: effects of substratum morphology on cell physiology," *Biotechnology and Bioengineering,* **43,** 764-771 (1994)

3. B.D. Ratner, "New ideas in biomaterial science - a path to engineered biomaterials," *J. Biomed. Mater. Res.*, **27,** 837-850 (1993)

4. A.S.G. Curtis, and Clark P, "The effects of topographic and mechanical properties of

materials on cell behavior," *Critical Reviews in Biocompatibility,* **5,** 344-362 (1990)

5. B. Chehroudi, T.R. Gould, and D.M. Brunette, "Effects of a grooved epoxy substratum on epithelial cell behavior in vitro and in vivo," *J. Biomed. Mater. Res.,* **22,** 459-473 (1988)

6. B. Chehroudi, T.R.L. Gould, and D.M. Brunette, "A light and electron microscope study of the effects of surface topography on the behavior of cells attached to titanium-coated percutaneous implants," *J. Biomed. Mater. Res.,* **25,** 387-405 (1991)

7. C.E. Campbell, and A.F. von Recum, "Microtopography and soft tissue response," *J.Invest. Surg.,* **2,** 51-74 (1989)

8. G.J. Picha, and R.F. Drake, "Pillared-surface microstructure and soft-tissue implants: Effect of implant site and fixation," *J. Biomed. Mater. Res.,* 30, 305-312 (1996)

9. J.A. Jansen, and K. de Groot, "Guinea pig and rabbit model for the histological evaluation of permanent percutaneous implants," *Biomaterials*, **9,** 268-272 (1988)

10. J.A. Jansen, J.P.C.M. van der Waerden, H.B.M. van der Lubbe, and K. de Groot, "Tissue response to percutaneous implants in rabbits," *J. Biomat. Mater. Res.,* **24,** 295-307 (1990)

11. J.A. Jansen, "Development of a new percutaneous access device for implantation in soft tissues," *J. Biomed. Mater. Res.*, **25,** 1535-1545 (1991)

12. J.A. Jansen, J.P.C.M. van der Waerden, and K. de Groot, "Fibroblast and epithelial cell interactions with surface-treated implant materials," *Biomaterials,* **12,** 25-31 (1991)

13. J.A. Jansen, E.T. den Braber, and Y. Paquay, "Percutaneous implants," in *Materials in Clinical Applications; Advances in Science and Technology, 12*, P. Vincenzini (ed.), Techna, Faenza, Italy, 1995, pp. 779-790

14. J.A. Schmidt, and A.F. von Recum AF, "Texturing of polymer surfaces at the cellular level," *Biomaterials* **12,** 385-389 (1991)

15. J.A. Schmidt, and A.F. von Recum, "Surface characterization of microtextured silicone," *Biomaterials* **13,** 675-681 (1992)

16. E.T. den Braber, J.E. de Ruijter, H.T.J. Smits, L.A. Ginsel, A.F von Recum, and J.A. Jansen, "Quantitative analysis of fibroblast morphology on microgrooved surfaces with various groove and ridge dimensions," *Biomaterials*, **17,** 2037-2044 (1996)

17. J.A. Jansen, and M.A. van't Hof, "Histological assessment of sintered metal-fibre-web materials," *J. Biomaterials Appl.* **9,** 30-54 (1994)

18. E.T. den Braber, J.E. de Ruijter, H.T.J. Smits, L.A. Ginsel, A.F. von Recum, and J.A. Jansen, "Effect of parallel surface microgrooves and surface energy on cell growth," *J. Biomed. Mater. Res.* **29,** 511-518 (1995)

19. L. Vacca, *Laboratory manual of histochemistry*, Raven Press, New York, 1985

20. E.T. den Braber, J.E. de Ruijter, L.A. Ginsel, A.F. von Recum, and J.A. Jansen, "Confocal laser scanning microscopical study of the cytoskeletal architecture, attachment complexes, and protein depositions of fibroblasts cultured on silicone micro grooved surfaces," *J. Biomed. Mater. Res.*, accepted 1997

21. J.A. Jansen, W.J.A. Dhert, J.P.C.M. van der Waerden, and A.F. von Recum, "Semi-quantitative and qualitative histologic analysis method for the evaluation of implant biocompatibility," *J. Invest. Surg.* **7,** 123-134 (1994)

22. C.A. Squier, and P. Collins, "The relationship between soft tissue attachment, epithelial downgrowth and surface porosity," *J. Perio. Res.* **16,** 434-440 (1981)

23. B. Chehroudi, T.R. Gould, and D.M. Brunette, "The role of connective tissue in inhibiting epithelial downgrowth on titanium-coated percutaneous devices," *J. Biomed. Mater. Res.*, **26,** 493-515 (1992)

24. S. Bern, A. Burd, and J. May jr., "The biophysical and histologic properties of capsules formed by smooth and textured silicone implants in the rabbit," *Plast. Reconstr. Surg.*, **89,** 1037-1042 (1992)

25. A.F. von Recum, H. Opitz, and E. Wu, "Collagen types I and III at the implant/tissue interface," *J. Biomed. Mater. Res.*, **27,** 757-761 (1993)

26. P. Clark, P. Connolly, A.S.G. Curtis, J.A.T. Dow, and C.D.W. Wilkinson, "Cell guidance by ultrafine topography *in vitro*", *J. Cell Sci.*, **99,** 73-77 (1991)

27. E.T. den Braber, J.E. de Ruijter, H.T.J. Smits, L.A. Ginsel, A.F von Recum, and J.A. Jansen, "Quantitative analysis of cell proliferation and orientation on substrata with uniform parallel surface micro-grooves," *Biomaterials*, **17,** 1093-1099 (1996)

28. B. Chehroudi, and D.M. Brunette, "Effects of surface topography on cell behavior," *Encyclopedic Handbook of Biomaterials and Bioengineering*, D.L. Wise, D.J. Trantolo, D.E. Altobelli, M.J. Yaszemski, J.D. Gresser, E.R. Schwartz (eds.), Marcel Dekker Inc., New York, 1995, 813-842

29. H.P. Ehrlich, "Regulation der Wundheilung aus der Sicht des Bindesgewebes," *Der Chirurg*, **66,** 165-173 (1995)

CHAPTER 8

SEM, TEM, and CLSM observation of fibroblasts cultured on microgrooved surfaces of bulk titanium substrata

E.T. den Braber[1],
H.V. Jansen[2], M.J. de Boer[2], H.J.E. Croes[3],
M. Elwenspoek[2], L.A. Ginsel[3], and J.A. Jansen[1]

[1]Department of Biomaterials, University of Nijmegen, Dental School,
POB 9101, NL-6500 HB Nijmegen, The Netherlands
[2]MESA Research Institute, Department of Electrical Engineering, University of Twente,
POB 217, NL-7500 AE Enschede, The Netherlands
[3]Faculty of Medical Sciences, Department of Cell Biology and Histology, University of Nijmegen,
POB 9101, NL-6500 HB Nijmegen, The Netherlands

CHAPTER 8

SEM, TEM, and CLSM observation of fibroblasts cultured on microgrooved surfaces of bulk titanium substrata

INTRODUCTION

Previous research has demonstrated that the response of cells and tissues to implant surfaces with micropatterns is unique and reproducible[1-3]. The results of these experiments have provided many investigators with the opportunity to hypothesize on the usefulness and advantages of textured implant surfaces over smooth ones. For example, in an extensive review by Curtis and Clark[3] on this subject, some suggestions are summed up in favour of the application of surface micropatterns to medical devices, e.g.

-1- Reduction of lymphocyte penetration into grafted skin.
-2- Improving nervous system regeneration, in particular spinal cord regeneration.
-3- Trapping cells such as tumour cells in topographical traps. Topographical traps in this case could be shapes that immobilize cells in certain positions.
-4- Aligning and improving connective tissue and intracellular material.
-5- Forming tubules of cells such as various ducts and capillaries.

Recognizing the possible potential of microtextured implant surfaces, many investigators have studied cellular behaviour to various micropatterns produced in glass, polystyrene, silicon, quartz, Epon surface replicas, and silicone rubber surface replicas[2, 4-9]. Although many silicone rubber implants do exist, other materials like titanium are usually used for implant purposes. However, until now this material was never applied in microtexturing experiments due to difficulties of producing micropatterns in the surface of this metal. Some have tried to solve this problem by coating plasma etched silicon surfaces with titanium[9]. But, although these studies have presented very useful results, this method offers no satisfactory solution for the fabrication of micropatterned titanium implant surfaces.

Therefore, the aim of this study was:

-1- to investigate the possibility of producing micropatterns in bulk commercially pure titanium (cpTi), a frequently used biomaterial.
-2- to compare fibroblast behaviour on these cpTi micropatterns with the results of our earlier experiments with microtextured silicone rubber substrata.

MATERIALS AND METHODS

Production and characterization of the titanium microtextured wafers

In order to produce cell culture substrata, circular titanium wafers with a diameter of 76.2 mm (3") were cut out of titanium plate material (cpTi Grade II, Engelhard-CLAL/ Drijfhout B.V., The Netherlands). Subsequently, these cpTi wafers were polished mechanically (grit size ≥0.25 μm) to create a smooth surface, which is indispensable for accurate patterning with photolithography techniques.

Standard lift-off photolithography was used to transfer gratings of 1.0, 2.0, 5.0, and 10.0 μm wide into Shipley 1805 photoresist. Before spinning the photoresist, the wafers

were cleaned carefully in boiling acetone and fuming 100% HNO_3 to remove particles and organic residues. After a prebake at 90°C, the titanium wafers were aligned and exposed using an ElectroVision Maskaligner. Finally, the exposed photoresist was removed in a Shipley developer (351), and a chromium layer of 50 nm was evaporated on the wafer surface by E-gun evaporation as mask material. Before plasma etching, the unexposed photoresist regions were removed by lift-off in an acetone ultrasonic bath.

After removal of the non-exposed chromium, SF_6/O_2 chemistry was used to etch the cpTi wafers with an ion energy of 250 eV in a standard RIE etcher (STS, PlasmaFab 340/310). Special precautions were taken to reduce condensation of TiF_4 on wafer surface and reactor wall. Therefore, the etch process was carried out at a pressure of 20 mTorr, while the chamber wall and electrode temperature were heated up to a temperature of 80°C. After etching, the chromium layer was stripped off and the surface examined by scanning electron microscope (SEM; JEOL 6310), surface profilometer (DEKTAK 3030, Sloan), and energy dispersive spectroscopy (EDS, Noran 5500).

Cell culture

For harvesting rat dermal fibroblasts (RDFs), abdominal skin grafts were taken from male Wistar rats (100-120 gram). After dissociation and culture of the RDFs as described earlier[4-8], the fifth generation of these cells was identified as (myo)fibroblasts and used for further experiments.

Before using the cpTi wafers for cell culture purposes, these substrata were given an ultrasonic rinse in 30% nitric acid (Merck) for 5 minutes, followed by flushing the wafers with tapwater for 15 minutes. Subsequently, the substrata were rinsed ultrasonically in 20% Na_2CO_3 solution (15 minutes; Merck), dried under a constant N_2 gas flow, rinsed ultrasonically in pure acetone (Merck) for 5 minutes, and rinsed twice in distilled, deionized water for 15 minutes. Finally, the wafers were sterilized for cell culture by boiling in 70% ethanol for 15 minutes.

After air-drying the titanium wafers in a laminar flow cabinet and positioning them in the petri dishes (∅=90mm; Bibby Sterilin Ltd., U.K.), 2.0 $x10^5$ viable RDFs in α-MEM with Earl's Salts and L-glutamine (Gibco), and 10% (v/v) heattreated fetal calf serum (Gibco) were added to each wafer. The cells were incubated for 3 days (37°C, 5% CO_2 -95% air) under static conditions, while the growth medium was changed after 2 days of culture. These experiments were performed in sixfold.

Scanning Electron Microscopy (SEM) and Transmission Electron Microscopy (TEM)

At the end of the incubation period, all cultures were given two 5 minute rinses with phosphate buffered saline without magnesium and calcium (PBS Dulbeco; pH 7.2) to remove non-attached cells. For SEM, the cells on the cpTi microgrooved substrata were fixed for 30 minutes with 2.5% glutaraldehyde 0.1M sodium cacodilate (pH 7.3), supplemented with 0.1M sucrose. After fixation, the wafers were rinsed twice with 0.1M phosphate buffer (30 minutes) and dehydrated using a graded ethanol series and tetramethylsilane (TMS, 5 minutes, Sigma)[10-11]. Subsequently, the samples were air dried, sputter-coated with gold, and viewed with SEM immediately after preparation.

For TEM, the cell cultures were treated as described before[8]. In short, the cells on the titanium wafers were fixed with 2.0% glutaraldehyde (Merck) in 0.1M phosphate buffer (pH 7.3) for 2 hours at 4°C and postfixed with a 1.0% OsO_4 (Merck) - 0.1M phosphate buffer solution for 1 hour. Following dehydration with a graded ethanol series, random areas on the wafer were covered with Epon, which was left to polymerize for 24 hours at 60°C. After polymerization, the Epon

blocks were removed from the titanium surface by N_2 freeze fracture. These Epon blocks, which contained the RDFs and a cast of the microgrooved wafer surface, were reembedded in Epon. Ultrathin sections perpendicular to the surface grooves were cut on a Reichert OMU-3 ultramicrotome with a diamond knife (DRUKKER International, The Netherlands). Sections were collected on Formvar-coated copper grids and stained with saturated uranylacetate (20 minutes) and leadcitrate (10 minutes) for contrast enhancement. All specimens were observed with a JEOL 1210 transmission electron microscope.

Confocal Laser Scanning Microscopy (CLSM)

CLSM preparation and observation of the RDFs on the cpTi microgrooved wafers was performed as described elsewhere[7]. In short, the titanium wafers were first rinsed with PBS to remove non attached cells. After this first rinse, the cells were fixed with 2.0% paraformalin (Merck) in PBS for 15 minutes, and permeabilized with 1.0% Triton X-100 for 5 minutes. For visualizing the vinculin containing focal adhesion points of the RDFs, mouse monoclonal antibody hVIN-1, specific for vinculin[12] (30 minutes; Sigma) and fluorescein *iso*-thiocyanate (FITC) conjugated goat anti-mouse IgG (30 minutes; Sigma) were used. The RDF stress fibres were visualized with thiorhodamine *iso*-thiocyanate (TRITC) labelled phalloidin (30 minutes; Sigma).

Immediately after performing the double stains, the RDFs were viewed with a Bio-Rad MRC 1000 CLSM (Bio-Rad Laboratories). To avoid possible damage of the samples due to the size of the titanium wafers, the stained areas were not covered with a coverslip. Consequently, the CLSM consisted out of a Nikon Diaphot microscope with non-cover glass (NCG) objectives (Nikon). Next to the fluorescence mode, the krypton/argon mixed gas laser (Ion Laser Technology, Salt Lake City, UT, USA) of the CLSM was used to visualize the underlying microtextured cpTi surface with the reflection mode. After capture of the digital images with a Synoptics Sprynt frame grabber and storage on an 1 GB optical disk cartridges (LM-D702W, Panasonic), Confocal Assistant V3.10 for Windows™ 3.1x (FTP.GENETICS.BIO-RAD.COM; copyright Todd Clark Brelje, 1995) was used to create 24 bits RGB (**R**ed-**G**reen-**B**lue) overlay images. These digital images made it possible to capture the fluorescent and reflection data in one picture. The RGB images were transferred to CD-ROM by using a CD-ROM writer (CDD2000, Philips) for permanent storage and analysis.

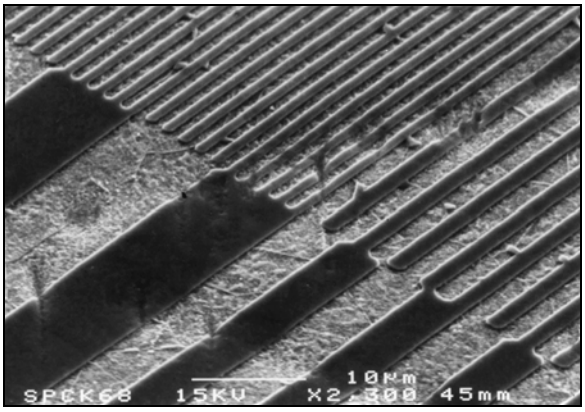

Figure 1 Scanning electron micrograph of the four different microtextures on the cpTi wafer surfaces. The dents in the surface and consequential pattern damage is clearly visible. Furthermore, the protrusions on the surface edge and the difference in the roughness of the groove bottom and ridge crest can be seen.

RESULTS

Characterization of the wafer surfaces

Examination of the microtextured wafer surface with SEM showed some imperfections of the surface patterns. Frequently, dents (Figure 1) and slopes (Figure 2) in the wafer surface were seen, causing damage or discontinuity of surface ridges and the etched surface pattern in general. Occasionally, protrusions on the ridge edges were seen (Figure 1). Further inspection revealed that the ridge crests were

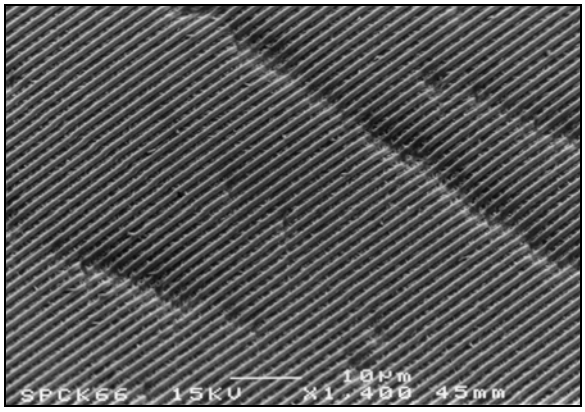

Figure 2 SEM image of a TiD01 surface. The slopes in the cpTi wafer surface cause imperfections of the etched surface pattern.

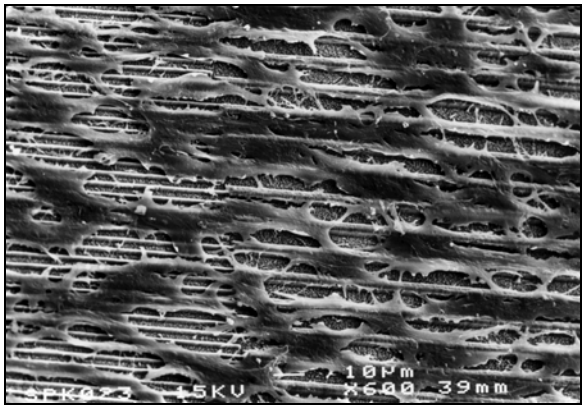

Figure 3 SEM photograph of RDFs on a TiD01 and TiD05 surface after 3 days of incubation. Although detection of the complete cell perimeter is difficult, the cells appear to be aligned parallel to the surface pattern.

smooth, while the bottom of the grooves possessed an aspecific roughness. Finally, deviations of the ridge shape were observed. Although most ridges possessed a rectangular shape with angles close to 90°, the 1.0 µm ridges (TiD01) occasionally displayed a triangular configuration. In addition, some 5.0 µm (TiD05) and 10.0 µm (TiD10) ridge edges displayed signs of underetch, giving these surface features a mushroom-like appearance.

Concerning the dimensions of the surface patterns, the DEKTAK profilometer showed that the measured values differed from the intended designer values. Both the designer and actual surface texture dimensions can be found in Table I. Measurements also showed that the titanium wafers possessed a curvature of the surface. This curvature proved to be ≤0.09%, causing the depth of the surface grooves to range from 1.1 and 2.2 µm. Finally, EDS showed no chromium, natrium, or vanadium impurities of the titanium wafer surfaces.

TABLE I
Designer and measured values of the micropatterns on the titanium wafers surfaces
(Gw=groove width, Rw =Ridge width)

Surface	***Designer values***		***Actual values***	
	Gw (µm)	*Rw (µm)*	*Gw (µm)*	*Rw (µm)*
TiD01	1.0	1.0	1.0	0.8
TiD02	2.0	2.0	2.1	1.4
TiD05	5.0	5.0	5.0	3.6
TiD10	10.0	10.0	9.2	8.0

Scanning electron microscopy (SEM) of the RDFs on the textured surfaces

Study of the RDFs on the microtextured cpTi surfaces with SEM showed large quantities of cells, which were arranged mainly as monolayers (Figure 3). Occasionally, RDFs were seen on top of other cells (Figure 4). This concerned single RDFs and not tightly packed, continuous multilayers of cells. Majority of the RDFs on the textured surfaces had formed many cell-cell contacts (Figure 3). These cell-cell contacts made the determination of the RDFs main direction of orientation difficult. Nevertheless, the main vector of orientation seemed to be directed parallel to the surface ridges on all patterns. This was especially clear on the TiD01, TiD02, and TiD05 surfaces.

Further, we observed that all cells

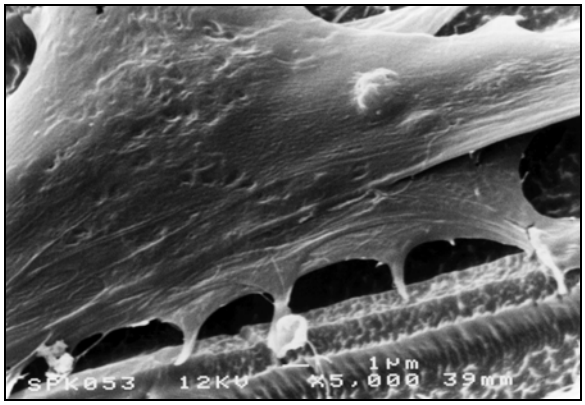

Figure 4 SEM image of two RDFs on a TiD02 surface after 3 days of incubation. Cell extensions of the bottom cell attach to the surface ridge.

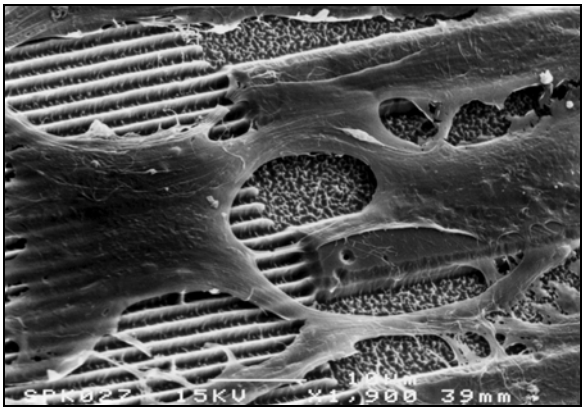

Figure 5 Scanning electron image of RDFs on a TiD01 and TiD10 surface after 3 days of incubation. The cells, which attach to the surface ridges or to each other through cell-cell contacts, appear to avoid contact with the bottom of the grooves.

spanned the surface grooves, disregarding the groove width or depth (Figure 3). Close examination of the RDF attachments frequently showed specific cell attachments to the surface ridges (Figure 4) and other cells (Figure 5) on all surface patterns. Distinct cell attachments to the bottom of the grooves could not detected by SEM.

Transmission electron microscopy (TEM)

General examination of the RDFs on the surfaces with TEM showed that these cells were arranged in a monolayer conformation. As with SEM, RDFs were seen occasionally on top of each other, but a continuous multilayer was not detected. Higher magnification learned that all cells on all surfaces displayed a normal appearance (Figure 6 to 10). The nucleus of the RDFs contained both euchromatin and heterochromatin, while in the cytosol intracellular components like the endoplasmatic reticulum (ER), the Golgi apparatus, mitochondria, lysosomes, and autophage vacuoles were observed. Widening of the ER was not found in any of the cells. Ribosomes were seen either as free ribosomes or associated with the ER. Finally, small quantities of glycogen were observed in the cytosol. Although the titanium wafers were removed during the preparation of the samples, an electron dense film outlined the features on the surface of the removed wafer. This film, that was seen in all samples, was approximately 6 nm thick and consisted probably out of adsorbed proteins originating from the culture medium. With the help of this film,

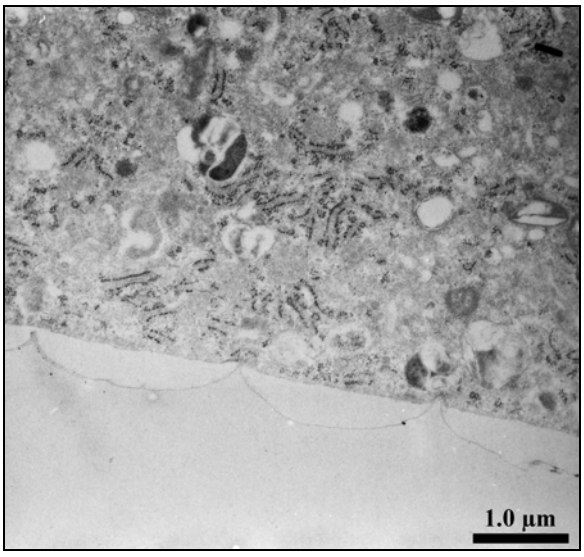

Figure 6 Transmission electron micrograph of a RDF on a TiD01 surface (3 day incubation). An electron dense protein layer outlines the textured wafer surface. Despite the triangular surface ridges, the cell membrane appears not to be punctured. Focal contacts can be found at the points of contact between the cell and the surface ridges. No contact can be found between the cell and the bottom of the grooves.

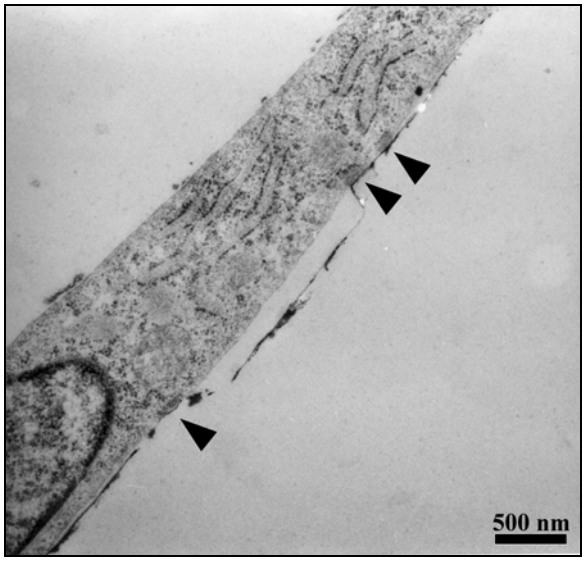

Figure 7 TEM micrograph of a RDF on a TiD02 surface (3 day incubation). Clearly defined focal adhesion points (⮜) can be seen on or near the edges of the surface ridges. There is no contact between the RDF and the bottom of the groove. The black electron dense areas are titanium residues, torn of the wafer surface during preparation.

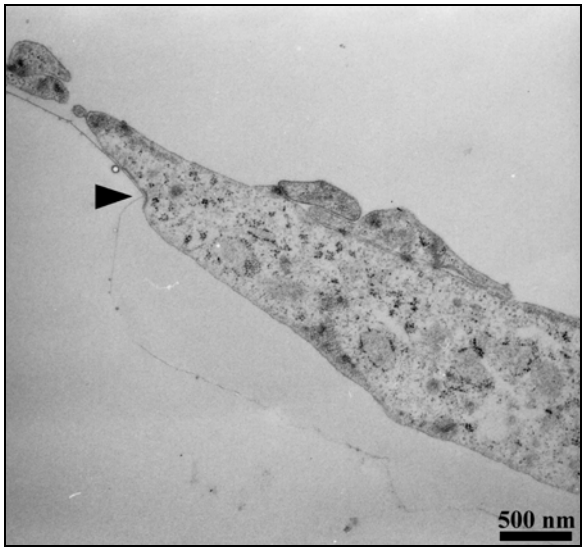

Figure 9 Higher TEM magnification of the RDF in Figure 8. A focal adhesion point (➢) is wrapped around the edge of the surface ridge.

it was possible to evaluate the quality of the etched surface features and the contact between these features and the RDFs.

TEM confirmed that some areas of the TiD01 surfaces possessed triangular ridges (Figure 6). RDFs on these triangular ridges only contacted the top of the ridges. Some focal adhesion points were found on the pointed ridges, but these structures were not defined as clearly as on the other surface pat-

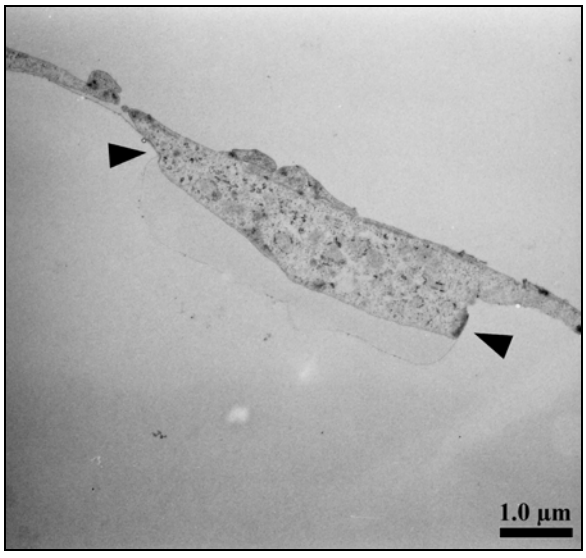

Figure 8 Transmission electron micrograph of a RDF on a TiD05 surface after 3 days of incubation. The cell protrudes into the groove, but does not contact the bottom of the groove. Focal adhesion points (⮜) can be seen on the edge of the ridge and the wall of the surface groove.

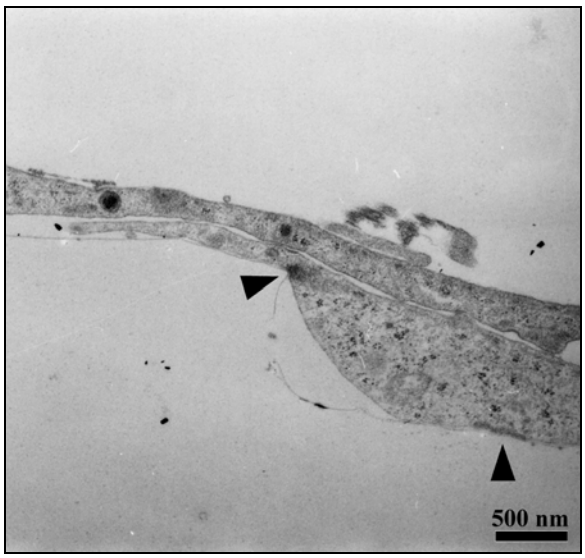

Figure 10 TEM image of RDFs on a TiD10 surface (3 day incubation). The underlying cell contacts and attaches to the bottom of the groove (see ➢ ⮜). Focal adhesion points are present on the edge of the ridge and the bottom of the groove.

terns. No contact was found between the RDFs and the bottom of the TiD01 grooves.

The patterns on the TiD02 surfaces existed solely out of ridges with (near) rectangular edges (Figure 7). Occasionally, electron dense residues were seen, which originated from the original titanium wafer surface. In contrast with the RDFs on the TiD01 surfaces, the cells on the TiD02 textures possessed many well defined focal adhesion points. In none of the investigated TiD02 sections RDFs contacted the bottom of the surface grooves.

The ridges of the TiD05 patterns possessed protruding edges, which gave the ridges a mushroom-like shape (Figure 8 and 9). Moreover, the angle between the walls and the floor of the surface grooves proved to be rounded. Although the RDFs on the TiD05 patterns protruded occasionally into the grooves, these cells never made contact with the floor of these grooves (Figure 8). Focal adhesion points were found on the crests and edges of the ridges and on the walls of the surface grooves. Occasionally, these structures were wrapped around the edges of the ridges (Figure 9).

Mushroom-like shaped ridges and rounded angles between the groove wall and groove floor were also found with the TiD10 textures. Furthermore, the RDFs on these surface patterns also protruded into the surface grooves, but this occurred more frequently than on the TiD05 surfaces. At many sites, the cells on the TiD10 textures contacted the bottom of the grooves, often resulting in the formation of focal adhesion points (Figure 10). In addition, the cells also showed the presence of focal adhesion points on the crests and edges of the ridges.

Confocal scanning laser microscopy (CLSM)

With the help of fluorescent staining techniques and additional imaging software, we studied the relation between the stress fibres, vinculin containing attachment complexes, and the surface features. Careful examination of these digital images showed that the RDFs on the TiD01 and TiD02 surfaces possessed stress fibres that were highly aligned with the surface grooves and ridges (Figure 11). Many of these fibres ended at the vinculin containing focal adhesion points, which were located specifically on the surface ridges of these patterns. These focal points had an elongated ecliptic shape and were also orientated parallel with the surface ridges.

Predominant orientation of the stress fibres and vinculin containing focal adhesion points were not observed on the TiD05 and TiD10 surfaces. On the TiD05 patterns for example, a wide variety of highly oriented and non-orientated stress fibres was observed. The orientation of the vinculin containing attachment complexes proved to be comparable with the orientation of the stress fibres which ended on these focal points (Figure 12). In contrast with the TiD01 and TiD02 surfaces, vinculin on the TiD05 surfaces was not orientated solely parallel, but also perpendicular to the surface ridge (Figure 12). Nevertheless, focal adhesion points were located on the surface ridges.

On the TiD10 surfaces, mainly non-orientated stress fibres and focal adhesion points were found. The differences in F-actin and vinculin orientation between different surface textures is demonstrated clearly in Figure 13. This CLSM image shows RDFs on a TiD01 and TiD10 surface texture. While the stress fibres and vinculin containing focal adhesion points of the RDF on the TiD01 surface pattern were highly aligned,these intracellular components of the cells on the TiD10 texture were not. In contrast with the other surface patterns, some vinculin was found on the bottom of the 10.0 μm grooves. However, the majority of vinculin containing focal adhesion points were located on the crests of the TiD10 ridges.

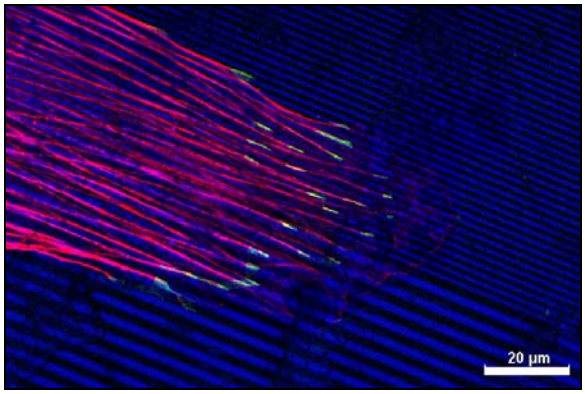

Figure 11 CLSM overlay image showing actin (RED) and vinculin (GREEN) and the cpTi surface (BLUE). Incubation lasted 3 days. On both the TiD01 (top) and the TiD02 (bottom) surface, the stress fibres and the focal adhesion points are orientated parallel to the surface pattern. Vinculin is located mainly on the surface ridges.

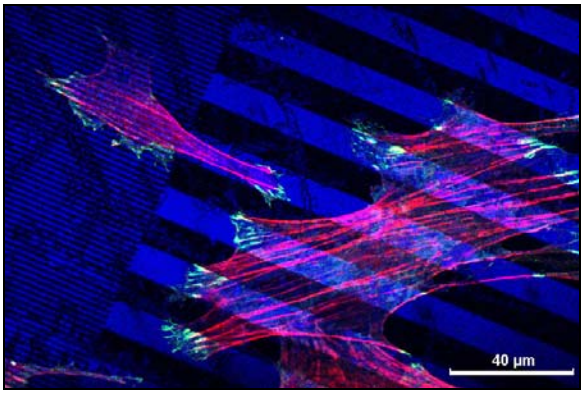

Figure 13 CLSM digital overlay image showing RDF F-actin (RED), RDF vinculin (GREEN), and the cpTi surface (BLUE). The image shows the transition from a TiD01 (left) to a TiD10 (right) texture. The cells were incubated for 3 days on these patterns. While the RDF on the TiD01 texture possesses highly aligned stress fibres and focal points, these intracellular components of the cell on the TiD10 surface are orientated differently.

DISCUSSION AND CONCLUSIONS

The results of this study show that it is possible to produce micropatterns in bulk commercially pure titanium. Although the quality of the micropatterns fell within set tolerance levels, results also made it clear that further minor adjustments will be required to optimize future cpTi microtextured surfaces. For instance, SEM showed dents, cavities, and slopes in the wafer surfaces. It is very likely that these features were remnants of damage inflicted during cutting the wafer to its appropriate size and shape, mechanical polishing of the wafer surface, the etching process, transport between laboratories, cell culture, or specimen preparation. An good example are the slopes (Figure 2), whose appearance suggests that they originated as scratches, which were reduced to slopes by polishing. The sharp edged dents and cavities on the other hand imply damage after polishing. Although these surface imperfections were seen on a limited scale, their impact on the eventual patterns emphasizes the importance of continuous surface checks during the various stages of the production process.

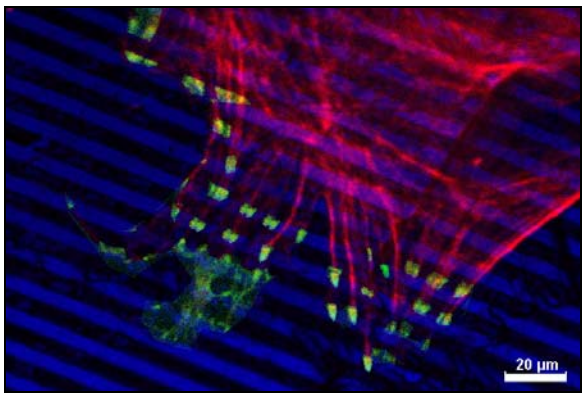

Figure 12 RGB overlay image of a RDF on a TiD05 surface (BLUE) after 3 days of incubation. The stress fibres (RED) and focal adhesion points (GREEN) are not orientated parallel to the surface grooves and ridges.

SEM and TEM showed that some 1.0 µm ridges had a triangular shape in stead of a battlement-like appearance with rectangular edges. This could be caused by variations in the SF_6/O_2 etching process. During this process, a plasma is created by dissociating SF_6 in a RF field into SF_5^+ ions and F^* radicals. While the SF_5^+ ions etch the bottom of the grooves physically through bombardment, the F^* radicals etch the walls and bottom of the grooves chemically. In both cases, these processes result in the formation of TiF_4 gas,

which is removed by maintaining a low pressure environment in the reaction chamber. Introduction of O_2 offers the possibility of regulation, since the addition of O_2 facilitates the formation of a passivation layer which changes the etching speed. Next to variations during this etching process, the observed triangular ridges could also be caused by the fact that the surfaces of the titanium wafers were not perfectly flat, but possessed a small curvature of 0.09%. A curved wafer surface could induce imperfections of the applied chromium mask, resulting in deviations of the appearance of the eventual microfeatures. Except from the aberrant triangular ridge shapes, the observed deviations in groove width, ridge width, and groove depth could also be explained by the transferal and etching of gratings on non-planar wafer surfaces.

In addition, SEM micrographs showed that the roughness of the floor of the grooves was clearly different from that of the crest of the ridges. This difference in roughness could be caused by the formation of TiO_3 in stead of TiO_4 during the etching process. Since TiO_4 has a much lower sublimation point than TiO_3, it is possible that the latter was deposited on the groove floor during etching, resulting in an aspecific rough surface. It is more likely however, that this roughness was caused by the polycrystalline composition of the used cpTi wafers. Polycrystallinity is known to induce isotropic etching, since the molecule matrix of the material is oriented along several orientational planes. Due to this reason, most investigators prefer anisotropic materials like silicon. But these materials are not used for the production of implants. Therefore, further tuning of the etching process or perhaps the use of single crystalline titanium seems to be a better option for enhancing the quality of etched micropatterns in titanium. Furthermore, subsequent etching of the wafer surface after removal of the protective chromium layer could produce a comparable roughness on both the groove floor and the ridge crest.

Concerning the behaviour of the RDFs, SEM results suggested that the cells orientated parallel to the 1.0, 2.0, and 5.0 μm surface patterns, while the main direction of orientation of the RDFs on the TiD10 surfaces was very different. These results corroborate with our earlier studies with microtextured silicone rubber substrata[4-6]. During these earlier studies, digital image analysis showed that RDFs on silicone rubber surfaces with 2.0 μm grooves and ridges (SilD02) aligned strongly along the surface patterns, while the cells on the 5.0 μm grooves and ridges (SilD05) were less aligned. RDFs on silicone rubber substrata with 10.0 μm grooves and ridges (SilD10) proved to be orientated randomly.

CLSM overlay images showed that the stress fibres of the cells on the TiD01 and TiD02 surfaces also were orientated strongly parallel to the surface ridges, while these fibres of the RDFs on the TiD05 and TiD10 patterns were not (Figures 11 to 13). This again proved to be identical with the results of one of our earlier studies[7], during which we found similar directional vectors for the microfilaments of the RDFs incubated on SilD02, SilD05, and SilD10 surfaces. Further similarities between the RDFs on microtextured cpTi and silicone rubber surfaces were found for the location and orientation of the vinculin containing focal adhesion points. On both the titanium and the silicone rubber surfaces, vinculin was located mainly on the ridges of the surface patterns. Furthermore, the orientation of these vinculin stains was highly comparable. On both the TiD02 and SilD02 surfaces, the vinculin stains were directed strictly parallel to the surface ridges, while on the TiD05, SilD05, TiD10, and SilD10 surfaces other vinculin orientations were observed.

Similarities were also found for the TEM results. TEM showed that the RDFs on the TiD01, TiD02, and TiD05 surfaces did not

touch the bottom of the grooves. This is in agreement with our findings on silicone rubber substrata[8] and earlier results by Rovensky and Slavnaya[13]. During an earlier TEM study[8], we also found that the focal adhesion points of RDFs on microgrooved silicone rubber substrata were located mainly on the ridges. Again, comparable cell behaviour was observed on the microgrooved titanium surfaces during this study. Finally, results showed that only the cells on the SilD10 and TiD10 textures contacted the floor of the grooves.

Recognizing the similarities between the results on the microtextured titanium and silicone rubber surfaces, it is possible to discuss the implications of these findings. For example, the physicochemical properties of silicone rubber and titanium are not identical. This, together with the role that these material properties play in cell attachment[1-3, 9], could cause the RDFs to orientate differently on titanium. However, our results show that the alignment of the RDFs does not differ from that of RDFs on microtextured silicone rubber substrata[4-7]. The similarities could imply that the orienting effect of surface micropatterns is not influenced or overruled by material related properties. However, this does not mean that the substratum material has no influence at all. This is demonstrated clearly by our SEM data, that show that large quantities of cells were found on the titanium surfaces after 3 days of culturing. Comparison with cell quantities on silicone rubber substrata[4-8] revealed that, although identical amounts of RDFs were seeded (45 viable RDF per mm^2), less cells were present on these substrata after 3 days of incubation. This dissimilarity in cellular proliferation rate could be caused by differences in physicochemical properties of both substrata materials[1, 14]. Material surface properties are considered crucial for cell adhesion and spreading[1], cell activities that are related directly to the ability of fibroblasts to proliferate[14]. Therefore, it is possible to suggest that the more hydrophillic titanium surfaces induce a higher proliferation rate than the more hydrophobic silicon rubber surfaces.

Finally, some remarks can be made concerning the focal adhesion points. TEM micrographs showed that the focal adhesion points were wrapped occasionally around the edges of the ridges (Figure 9). This implies that focal adhesion points possess the ability to bend, and are therefore not rigid structures. This fact, together with the observed focal adhesion points on the walls of the ridges, seems to contradict with the hypothesis by Ohara and Buck[6, 15]. This hypothesis suggests that the geometrical dimensions of the focal adhesion points and the available area for attachment to the surface ridges are crucial elements in the process of cellular orientation. According to this theory, only one major orientational vector of attachment is possible on ridges with a width smaller than the minimum length required for focal adhesion point attachment, i.e. parallel to the surface grooves and ridges. However, if the focal adhesion points are not rigid, cell attachment is not limited due to this cause. Subsequently, this would mean that other phenomena cause the cell to orientate and elongate on microgrooved surfaces.

ACKNOWLEDGEMENT

This study is supported by the Technology Foundation (STW).

REFERENCES

1. A.F. von Recum and T.G. van Kooten, "The influence of micro-topography on cellular response and the implications for silicone implants" *J. of Biomat. Sci. Polymer Edition,* **7,** 181-198 (1995)

2. R. Singhvi, G. Stephanopoulos, D.I.C. Wang, "Review: effects of substratum morphology on cell physiology," *Biotechnology and Bioengineering,* **43,** 764-771 (1994)

3. A.S.G. Curtis, and Clark P, "The effects of topographic and mechanical properties of materials on cell behavior," *Critical Reviews in Biocompatibility,* **5,** 344-362 (1990)

4. E.T. den Braber, J.E. de Ruijter, H.T.J. Smits, L.A. Ginsel, A.F. von Recum, and J.A. Jansen, "Effect of parallel surface micro grooves and surface energy on cell growth," *J. Biomed. Mater. Res.* **29,** 511-518 (1995)

5. E.T. den Braber, J.E. de Ruijter, L.A. Ginsel, A.F. von Recum, and J.A. Jansen, "Quantitative analysis of cell proliferation and orientation on substrata with uniform parallel surface micro grooves," *Biomaterials* **17,** 1093-1099 (1996)

6. E.T. den Braber, J.E. de Ruijter, H.T.J. Smits, L.A. Ginsel, A.F von Recum, and J.A. Jansen, "Quantitative analysis of fibroblast morphology on microgrooved surfaces with various groove and ridge dimensions," *Biomaterials*, **17,** 2037-2044 (1996)

7. E.T. den Braber, J.E. de Ruijter, L.A. Ginsel, A.F. von Recum, and J.A. Jansen, "Confocal laser scanning microscopical study of the cytoskeletal architecture, attachment complexes, and protein depositions of fibroblasts cultured on silicone micro grooved surfaces," *J. Biomed. Mater. Res.*, accepted 1997

8. E.T. den Braber, J.E. de Ruijter, H.J.E. Croes, L.A. Ginsel, and J.A. Jansen, "Transmission electron microscopical study of fibroblast attachment to microtextured silicone rubber surfaces," *Cells and Materials* accepted 1997

9. B. Chehroudi, and D.M. Brunette, "Effects of surface topography on cell behavior," *Encyclopedic Handbook of Biomaterials and Bioengineering*, D.L. Wise, D.J. Trantolo, D.E. Altobelli, M.J. Yaszemski, J.D. Gresser, E.R. Schwartz (eds.), Marcel Dekker Inc., New York, 1995, 813-842

10. W.J. Reville, and M.P. Cotter, "An evaluation of the usefulness of air-drying biological samples from tetramethylsilane in preparation for scanning electron microscopy," *J Electron Microsc.,* **40,** 198-202 (1991)

11. S. Dey, T.S. Basu Baul, and B. Roy, "A new rapid method of air-drying for scanning electron microscopy using tetramethylsilane," *Journal of Microscopy,* **156,** 259-261 (1989)

12. R. Benori, D. Salomon, and B. Geiger, "Identification of two distinct domains on vinculin involved in its association with focal contacts," *J. Cell. Biol.,* **108,** 2383-2393 (1989)

13. Y.A. Rovensky, and I.L. Slavnaya, "Spreading of fibroblast- like cells on grooved surfaces," *Exp. Cell Res.,* **84,** 199-206 (1974)

14. T. Groth and G. Altankov, "Studies on cell-biomaterial interaction: role of tyrosine phosphorylation during fibroblast spreading on surfaces varying in wettability," *Biomaterials,* **17,** 1227-1234 (1996)

15. P.T. Ohara and R.C. Buck, "Contact guidance in vitro," *Exp. Cell. Res.,* **121,** 235-249 (1979)

CHAPTER 9

Overall conclusions and new questions...

CHAPTER 9

Overall conclusions and new questions...

Reviewing the results presented in this thesis, it can be concluded that the experiments in this thesis did not provide a final model or explanation for the working mechanisms of cellular behaviour to microtextured surfaces. The used and demonstrated techniques did however offer exciting opportunities, not only to create textured surfaces, but also to get insight in the modulation of the cell responses to these surfaces. In the following paragraphs the results in the chapters 2 to 8 will be discussed in relation to earlier published results and hypotheses.

Although the overall mechanism of contact guidance was not explained, some questions concerning the fascinating phenomena of contact guidance were answered. One of these main questions was which parameter of the standardized microgrooved surfaces manipulated fibroblast behaviour. Concerning the major determining factor for contact guidance of cells on these surfaces, there are two generally accepted hypotheses available. The first one by Clark et al.[1-2] suggests that the degree of cell alignment on surfaces with parallel grooves is a strong function of the groove depth and a weaker function of the repeat spacing. However, this hypothesis contradicts the results of the digital image analysis (DIA) experiments in chapter 4, which showed no significant difference between the alignment of RDFs on 0.5 and 1.0 μm deep grooves. In addition, the rat dermal fibroblasts (RDFs) incubated on the titanium microgrooved wafers (chapter 8) displayed no differences in alignment between the 1.1 and 2.2 μm deep grooves, or the earlier investigated grooves on the silicone rubber surfaces.

However, the results of the experiments in this thesis and data of studies by other investigators[3-6] seem to indicate at a limited importance of the groove depth and a major influence of the ridge width on cell alignment. Such a statement would corroborate the second hypothesis by Ohara and Buck[5], which proposes that, if the cells bridge the grooves, there will be no effect of the depth of these grooves on cellular alignment. Accordingly, the ridge width is the main determining factor in contact guidance. In chapter 3 and 4, quantitative DIA data demonstrated that the morphological changes of the RDFs on the microgrooved surfaces was a result of the ridge width, and not the groove width or depth. Specifically, experiments showed that ridges ≤ 4.0 μm can be used successfully to orientate (≤10°) RDFs along the surface microgrooves. In addition, other indications for the importance of the ridge were found with other forms of microscopy. For example, phase contrast microscopy (chapter 4), confocal laser scanning microscopy (CLSM; chapters 5 and 8) and transmission electron microscopy (TEM; chapters 6 and 8) showed that RDFs attached specifically to the ≤ 5.0 μm ridges of the microgrooved substrata.

CLSM also revealed that the alignment of the intracellular cytoskeletal components matched the orientation of the cells. Since no clear relation could be demonstrated between the ridge width and the deposited extracellular matrix (ECM) proteins, or the cytoskeletal and ECM alignment, other cell functions apparently

cause cell guidance. For example, there is some evidence that specific cell adhesion receptors, like integrin, can direct cell movement[7-9]. These studies show that integrin does not only play a role in cell adhesion, but also participates in processes like mechano-reception, interpretation, transduction, and various cell signalling pathways. This is also illustrated by earlier studies that report changes in many cellular processes like cellular differentiation, DNA/RNA transcription, cell metabolism, and protein production[3-4, 10-11]. Moreover, changes in the regulation of fibronectin mRNA levels, mRNA stability, and fibronectin stability/assembly on surfaces with microgrooves were found[10]. Therefore, further research into the cell response to surface topography should include a detailed study of the involvement of cellular adhesive molecules.

An other point of attention is the fact that during all experiments in this thesis only rat dermal fibroblasts (RDFs) were used. Although fibroblasts are very important in processes concerning connective tissue, many implants contact other cells and tissues. A good example are bone anchored implants, which interface with osteoblasts, osteocytes, osteoclasts, chondrocytes, or chondroblasts. It is paramount to note that the response of these cells to microgrooved surfaces could differ from that of fibroblasts. This was stressed earlier by Curtis and Clark[12], who concluded their review with the statement that `the topographical reactions of cells vary considerably from type to type, perhaps reflecting differing cytoskeletal organizations'. Therefore, the behaviour of these cells with microtextured surfaces should be investigated thoroughly before any statement can be made on microtextured bone anchored implants.

Many investigators have already speculated on the benefits of microtextured implants. For example, Ratner[13] speculated on the benefits of an implant surface that would not cause the formation of a fibrous capsule. According to Ratner, such an implant would not `be walled off', but the cells contacting the implant surface would respond `as if they are not seeing and interacting with the biomaterial'. This woundhealing reaction would be preferable for the clinical success of several frequently used implants. For example, reduction of the capsule thickness around an implant could mean a reduction of the capsule contraction that is often observed with silicone breast implants[14]. Furthermore, capsule reduction would enhance the performance of many implanted biosensors, pacemakers, and infusion pumps[3]. These devices all benefit from an optimal contact between the tissues and the implant for the transduction of signals. For instance, the necessary electrical pulse of a pacemaker would be conducted better to the heart muscle if the capsule around the electrode of this device was minimized. An other good example is the sensor of an implanted insulin infusion pump. For optimal detection of insulin levels, maximal contact between the sensor of this device and the surrounding tissues is required. However, if a fibrous capsule shields the sensor from the crucial signal, the performance of the implant will be insufficient.

Unfortunately, the *in vivo* experiments in chapter 7 proved to be inconclusive. First of all, no reduction of the fibrous capsule around the microtextured implants was found. Although several possible explanations have been presented in the Discussion and Conclusions section of chapter 7, the most valid argument appears to be the depth of the groove. Even when this pattern dimension does not provoke cellular orientation *in vivo* due to the existing cell-cell contacts[12], it could facilitate mechanical interlocking of the implant. This could lead eventually to a fixation of the implant, a minimum of damage to the surrounding tissues, and subsequently, a reduction of the fibrous capsule thickness. However, that micropatterned surfaces are

able manipulate woundhealing processes around implants was demonstrated by the significant differences in the number of inflammatory cells and bloodvessels around the microgrooved implants. Therefore, further research seems mandatory, especially since textured surfaces could present a possible tool in the manipulation of tissue growth and regeneration. Examples of this potential have been shown before with for instance percutaneous implants[3-4, 12-13, 17-18]. Furthermore, guided regeneration could reduce the formation of scarring tissue and enhance the repair of highly orientated structures like tendons[19-21]. In addition, the orienting effect of microgrooved surfaces could induce endothelial orientation in artificial grafts[13, 22] or reduce marsupialization with many percutaneous and permucosal implants[19]. Other applications of microtextured biomaterials has been reported in the discipline of tissue engineering. By using orienting scaffolds, skin autografts have been generated out of individual keritinocytes[23]. Moreover, attempts have been made to produce large tubular morphologies that could function as intestine or ureter segmental replacements[24]. In addition, microtextured surfaces have been used in *in vitro* experiments to decrease hepatocyte dedifferentiation[25-26] or induce guided nerve regeneration[1-2, 27].

Given these large number of possible applications for microtextured surfaces, experiments with other types of microtextured (bio) materials could prove to be very useful. This appears to be possible, since the experiments in chapter 8 did show that microtextured surfaces can be produced in bulk titanium. Although more research is necessary to optimize the production process of micropatterned surfaces, the presented preliminary results showed that RDFs display comparable behaviour on silicone rubber and titanium microgrooved surfaces. This does only apply to the orientation and not to the proliferation of the cells, probably because the latter is a process that is influenced by the differences in physicochemical properties between titanium and silicone rubber. This could very well be a result of differences in the surface free energy of the used materials, a conclusion that is supported by the results of chapter 2. Recognizing the large number of existing implants made of titanium, further research with micropatterned titanium surfaces and various cell types seems justified. In addition, many other materials are used in implantology and tissue engineering. Applying microtextures to the surfaces of these materials could benefit the development of successful implants and scaffolds.

An additional point of interest is the production of different shaped, microgrooved titanium surfaces. As stated before, many currently used implants are made of titanium. However, these implants are often cylindrical, and not planar. In order to study a possible design for a microtextured implant, development of microfabrication techniques is imperative. This can include the production of complex surface topographies[15] and the fabrication of microstructures on non-planar surfaces[16]. Using the latter, it will for example be possible to apply a microtexture to non-planar, curved implant surfaces. Development of these techniques will not only benefit biomaterial research, but also the production of microelectronic, mechanical, and optical devices and subsystems[15-16]. Subsequently, it is possible that the development of microfabrication techniques will not only result in the production of microtextured implants, but also in the construction smaller implant devices. Therefore, it is recommended that research of microtextured surfaces, as started with this thesis, is exploited further to determine whether microfabrication can offer a major advantage for the engineering of `smart' manipulative implants and (smaller) implants with higher clinical success rates. In addition, these new studies could also contribute to a better understanding of the

mechanisms that cause cellular contact guidance. Such insight would not only enlarge the general knowledge of these processes, but also offer implant designers a tool for designing more successful implants with predicable qualities.

REFERENCES

1. P. Clark, P. Connolly, A.S.G. Curtis, J.A.T. Dow, and C.D.W. Wilkinson, "Topographical control of cell behaviour: II. multiple grooved substrata," *Development,* **108,** 635-644 (1990)

2. P. Clark, P. Connolly, A.S.G. Curtis, J.A.T. Dow, and C.D.W. Wilkinson, "Cell guidance by ultrafine topography in vitro," *J. Cell Sci.,* **99,** 73-77 (1991)

3. A.F. von Recum and T.G. van Kooten, "The influence of micro- topography on cellular response and the implications for silicone implants," *Journal of Biomaterials Science - Polymer Edition,* **7,** 181-198 (1995)

4. R. Singhvi, G. Stephanopoulos, D.I.C. Wang, "Review: effects of substratum morphology on cell physiology," *Biotechnology and Bioengineering,* **43,** 764-771 (1994)

5. P.T. Ohara and R.C. Buck, "Contact guidance in vitro," *Exp. Cell Res.,* **121,** 235-249 (1979)

6. G.A. Dunn and A.F. Brown, "Alignment of fibroblasts on grooved surfaces described by a simple geometric transformation," *J. Cell Sci.,* **83,** 313-340 (1986)

7. N. Wang, J.P. Butler, and D.E. Ingber, "Mechanotransduction across the cell surface and through the cytoskeleton," *Science*, 260, 1124-1127 (1993)

8. A.J. Banes, M. Tsuzaki, J. Yamamoto, T. Fisher, B. Brigman, T. Brown, and L. Miller, "Mechanoreception at the cellular level: the detection, interpretation, and diversity of responses to mechanical signals," *Biochem. Cell Biol.,* **73,** 349-365 (1995)

9. N.A. Hotchin and A. Hall, "The assembly of integrin adhesion complexes requires both extracellular matrix and intracellular rho/rac GTPases," *J. Cell Biol.*, **131,** 1857-1865 (1995)

10. L.S. Chou, J.D. Firth, V.J. Uitto, and D.M. Brunette, "Substratum surface topography alters cell shape and regulates fibronectin mRNA level, mRNA stability, secretion and assembly in human fibroblasts," *J. Cell Sci.,* **108,** 1563-1573 (1995)

11. B. Wójciak-Stothard, Z. Madeja, W. Korohoda, and A.S.G. Curtis, "Activation of macrophage-like cells by mutiple grooved substrata. Topographical control of cell behaviour," *Cell Biol. Internat.,* **19,** 485-490 (1995)

12. A.S.G. Curtis and P. Clark, "The effects of topographic and mechanical properties of materials on cell behavior," *Critical Reviews in Biocompatibility,* **5,** 344-362 (1990)

13. B.D. Ratner, "New ideas in biomaterial science - a path to engineered biomaterials," *J. Biomed. Mater. Res.*, **27,** 837-850 (1993)

14. S. Bern, A. Burd, and J. May jr., "The biophysical and histologic properties of capsules formed by smooth and textured silicone implants in the rabbit," *Plast. Reconstr. Surg.*, **89,** 1037-1042 (1992)

15. B. Wagner, H.J. Quenzer, W. Henke, W. Hoppe, and W. Pilz, "Microfabrication of complex surface topographies using grey-tone lithography," *Sensors and Actuators,* **A 46-47,** 89-94 (1995)

16. S.C. Jacobsen, D.L. Wells, C.C. Davies, and J.E. Wood, "Fabrication of micro-structures using non-planar lithography (NPL)," *In: IEEE Micro Elctro Mechanical Systems MEMS '91*, Anon (ed.), IEEE, Piscataway, N.J., U.S.A., 1991, pp. 45-50

17. B. Chehroudi, T.R. Gould, and D.M. Brunette, "Effects of a grooved epoxy substratum on epithelial cell behavior in vitro and in vivo," *J. Biomed. Mater. Res.,* **22,** 459-473 (1988)

18. B. Chehroudi, T.R.L. Gould, and D.M. Brunette, "A light and electron microscope study of the effects of surface topography on the behavior of cells attached to titanium-coated percutaneous implants," *J. Biomed. Mater. Res.,* **25,** 387-405 (1991)

19. B. Chehroudi, and D.M. Brunette, "Effects of surface topography on cell behavior," *Encyclopedic Handbook of Biomaterials and Bioengineering*, D.L. Wise, D.J. Trantolo, D.E. Altobelli, M.J. Yaszemski, J.D. Gresser, E.R. Schwartz (eds.), Marcel Dekker Inc., New York, 1995, 813-842

20. H.P. Ehrlich, "Regulation der Wundheilung aus der Sicht des Bindesgewebes," *Der Chirurg*, **66,** 165-173 (1995)

21. B. Wòjciak, J. Crossan, A.S.G. Curtis, and C.D.W. Wilkinson, "Grooved substrata facilitate *in vitro* healing of completely divided

flexor tendons," *J. Mat. Sci.: Mat. in Med.,* **6,** 266-271 (1995)

22. B.J. Spargo, M.A. Testoff, T.B. Nielson, D.A. Stenger, J.J. Hickman and A.S. Rudolph, " Spatially controlled adhesion, spreading, and differentiation of endothelial cells on self-assembled molecular monolayers," *Proc. Nat. Acad. Sci. USA,* **91,** 11070-11074 (1994)

23. E. Bell, M. Rosenberg, P. Kemp, R. Gay, G.D. Green, N. Muthukumaran, and C. Nolte, "Recipies for reconstituting skin," *J. Biomech. Eng. Trans. ASME,* **113,** 113-119 (1991)

24. D.J. Mooney, G. Organ, J.P. Vacanti, R. Langer, "Design and fabrication of biodegradable polymer devices to engineer tubular tissues," *Cell Transplant,* **3,** 203-210 (1994)

25. L.G. Cima, D.E. Ingber, J.P. Vacanti, and R. Langer, "Hepatocyte culture on biodegradable polymeric substrates," *Biotech. Bioengineering,* **38,** 145-158 (1991)

26. J.C.Y. Dunn, R.G. Thomkins, and M.L. Yarmush, "Hepatocytes in collagen sandwich: evidence for transcriptional and translational regulation," *J. Cell Biol.,* **116,** 1043-1053 (1992)

27. V. Guenard, N. Kleitman, T.K. Morrissey, R.P. Bunge, and P Aebischer, "Syngeneic Schwann cells derived from adult nerves seeded in semipermeable guidance channels enhance the peripheral nerve generation," *J. Neurosci.,* **12,** 3310-3320 (1992)

SUMMARY

SUMMARY

More and more implants are being used in medicine. The clinical success of such implants will depend for a very large part on the physico-chemical properties of the (bio)-material. New techniques, which are also used in the field of tissue engineering, open up new possibilities for manipulating woundhealing related processes. Manipulation in this case means steering of cell and tissue related processes during woundhealing around the implant. One of the tools in the task of creating a manipulative implant surface could be the application of surface microtextures.

Chapter 2 describes how, in order to evaluate the effect of surface treatment and surface microtexture on cellular behaviour, smooth (SilD00) and microtextured silicone substrata were produced. The microtextured substrata that were used for this purpose possessed parallel surface grooves with a groove and ridge width of 2.0 (SilD02), 5.0 (SilD05), and 10.0 μm (SilD10). The depth of the surface grooves was approximately 0.5 μm. Subsequently, these substrata were either left untreated (NT) or treated by ultraviolet irradiation (UV), radio frequency glow discharge treatment (RFGD), or both (UVRFGD). After characterization of the substrata with scanning electron microscopy (SEM), scanning probe microscopy (SPM), and wettability measurements according to the Wilhelmy plate technique, rat dermal fibroblasts (RDFs) were cultured on the UV, RFGD, and UVRFGD treated surfaces for 1, 3, 5, and 7 days. Comparison between the NT and UV substrata revealed that UV treatment did not influence the contact angles and surface energies of surfaces with a similar surface topography. However, the contact angles of the RFGD and UVRFGD substrata were significantly smaller than those of the UV and NT substrata. The dimension of the surface events did not influence the wettability characteristics. Cell culture experiments revealed that RDF cell growth on UV treated surfaces was lower than on the RFGD and UVRFGD substrata. SEM examination demonstrated that the parallel surface grooves on the SilD02 and SilD05 substrata were able to induce stronger cell orientation and alignment than the events on SilD10 surfaces. By combining all the findings, the most important conclusion is that physicochemical parameters such as wettability and surface free energy influence the cell growth, but play no measurable role in the shape and orientation of cells on microtextured surfaces.

In **chapter 3**, a study is described to quantify the effect of the substrata surface topography on cellular behaviour. For this purpose smooth and microtextured silicone substrata were produced, and made suitable for cell culture by radio frequency glow discharge treatment. The silicone rubber substrata used during this study had the same surface patterns as the substrata described in chapter 2. RDFs were cultured on these silicone rubber substrata and a tissue culture polystyrene control surface for 1, 2, 3, 5, and 7 days. After incubation the cell proliferation was quantified with a Coulter Counter, and RDF size, shape, and orientation with digital image analysis (DIA). Again, cell counts proved that neither the presence of the surface grooves, nor the dimension of these grooves had an effect on the cell proliferation. However, RDFs on SilD02, and to a lesser extent on SilD05 substrata, were elongated

and aligned parallel to the surface grooves. Orientation of the RDFs on SilD10 substrata proved to be comparable to the SilD00 substrata. The cells were capable of spanning the surface grooves on all textures.

The results of the studies in chapter 2 and 3 showed that fibroblasts respond to substratum surface roughness. **Chapter 4** investigates how changing surface feature dimensions affects their size, shape, and orientation. Therefore, the microtextured substrata possessed parallel surface microgrooves and ridges that ranged in width from 1.0 to 10.0 μm. The grooves were either 0.45 or 1.00 μm deep. Prior to incubation, the substrata were cleaned and given a radio frequency glow discharge treatment. The RDFs were incubated on these substrata for 5 days. During incubation, the RDFs were photographed on day 1, 2, 3, 4, and 5, using phase contrast microscopy. Digital image analysis of these images revealed that on surfaces with a ridge width ≤4.0 μm, cells were highly orientated (<10°) and elongated along the surface grooves. Protrusions contacting the ridges could be seen. If the ridge width was larger than 4.0 μm, cellular orientation was random (≈45°) and the shape of the RDFs became more circular. Furthermore, results showed that the ridge width is the most important parameter, since varying the groove width and groove depth did not affect the RDF size, shape, or the angle of cellular orientation.

In **chapter 5**, the microfilaments and vinculin containing attachment complexes of RDFs incubated on microtextured surfaces, were investigated with confocal laser scanning microscopy (CLSM) and DIA. In addition, depositions of bovine and endogenous fibronectin and vitronectin were studied. To enable comparison with our previous data, smooth (SilD00) and microtextured silicone substrata (SilD02, SilD05, and SilD10) were used. Results first of all showed that CLSM and DIA make it possible to visualize and analyze intracellular and extracellular proteins and the underlying surface simultaneously through the creation of digital overlay images. Furthermore, it was observed that the microfilaments and vinculin aggregates of the RDFs on the 2.0 μm grooved substrata were orientated along the surface grooves, while these proteins were significantly less orientated on the 5.0 and 10.0 μm grooved surfaces. In contrast, bovine and endogenous fibronectin and vitronectin were orientated along the surface grooves on all textured surfaces. These proteins did not seem to be hindered by the surface grooves, since many groove spanning filaments were found on all microgrooved surfaces. Vinculin was located mainly on the surface ridges on all textured surfaces. Based on the results of this study, it was concluded that the observations did not confirm nor reject unequivocally one of the earlier published hypotheses concerning contact guidance.

In **chapter 6**, transmission electron microscopy (TEM) was used to test the hypothesis whether cellular attachment is highly influenced by the micromorphology of the substratum surface. After culturing RDFs on the SilD00, SilD02, SilD05, and SilD10 substrata for 3 and 5 days, the samples were prepared and sectioned for TEM by using a specially developed preparation technique. On the SilD02 and SilD05 surfaces it was found that the RDFs attached specifically to the ridges and did not contact the bottom of the surface grooves. In some instances, cell protrusions extended into the grooves, but none of these were found to contact or attach to the bottom of the microgrooves. Focal adhesion points (FAPs) were observed on the ridges of the surface patterns. In contrast, on the SilD10 substrata FAPs were observed on the surface ridges as well as in the surface grooves. Furthermore, close examination sug-

gested orientation of the filamentous cytoskeletal components parallel to the surface grooves on the SilD02 and SilD05 surfaces, which might be related to earlier observed overall cellular alignment along parallel surface grooves.

Chapter 7 investigates and discusses the proposed ability of microtextured implant surfaces to alter events at the interface between implant surface and surrounding tissues during woundhealing. To investigate this phenomenon, silicone rubber implants with SilD00, SilD02, SilD05, and SilD10 surfaces were implanted subcutaneously in rabbits for 3, 7, 42, and 84 days. SEM observation showed fibroblasts, erythrocytes, lymphocytes, macrophages, fibrin, and collagen on all implant surfaces after 3 and 7 days. After 42 and 84 days only little collagen, a small number of fibroblasts, but no inflammatory cells, were seen on the implant surfaces. The fibroblasts were not orientated along the surface grooves on all textured surfaces. Three dimensional reconstruction of CLSM images and normal light microscopy showed no significant differences between the thickness of the capsule surrounding the smooth and microgrooved implants. In contrast, normal light microscopy did show a significantly lower number of inflammatory cells, and a significantly higher number of blood vessels in the capsules surrounding the microgrooved implants. Differences between the 2.0, 5.0, and 10.0 μm grooved implants were not detected, although our results concerning the capsule thickness suggest that the depth of the grooves used was not sufficient to facilitate mechanical interlocking. The cause for the observed differences in inflammatory response and number of blood vessels remains unclear.

Up until the study in chapter 7, only silicone rubber substrata were used to investigate RDF behaviour on microtextured surfaces. In order to determine whether micropatterns can be produced in the frequently used biomaterial titanium, and to investigate the effect of these surfaces on RDF behaviour, photolithography and SF_6/O_2 chemistry were used in **chapter 8** to produce gratings of 1.0 (TiD01), 2.0 (TiD02), 5.0 (TiD05), and 10.0 μm wide (TiD10) into commercially pure titanium wafers. After incubation of RDFs on these surfaces for 3 days. Results showed that the RDFs as a whole and their stress fibres orientated strictly parallel to the surface pattern on the TiD01 and TiD02 surfaces. On the TiD05 and TiD10 surfaces this was not observed. In addition, TEM and CLSM demonstrated that the FAPs were located mainly on the surface ridges. TEM also revealed that these FAPs were wrapped occasionally around the edges of the ridges. Only the RDFs on both the TiD05 and TiD10 surfaces protruded into the grooves and possessed FAPs on the walls of the grooves. Attachment to the groove floor was observed only on the TiD10 textures. Comparison of these results with the observations on microtextured silicone rubber substrata suggests that material specific properties do not influence the orientational effect of the surface texture on the observed RDF cellular behaviour. The proliferation rate of the RDFs however seems to be much higher on titanium than on silicone rubber substrata.

The conclusions of this thesis, and their implication for future research and implant design are described in **chapter 9**.

SAMENVATTING

SAMENVATTING

In de geneeskunde wordt steeds meer gebruik gemaakt van implantaten. Het klinisch succes van implantaten hangt voor een zeer groot deel af van de fysisch-chemische eigenschappen van het (bio)materiaal waaruit dit implantaat gemaakt is. Nieuwe technieken, die ook gebruikt worden in de tissue engineering, zouden manipulatie van wondgenezingsprocessen mogelijk kunnen maken. Met manipulatie wordt een sturing van de cel- en weefselreactie tijdens het wondgenezingsproces bedoeld, welke uiteindelijk kan leiden tot een verhoogd klinisch succes van het implantaat. Oppervlakken met microtexturen hebben deze potentie.

In **hoofdstuk 2** is onderzocht wat de invloed van verschillende oppervlakte behandelingen en microtexturen is op het gedrag van cellen. Ten behoeve van deze experimenten werden siliconen substraten geproduceerd die in het bezit waren van een glad (SilD00) of gegroefd oppervlak. De groeven en de tussenliggende richels in het oppervlak hadden beiden een breedte van 2.0 (SilD02), 5.0 (SilD05) of 10.0 μm (SilD10). De diepte van alle groeven was ± 0.5 μm. Na productie zijn deze substraten verdeeld over verschillende groepen, die bestonden uit substraten die geen verder behandeling ondergingen (NT), die bestraald werden met UV licht (UV), een plasma behandeling ontvingen (RFGD), of zowel met UV als een plasma behandeld werden (UVRFGD). Na deze behandelingen werd het oppervlak van de substraten geïnspecteerd met behulp van scanning electronen microscopie (SEM), scanning probe microscopie (SPM) en bevochtigbaarheidsmetingen volgens de techniek van Wilhelmy. Hierna zijn er fibroblasten, afkomstig waren uit de huid van de rat (RDFs), op deze verschillend behandelde substraten gekweekt voor 1, 3, 5 en 7 dagen. De resultaten lieten zien dat de bevochtigbaarheid en oppervlakte vrije energie van de NT en UV substraten niet verschilde. Vergelijking met de RFGD en UVRFGD groepen liet echter zien dat de bevochtigbaarheid van deze substraten significant lager was dan die uit de NT en UV groep. Verschillen binnen één behandelingsgroep als gevolg van verschillende groef en richel breedten werden niet waargenomen. Wel werden er verschillen gevonden in de groeisnelheid van de cellen. Het bleek nl. dat de RDFs op de RFGD en UVRFGD substraten significant sneller groeiden dan op de UV substraten. Verder toonde SEM aan dat de SilD02 en SilD05 oppervlakte patronen een sterkere orintatie van de cellen parallel aan de groeven induceerde dan de SilD10 oppervlakken. De belangrijkste conclusie van deze studie was dan ook dat fysisch-chemische parameters zoals bevochtigbaarheid en oppervlakte vrije energie wel invloed hebben op de groeisnelheid van RDFs, maar niet op de oriëntatie van deze cellen.

In **hoofdstuk 3** zijn de effecten van oppervlakte structuren op het gedrag van cellen gekwantificeerd. Hiervoor werd wederom gebruik gemaakt van gladde en gegroefde siliconen substraten. Deze maal ontvingen alle substraten enkel een RFGD behandeling. Na deze oppervlakte behandeling werden er RDFs op de siliconen en polystyreen controle substraten gekweekt voor periodes van 1, 2, 3, 5 en 7 dagen. Ook deze keer bleek dat, noch de aanwezigheid van groeven in het substraat oppervlak, noch de grootte van de groeven en richels invloed hadden op de groeisnelheid van de cellen. Wel was te zien met digitale beeldanalyse (DIA) dat de RDFs op de SilD02, en in mindere mate op de SilD05 substraten, langgerekt waren en zich parallel richtten aan de oppervlakte groeven. De orintatie van de RDFs op de SilD10 substraten bleek vrijwel identiek aan de willekeurige oriëntatie van de cellen op

de gladde SilD00 oppervlakken. Tenslotte werd waargenomen dat de RDFs in alle gevallen de groeven overbrugden.

De resultaten van de in de hoofdstukken 2 en 3 beschreven studies lieten zien dat het gedrag van fibroblasten beïnvloed wordt door de ruwheid van het oppervlak waarop zij gekweekt worden. **Hoofdstuk 4** gaat nader in op de vraag welke groef en richel breedten specifieke veranderingen in celgrootte, celvorm en celorientatie veroorzaken. Om dit nader te kunnen onderzoeken werden er gegroefde siliconen substraten geproduceerd met diverse patronen. Dit maal varieerden zowel de groef als de richelbreedte tussen de 1.0 en 10.0 μm. Verder waren de groeven 0.45 of 1.0 μm diep. Na een RFGD behandeling werden RDFs op deze substraten gekweekt voor 5 dagen. Gedurende deze 5 dagen werden de levende fibroblasten op de gladde en gegroefde substraten gefotografeerd op dag 1, 2, 3, 4 en 5 met behulp van een fase contrast microscoop. Aan de hand van deze foto's liet DIA o.a. zien dat RDFs op oppervlakken met richels kleiner of gelijk aan 4.0 μm langer waren en in hoge mate georinteerd lagen in de richting van de groeven (afwijking kleiner dan 10°). Verder hadden deze cellen uitstulpingen die specifiek contact maakten met de oppervlakte richels. RDFs op substraten met richels groter dan 4.0 μm waren ronder van vorm en willekeurig georinteerd (gemiddeld ongeveer 45°). Aan de hand van de resultaten kan geconcludeerd worden dat de breedte van de richel de belangrijkste parameter is, daar variatie van groefbreedte en diepte geen invloed heeft op de grootte, vorm en oriëntatie van de cellen.

In **hoofdstuk 5** worden de microfilamenten en vinculine bevattende hechtingscomplexen van RDFs op gegroefde oppervlakken onderzocht met behulp van CLSM en DIA. Naast deze intracellulaire componenten werden ook bovine en endogeen fibronectine en vitronectine bestudeerd. Om vergelijking met eerdere resultaten mogelijk te maken, werden wederom de SilD00, SilD02, SilD05 en SilD10 substraten gebruikt. Uit de resultaten van deze studie werd allereerst duidelijk dat het mogelijk is met behulp van confocale laser scanning microscopie (CLSM) en DIA intra- en extracellulaire fluorescent gelabelde protenen samen met het oppervlak van het materiaal in beeld te brengen en te analyseren. Verder bleek dat de actine microfilamenten en de focale adhesie punten, waarvan vinculine een onderdeel is, zich oriënteren in de richting van het oppervlakte patroon. Op de SilD05 en SilD10 substraten waren deze intracellulaire componenten significant minder georiënteerd. Vinculine bevond zich voornamelijk op de richels van alle oppervlakte patronen. Het bovine en endogeen fibronectine en vitronectine was, in tegenstelling tot de eerder genoemde microfilamenten en vinculine, sterk georinteerd op alle oppervlakte texturen. Deze proteïnen leken geen hinder te ondervinden van de groeven in het substraat oppervlak, daar werd waargenomen dat zij alle groeven overspanden. Aan de hand van de resultaten van deze studie was het echter niet mogelijk een uitspraak te doen over de (on)juistheid van eerder gepubliceerde theorieën met betrekking tot celorientatie en "contact guidance".

In **hoofdstuk 6** is transmissie electronen microscopie (TEM) gebruikt om de hypothese te testen, die stelt dat cel hechting in hoge mate beïnvloed wordt door oppervlakte ruwheid. Na het kweken van RDFs op SilD00, SilD02, SilD05 en SilD10 substraten voor 3 en 5 dagen, zijn er ultra dunne coupes gemaakt met behulp van een speciaal voor dit doel ontwikkelde preparatie techniek. Aan de hand van deze coupes werd waargenomen dat de RDFs op de SilD02 en SilD05 substraten specifiek hechten aan de richels van het oppervlakte patroon. Verder kwamen de fibroblasten enkel in contact met de top van de richels en niet met de bodem van de groeven. In sommige gevallen werden er wel celprotrusies in de groeven aangetroffen, maar hechting van deze uitstulpingen aan de bodem van de groef werden niet waargenomen. Focale adhesie punten (FAPs) werden enkel

gezien op de richels. In tegenstelling tot de RDFs op de SilD02 en SilD05 substraten, hechten de cellen op de SilD10 oppervlakken zowel aan de toppen van richels als aan de bodem van de groeven. Tenslotte wees observatie van de cytoskeletaire filamenten uit dat deze parallel aan de groeven waren georiënteerd op de SilD02 en SilD05 substraten. Dit laatste kan verband houden met de eerder waargenomen oriëntatie van de gehele cel op deze oppervlakte patronen.

Hoofdstuk 7 onderzoekt en bespreekt de eventuele potentie van gegroefde implantaat oppervlakken om genezingsprocessen op het scheidingsvlak tussen implantaat en weefsels te beïnvloeden. Om dit te kunnen onderzoeken, werden siliconen implantaten met SilD00, SilD02, SilD05 en SilD10 oppervlakken onder de huid van konijnen geplaatst voor 3, 7, 42 en 84 dagen. Na verwijdering van deze implantaten bleek met behulp van SEM dat na 3 en 7 dagen fibroblasten, erytrocyten, lymfocyten, macrofagen, fibrine en collageen aanwezig waren op het oppervlak van alle implantaten. Na 42 en 84 dagen werden wel slechts kleine hoeveelheden collageen en niet georinteerde fibroblasten, maar geen ontstekingscellen waargenomen op alle implantaat oppervlakken. Drie dimensionale reconstructie van CLSM beelden van de weefsels en normale licht microscopie (LM) lieten zien dat er geen significante verschillen waren tussen de dikte van het kapsel rond de gladde en gegroefde implantaten. Daarnaast toonde LM wel aan dat rond de gegroefde implantaten significant minder ontstekingscellen en significant meer bloedvaten aanwezig waren. Verschillen tussen de verschillend gegroefde oppervlakken werden niet gevonden. Uit de resultaten met betrekking tot de dikte van het kapsel kan mogelijk geconcludeerd worden dat de groeven in deze implantaten niet diep genoeg waren om "mechanical interlocking" te veroorzaken. Dit betekent dat het implantaat op zijn plaats wordt gefixeerd door het in de groeven ingegroeide weefsel. De oorzaak van het lagere aantal ontstekingscellen en hogere aantal bloedvaten rond de gegroefde implantaten is onduidelijk.

Tot aan de studie in hoofdstuk 7 zijn er enkel siliconen substraten gebruikt. Om de productie van micropatronen in andere implantatie materialen en de reactie van cellen op deze alternatieve materialen te onderzoeken, werden in **hoofdstuk 8** microgroeven van 1.0 (TiD01), 2.0 (TiD02), 5.0 (TiD05) en 10.0 μm (TiD10) in titanium aangebracht met behulp van fotolithografie en SF_6/O_2 chemie. Na een incubatie van 3 dagen, oriënteerde de gehele cel en de intracellulaire actine filamenten zich langs de TiD01 en TiD02 microgroeven. Op de TiD05 en TiD10 oppervlakken was deze oriëntatie niet aanwezig. Verder toonden TEM en CLSM aan dat de focale adhesie punten zich voornamelijk bevonden op de richels. Herhaaldelijk was met TEM te zien dat deze FAPs ook om de hoek van een richel kunnen buigen. Uitstulping van de fibroblasten in de groeven werd alleen gezien op de TiD05 en TiD10 oppervlakte patronen. Hoewel de cellen op deze texturen FAPs bezaten op zowel de richels als de wanden van de groeven, hechten slechts de cellen op de TiD10 oppervlakken aan de bodem van de groeven. Vergelijking van deze resultaten met die uit eerdere experimenten met siliconen substraten geven aan dat de materiaal gerelateerde eigenschappen geen invloed hebben op de oriëntatie van de cellen. De groeisnelheid van de fibroblasten daarentegen lijkt weldegelijk benvloed te worden door de eigenschappen van het substraat materiaal.

De belangrijkste conclusies van dit proefschrift en eventuele suggesties voor verder onderzoek en eventuele toekomstige implantaat ontwerpen worden besproken in **hoofdstuk 9**.

ACKKNOWLEDGEMENTS

Writing a thesis can be a lonely task. If you don't do it properly, it can result in long nights, staring at a blank computer screen, not knowing where the train is taking you. Don't get me wrong. This thesis wasn't written in a jiffy. I've had my share of sleepless nights. But in my case the damage was limited because I had some people around who kept me on track. This section is dedicated to them.

First of all I would like to thank **prof. dr. John Jansen**. I guess I annoyed John over the years, refusing to stop calling him THE CHIEF. But that was all well meant, believe me. During these last 4 years, he managed to keep me on track, although he never forced me to live by a strict time table or master plan. A good example was when I asked him how things were supposed to go concerning holidays. Mind you, this was 2 weeks after I had started. He smiled at me, waved his arms according his personal trademark and said, `Well, all I expect from you is that you finish the job on time. How you do or plan it, is your responsibility.' I don't know if he ever regretted that he said that. I hope not. But I'm grateful for the freedom and trust he gave me.

Furthermore, I would like to thank **prof. dr. Leo Ginsel**. The first time I met Leo, he probably must have thought something like, `What in heavens name is this moron doing on my department?' For the record I've to say that I had consumed a lot of beer the first time I saw him. That always makes people behave, ...huh..., differently. But he kept an open mind and made me feel that I was always welcome on the Department of Cell Biology and Histology over the years. He never was too busy to listen to my stories and provided me with different angles on subjects. Thanks Leo...

Sometimes distance can be a nuisance. If you've to cooperate with someone in the U.S.A. while you're in Europe, it can lead to impersonal contacts and general discussions. Happily, this is no golden rule. There are always exceptions. And **prof. dr. Andreas von Recum** of Clemson University is such an exception. When I met him in Clemson, he never struck me as the big biomaterials guru he actually is. He didn't hesitate to invite me into his home, meet his family, and show me his favourite hobby, i.e. raising sheep. Especially now that this thesis is ready, I am glad that I had the honour of calling him a part of my team.

Speaking of teams, we would never have got where we are now, if I couldn't have counted on **Anja de Ruijter**. This tiny lady with big potential helped me with all the work that had to be done. God knows how many times she helped me back on track when I went blank. When I felt buried under things to do, she eliminated problems with a few words and took huge loads of work off my back. The same thing goes for **Huib Croes**, who probably developed a throbbing headache every time I gave him those atrocious silicone substrata. Wonderman Huib proved that making TEM sections is a Craft that he mastered a long time ago.

Thanks also to all those people who made those little differences. **Joop Wolke** for teaching me everything there is to know about congresses and teasing me about my alleged

successes with foreign ladies, **Kitty van Dijk** for putting up with my loud music and cigarette smoke, and **Hein van der Lee** for showing me that there ALWAYS is a way to get the job done. Thank you **Saskia Onck** from Onck Graphic Design for giving me access to all your equipment and helping me with this thesis. Thanks to **Hans Smits** for all the help and tech hints, **dr. Paul Jap** for all the time and useful discussions (burp), **dr. Jack Fransen** for the (golden) tips, and **prof. dr. Nico Creugers** for showing me that *Star Trek* is no mental disorder. Thanks also to everybody at the Departments of Biomaterials, Oral Function, and Cell Biology and Histology of the University of Nijmegen for the good times over the years, the people of the CDL (Centraal Dieren Laboratorium) and the MESA Research Institute of the Technical University of Twente for all their help. If you are not mentioned in these acknowledgements, please keep in mind that you're always liable to forget somebody. So if I forgot you, please don't hold it against me.

To end this, I would like to finish with some people that I will never forget, whatever happens. First of all my **mum and dad**. They always saw the potential, even when I didn't, and shared everything they had to get me where I am now. Talking about opportunities... Thanks also to **Gabrie and Lydia**, who took a stray cat in and treated it as something special. I'll never know how to make it up to U 2. And finally, I would like to thank **Patricia**, my partner in crime. She ran the whole show single-handedly when I was putting all this down on paper. Luckily, she always kept me in touch with the `real world' when I slid off into a `Walter Mitty' syndrome. Or as James Thurber wrote it: `I was thinking,' said Walter Mitty. `Does it ever occur to you that I am sometimes thinking?' She looked at him. `I am going to take your temperature when I get you home.'

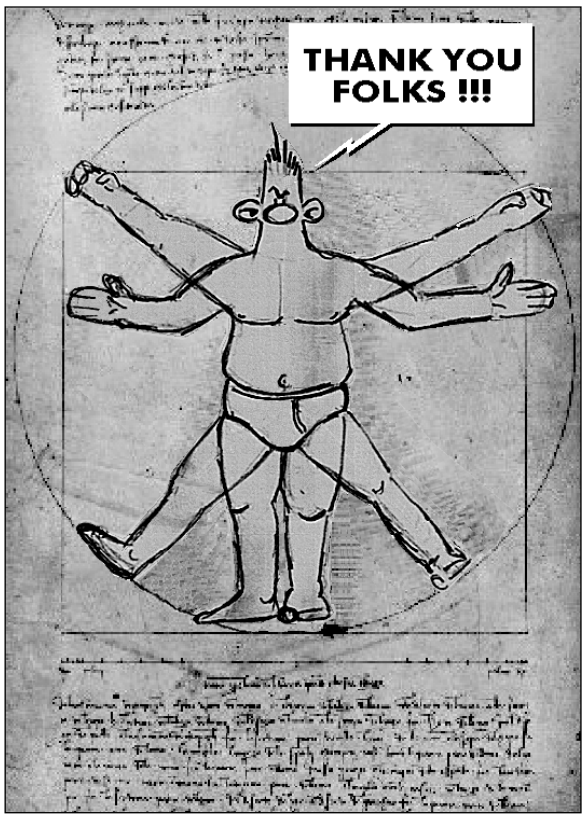

CURRICULUM VITAE

Edwin Teunis den Braber was born in Rotterdam, the Netherlands, on April 22th, 1965. In 1982, he graduated from the HAVO (high school) at the `Christelijke Scholengemeenschap Johannes Calvijn' in Rotterdam. Two years later, in 1984, he graduated successfully from the VWO (college) at the same institute. After performing his military obligations in several EC countries in 1985 and 1986, he entered the Faculty of Medicine and Dentistry of the University of Nijmegen in 1987 to pursue a MSc. degree in Biomedical Sciences. During this study, he participated in the studies `The effects of intra-tracheal cyclophosphamide administration on the morphology of the lung and the immune system of the rat' under the supervision of dr. A.A.J. Verhofstad and dr. J.H.J. Copius Peereboom Stegeman at the Institute of Pathology, University Hospital Nijmegen, and `Effect of the consumption of fermented foodstuffs on the human NK-activity through the ^{51}Cr and the (newly developed) LDH-release assay' under the supervision of prof. dr. Th. Ockhuizen, dr. G.J. Schaafsma, and S. Spanhaak MSc., at TNO Toxicology and Nutrition Institute in Zeist. In 1991, he completed his Biomedical Sciences study successfully with Toxicology as a specification. In December 1992, the project described in this thesis was initiated. The work was performed at the Department for Biomaterials (prof. dr. J.A. Jansen) and Department of Cell Biology and Histology (prof. dr. L.A. Ginsel) of the Faculty of Medical Sciences of the University of Nijmegen. During this study, close cooperation was established with the Dept. of Engineering (Clemson University, U.S.A.) of prof. dr. A.F. von Recum and the Dept. of Electrical Engineering (MESA Research Institute, University of Twente, The Netherlands) of prof. dr. M. Elwenspoek. In addition, the laboratories of prof. dr. D.M. Brunette at the University of British Colombia, Vancouver, Canada, were visited during this period.

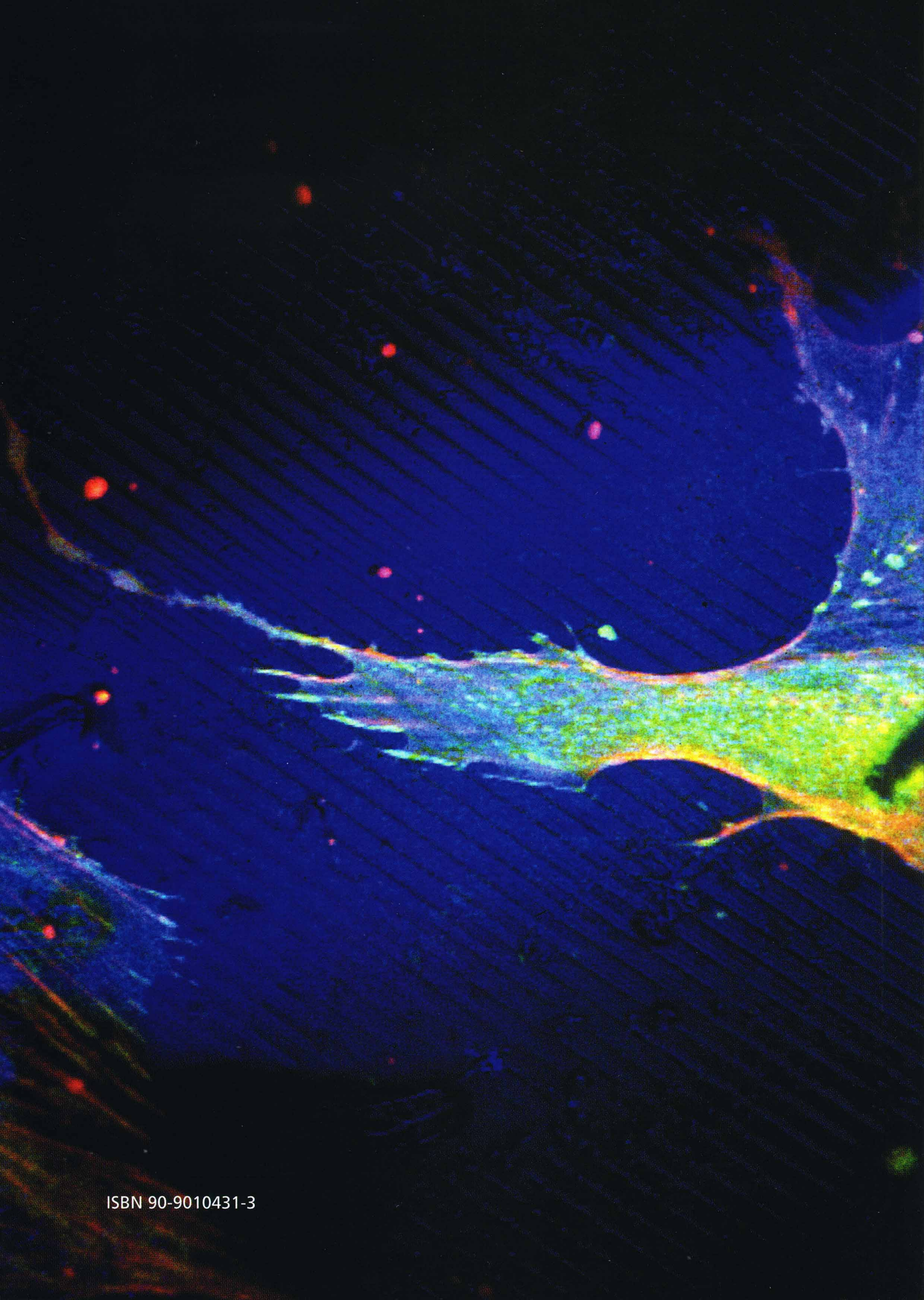

ISBN 90-9010431-3